# Seesaw and seesaw-like scenarios : Some phenomenological implications

*By*

**Avinanda Chaudhuri**

PHYS08201004006

*Harish-Chandra Research Institute, Allahabad*

*A thesis submitted to the*
*Board of Studies in Physical Sciences*

*In partial fulfillment of requirements*
*For the degree of*

**DOCTOR OF PHILOSOPHY**

*of*

**HOMI BHABHA NATIONAL INSTITUTE**


**June, 2016**

# STATEMENT BY AUTHOR

This dissertation has been submitted in partial fulfillment of requirements for an advanced degree at Homi Bhabha National Institute (HBNI) and is deposited in the Library to be made available to borrowers under rules of the HBNI.

Brief quotations from this dissertation are allowable without special permission, provided that accurate acknowledgement of source is made. Requests for permission for extended quotation from or reproduction of this manuscript in whole or in part may be granted by the Competent Authority of HBNI when in his or her judgment the proposed use of the material is in the interests of scholarship. In all other instances, however, permission must be obtained from the author.

Avinanda Chaudhuri

# DECLARATION

I, hereby declare that the investigation presented in the thesis has been carried out by me. The work is original and has not been submitted earlier as a whole or in part for a degree/diploma at this or any other Institution/University.

Avinanda Chaudhuri

# List of Publications arising from the thesis

**Journal**

1. **A. Chaudhuri**, W. Grimus and B. Mukhopadhyaya, *"Doubly charged scalar decays in a type II seesaw scenario with two Higgs triplets"*, *JHEP* **1402** *(2014) 060*.
2. **A. Chaudhuri**, N. Khan, B. Mukhopadhyaya and S. Rakshit, *"Dark matter candidate in an extended type III seesaw scenario"*, *Phys. Rev. D* **91** *(2015) 055024*.
3. **A. Chaudhuri** and B. Mukhopadhyaya, *"CP -violating phase in a two Higgs triplet scenario: Some phenomenological implications"* , *Phys. Rev. D* **93** *(2016) no.9, 093003*.

**Conferences**

*"Texture zeros and type II seesaw mechanism"*,
**A. Chaudhuri**,
*Nu Horizon, Harish-Chandra Research Institute, Allahabad, 17-19 th March, 2016*.

Avinanda Chaudhuri

*Dedicated to*

*my parents*

# Acknowledgements

It is not possible for me to describe in words the inspiration, encouragement and love I received from my parents, without which it would have been impossible for me to reach upto the stage where I am now.

I would like to express my deepest gratitude to my thesis supervisor Professor Biswarup Mukhopadhyaya for his invaluable guidance at every step of my research work. He has encouraged me to think and work independently all along.

I have learnt a lot from my collaborators. I would like to thank Prof. Walter Grimus for his wonderful guidance during the period of our collaboration. I take this opportunity to thank Prof. Subhendu Rakshit and Mr. Najimuddin Khan for the collaborating work. I would like to acknowledge the financial support I have received from the Regional Centre for Accelerator-based Particle Physics (RECAPP), HRI and Department of Atomic Energy, Govt. of India.

I thank all my friends at HRI, seniors, batchmates, juniors and post doctoral fellows for their support. I would like to specially thank Dr. Tanumoy Mondal and Dr. Subhadeep Mondal for their understanding and numerous help.

I would like to express my sincere regards to my teacher Prof. Asoke Sen, under whose guidance I have done a project work during my course of study at HRI, for his inspiration.

My regards are due to Dr. Aditi Mukhopadhyaya for her help in variours ways during my stay at HRI, Allahabad.

I want to take this opportunity to express my deepest respect to Prof. Sourov Roy (or Sourov da, as I call him) for being a constant source of inspiration to me.

I would like to convey my regards to my teachers at HRI, Prof. Rajesh Gopakumar, Prof. Sumathi Rao, Prof. Raj Gandhi, Prof. Asesh Krishna Datta, Prof. Ujjwal Sen, Prof. Sandhya Choubey, Prof. Aditi Sen(De), Prof. L. Sriramkumar, Prof. Satchidananda Naik, Prof. Dileep Jatkar, Prof. Pinaki Majumdar, Prof. V. Ravindran, Prof. Tirthankar Roy Choudhury, for their help during my stay at HRI.

My thanks are also due to Rukmini di (Dr. Rukmini Dey) for the music evenings that I enjoyed in her house.

Lastly, I would like to thank all the employees of HRI, Allahabad for their help during my research work.

# Contents

# SYNOPSIS

## Introduction

The Standard Model (SM) of particle physics has been extremely successful in describing most of the observed phenomena in particle physics. However, there is a strong motivation for physics beyond the SM, to address some yet unexplained observations, which include, small masses and mixing pattern of neutrinos, existence of Dark Matter (DM) and Dark energy in the Universe, matter-antimatter asymmetry of Universe and so on. Also, in the Large Hadron Collider (LHC) era, we hope to test the theory beyond the SM, which describes physics at the TeV scale. So, physics beyond the SM is a serious study for any aspiring physicist.

The electroweak symmetry $SU(2)_L \times U(1)_Y$ is broken by the vacuum expectation value (vev) of the Higgs doublet $v \simeq 246$ GeV, which gives mass to the gauge bosons and all the fermions except the neutrino. There is no $SU(2)_L$ singlet neutrino-like field in the SM, that can generate a Dirac mass term for the neutrino. Thus, neutrino is massless in the SM, at tree level. It can be seen that, to all orders in perturbation theory within SM, the neutrino is massless and also their masses remain zero even in the presence of non-perturbative effects.

Thus, one must seek physics beyond the SM, to explain observed evidence for neutrino masses. While there are many possibilities that lead to small neutrino masses, in this proposed thesis we focus on seesaw frameworks — which are considered as the most elegant way of explaining the smallness of neutrino mass. There are only four mechanisms in physics beyond the SM, to generate Majorana neutrino masses at tree level. They are called the — Type I, II, III seesaw mechanism and the Inverse Seesaw mechanism. Type I seesaw mechanism is the simplest possible extension of SM that leads to non-zero mass for the neutrino. In this case, only a right-handed neutrino is added to the SM. Sub-eV neutrino mass can be obtained as functions of Dirac Yukawa couplings, the SM Higgs vev and heavy mass of the right-handed neutrino. Type II seesaw is a way to generate non-zero neutrino masses without using the right-handed neutrino. In this framework, an $SU(2)_L$ scalar triplet field $(\Delta^{++}, \Delta^{+}, \Delta_0)$ , with $Y = 2$ hypercharge, is included in the

SM. This allows an additional $\Delta L = 2$ Yukawa coupling between the scalar triplet and the lepton doublet. When the neutral member of the scalar triplet $\Delta_0$ acquires a vev, then this yukawa term produces small neutrino masses in terms of combinations between yukawa coupling constants and triplet vev. In the case of Type III seesaw mechanism, at least two extra matter fields (normally taken as fermion triplets) with zero hypercharge are added to the SM. This in turn produces sub-eV neutrino mass as function of Yukawa coupling, vev of SM Higgs and heavy mass of the fermion triplets. Another realization of seesaw mechanism is the so-called 'Inverse Seesaw mechanism', where small neutrino mass arise as a result of new physics at TeV scale, which may be probed at the LHC experiments. The implimentation of this mechanism requires the addition of three right-handed neutrinos and three extra singlet neutral fermions to the three active neutrinos in SM. Then, considering a definite hierarchy between various mass terms of the right-handed neutrinos and singlet states, small neutrino mass can be generated.

Of all these scenarios, the works presented in this proposed thesis are based on Type II and Type III seesaw framework. The content of the proposed thesis is divided into two parts.

- In the first part of the thesis, phenomenology of doubly-charged scalar decays in Type II seesaw framework and usefulness of these decays at the LHC has been described.

- The second part of the thesis describes the prediction of a Dark Matter (DM) candidate within a scenario inspired by the Type III seesaw framework.

The following sections contain brief descriptions of the above topics.

## Doubly-charged scalar decays in Type II seesaw framework

The motivation behind these works is two-fold. Firstly, strong evidence has accumulated in favour of neutrino oscillation from the solar, atmospheric, reactor and accelerator neutrino experiments over the last few years. A lot, however, is yet to be known, including the mass generation mechanism and the absolute values of the masses, as opposed to mass-squared differences which affect oscillation rates. A gateway to information of both of the above kinds is some idea about the light neutrino mass matrix, in a basis where the charged lepton mass matrix is diagonal. Here, too, in absence of very clear guidelines, various 'textures' for the neutrino mass matrix are often investigated. A possibility that

frequently enters into such investigations is one where the mass matrix has some zero entries. Such 'zero textures' lead to a higher degree of predictability and inter-relation between mass eigenvalues and mixing angles, by virtue of fewer free paramaters. In the context of Majorana neutrinos which have a symmetric mass matrix, various texture zeros have thus been studied from a number of angles. Of them, two-zero textures have rather wide acceptability from the viewpoint of explaining observed data. It has been shown that, none of the seven possible two-zero-texture cases can be achieved by assuming only one scalar triplet in the theoretical framework of Type II seesaw. It has also been shown that, the contradictions that appear with a single triplet can be avoided, if two or more scalar triplets are present in the theory. So, we see that, there is need for an extended scalar triplet sector, if Type II seesaw has to be consistent with two-zero-textures of neutrino mass matrix. Secondly, when a single triplet is present in a Type II seesaw framework, then most conspicuous signal consists in the decay of doubly-charged scalar into a pair of same-sign leptons and alternatively, the decay into a pair of same-sign W-bosons, which is dominant in a complementary region of the parameter space. It occured to us that, a third decay channel is also possible, where, a doubly-charged scalar decays into a singly-charged scalar plus a $W$ boson of same sign. But, such a decay mode is usually suppressed, since the underlying $SU(2)$ invariance implies relatively small mass splitting among the members of a triplet. However, when more than one triplet of a similar nature are present, and mixing among them is allowed, a transition such as the third decay channel mentioned above is possible between two scalar mass eigenstates. So, motivated by the necessity of more than one triplet in applying the Type II seesaw to a class of neutrino mass textures and to examine whether the $SU(2)$ gauge coupling driven decay where a doubly-charged scalar decays into a singly-charged scalar plus a $W$ boson of same sign really overrides the other two decay channels as mentioned above, we take up the case of two coexisting triplets in our work.

We have shown that, this decay really dominates over all other decays, by choosing several benchmark points(BPs) over a wide range of parameter space and by taking all the vevs and coefficients of Lagrangian to be real. In other words, in our first attempt, we have neglected all the CP-violating effects. We have also pointed out the distinction between having a single triplet and two triplets in the scenario, at the LHC, by defining ratios of events emerging from two, three and four-lepton final states with missing transverse energy(MET). We found that, after applying suitable cuts to suppress the SM background, these ratios are widely different in two-triplet case as compared to single-triplet model — this provides a way to distinguish between the two scenarios at the LHC.

To see the phenomenology including CP-violation, we make a minimal extension of the simplified scenario by postulating *one* CP-violating phase to exist. This entails a complex vev for any one triplet, at the same time, there is a complex phase in the coefficient of the Lagrangian. We found that phases of complex vev and coefficients are inter-related. We have chosen our BPs over a wide range of parameter space and adjusted the free parameters in such a way, that a new decay channel of doubly-charged scalar opened up, in addition to the previously mentioned one, as a result of increase in mass separation between heavier and lighter doubly-charged scalars. We observed that the heavier doubly-charged scalar decays dominantly into lighter doubly-charged scalar plus SM Higgs. This, in turn, opens up a spectacular signal at LHC, especially when the lighter doubly-charged scalar mostly decays into two same sign leptons, leading to the decay of heavier doubly-charged scalar into a pair of same-sign leptons plus SM Higgs. We noticed that, when the phase space needed for this decay is not available, the process where the heavier doubly-charged scalar decays into a singly-charged scalar plus a same-sign $W$ boson, dominates over all other remaining decays — this situation has already been discussed. We pointed out some rather interesting effect of presence of phase. If the mass differences do not allow the above mentioned decays when the phase is absent, they eventually open-up with the increase in phase of triplet vev, when all other parameters are at fixed values. Another notable effect of presence of phase is that, the contribution of triplet vev to neutrino masses gets suppressed. This results in an increase in corresponding Yukawa couplings. This is reflected in the fact that, the decay of a doubly-charged scalar into two same-sign leptons too has non-negligible branching ratios for some BPs. We have simulated same-sign di-lepton final states from both the doubly-charged scalars to confirm our findings. Also, we have ensured that the lightest neutral scalar must have mass $\sim 125$ GeV for all BPs.

In short, in these works we have attempted to explore the trademark signals of scalar triplets in the Type II seesaw framework, that are contained in the doubly-charged components.

## Prediction of a new Dark Matter (DM) candidate

We have already emphasized the importance of Type III seesaw mechanism in the context of generating small mass of neutrino. On the other hand, there is strong empirical evidence for the existence of dark matter in the Universe. A simple and attractive candidate for DM should be a new elementary particle that is electrically neutral and stable on cos-

mological scales. Our proposal is an extension of the type-III seesaw model for neutrino masses. As two fermion triplets are required to generate neutrino masses, we need to introduce a third triplet to take care of the DM candidate. This triplet needs to be protected by a $Z_2$ symmetry to ensure stability of the DM particle. This third triplet does not contribute to neutrino mass generation through seesaw, because, it is odd under imposed $Z_2$ symmetry. The $SU(2)$ symmetry will in general demand the charged and neutral components of the fermion triplet to be degenerate. However, we need a mass splitting between the charged and neutral component to obtain a DM particle of mass of the order of the electroweak scale. In some models this mass splitting between the charged and neutral components of the fermion triplet have been obtained through radiative correction. The mass of the charged member of the triplet in such a case has to be well above $\sim$ TeV, in order to avoid fast $t$-channel annihilation and a consequent depletion in relic density. As a result, such models end up with somewhat inflexible prediction of DM mass in the region $2.5 - 2.7$ TeV. We propose, as an alternative, two $Z_2$-odd fermion fields: a $Y = 0$ triplet and a neutral singlet that appears as a heavy sterile neutrino. All SM fields and the first two fermion triplets are even under this $Z_2$ symmetry. Mixing between neutral component of the triplet and the sterile neutrino can yield a $Z_2$ odd neutral fermion state that is lighter than all other states in the $Z_2$ odd sector. This fermionic state emerges as the DM candidate in this work. The requisite rate of annihilation is ensured by postulating some $Z_2$ preserving dimension-five operators. Choice of a light sterile neutrino can lead to light DM candidates, in our model, we worked with DM masses of more than 62.5 GeV to avoid an unacceptably large invisible Higgs decay width.

The DM mass, relic density has been calucated as function of the five independent parameters present in the theory, given by — Mass of the fermion triplet ($M_\Sigma$), Mass of sterile neutrino ($M_{\nu_s}$) and three coefficients of the dimension-five operators introduced in the theory. Two different situations may arise : (i) $M_\Sigma \gg M_{\nu_s}$ and (ii) $M_\Sigma \simeq M_{\nu_s}$. In the first case, self annihilation of DM mainly contributes in the calculation of relic density. While, in the second case, coannihilation between the charged components of the triplet, the neutral eigenstate of higher mass and the dark matter candidate becomes important in the calculation of relic density. We have shown by varying one parameter at a time and keeping other parameters at fixed values that it is possible to obtain a wide region of DM mass from $200$ GeV to TeV range that satisfies the correct relic density range and the constrains imposed on WIMP-nucleon cross section by XENON 100 and LUX data. We also got a large region of parameter space that satisfies the correct relic density requirement and the bound imposed by XENON 100 and LUX data on WIMP-nucleon

cross section in both the cases of self-annihilation and co-annihilation of DM candidate. Dark matter direct detection experimental results are rather conflicting. While CDMS, DAMA, CoGeNT, CRESST point towards a DM mass of $\sim 10$ GeV, XENON 100 and LUX claim to rule out these observations. Given this scenario, we keep our options open and explore all DM masses allowed by experimental observations.

# List of Figures

# List of Tables

# Chapter 1

# Introduction

## 1.1 Standard Model and beyond

The Standard Model (SM) of particle physics encompasses our current knowledge of elementary particles. The SM is a successful quantum field theory, based on the $SU(3)_C \times SU(2)_L \times U(1)_Y$ gauge group, which describes the interactions among elementary particles and three of the four fundamental interactions. In Nature, all the known phenomena observed so far, can be described in terms of four fundamental forces :

- Strong Interaction
- Weak Interaction
- Electromagnetic interaction
- Gravitational Interaction

The $SU(3)_C$ is the gauge group of strong forces, where '$C$' denotes the color quantum number carried by quarks as well as gluons, which are mediators of strong interaction. The symmetry group corresponding to electroweak interaction is $SU(2)_L \times U(1)_Y$, where '$L$' refers to the left-chirality of fermions and '$Y$' stands for the weak hypercharge, which is defined by the relation

$$Q = T_3 + \frac{Y}{2} \tag{1.1}$$

'$Q$' and $T_3$ being respectively the electric charge and third component of the weak isospin of the fields involved.

So, SM describes only the first three of four fundamental forces previously mentioned. Gravity effects are negligible at the highest energy scale of particle accelerator experi-

ments performed till date and therefore its exclusion does not affect the explanation of whatever has been observed so far in the world of fundamental particles.

## 1.2 Particle content of SM

The fermionic sector of the SM consists of six types each of quarks and leptons, which come in three generations or flavors. The transformation properties of these fields under SM gauge group are determined by their respective charges under the gauge groups. The quark fields transform as triplets (fundamental representation) of $SU(3)_C$, whereas the leptons are singlet under this gauge group. The leptons do not possess any color charge and hence they do not take part in strong interactions. SM being a chiral theory, treats left-handed and right-handed fermion fields differently with respect to $SU(2) \times U(1)$ gauge interactions. The left-handed fields transform as doublets (fundamental representation) under $SU(2)$, while the right-handed fields are singlets under this group. Thus we have the particle content for the quark sector as follows

$$\text{Doublets}: \begin{pmatrix} u \\ d \end{pmatrix}_L ; \begin{pmatrix} c \\ s \end{pmatrix}_L ; \begin{pmatrix} t \\ b \end{pmatrix}_L$$
$$\text{Singlets}: u_R,\ d_R;\ c_R,\ s_R;\ t_R,\ b_R.$$

For the leptonic sector we have

$$\text{Doublets}: \begin{pmatrix} \nu_e \\ e \end{pmatrix}_L ; \begin{pmatrix} \nu_\mu \\ \mu \end{pmatrix}_L ; \begin{pmatrix} \nu_\tau \\ \tau \end{pmatrix}_L$$
$$\text{Singlets}: e_R;\ \mu_R;\ \tau_R.$$

The left-handed chiral component of the field $\Psi$ is defined as $\psi_L = P_L\psi = [(1-\gamma_5)/2]\psi$ and for the right-handed one, $\psi_R = P_R\psi = [(1+\gamma_5)/2]\psi$. With the convention followed so far, the lepton doublets will have hypercharge $(-1)$ and for lepton singlets it is $(-2)$. The quark doublets are of hypercharge $+1/3$, for up-type quark singlets it is $+4/3$ and down-type quark singlets will have hypercharge $(-2/3)$.

The gauge sector of SM contains eight massless vector fields $G^a_\mu (a = 1, 2, ...8)$, known as the gluons, the gauge bosons of $SU(3)_C$. The gauge bosons corresponding to the broken $SU(2)_L \times U(1)_Y$ group are, $\gamma$(photon), $W^\pm$ and $Z$. The gluons are electrically neutral and carry color quantum numbers. So, they have self-interactions (both trilinear and quartic). The $W^\pm$ are massive, charged particles and $Z$ boson is massive but electrically neutral. The $W^\pm$ and $Z$ bosons are self-interacting also, whereas the photon is non self-interacting, massless and neutral.

## 1.3 Origin of mass : Higgs mechanism

The particle spectrum of SM described so far is incomplete. Till now, we have considered only those interactions among the particles, which arise as a consequence of local gauge invariance. However, invariance under $SU(2)_L \times U(1)_Y$ gauge group implies that all the fermions as well as gauge bosons have to be massless. Introduction of explicit mass terms for them threatens to destroy the good features of SM, such as, renormalizability and unitarity. The solution to this, is to generate the mass term in the Lagrangian by breaking the gauge symmetry spontaneously, that is to say, not in the original Lagrangian but through a selective (non-symmetric) choice of the vacuum. This phenomena is known as *'Spontaneous Symmetry Breaking'(SSB)* [1–9].

It has been observed that in the SM the electric charge is conserved and therefore the concerned gauge group of electromagnetism i.e $U(1)_{em}$ is an exact symmetry of the theory. So under *SSB*, we should have the following symmetry breaking pattern

$$\mathrm{SU(2)}_L \times \mathrm{U(1)}_Y \xrightarrow{SSB} \mathrm{U(1)}_{\mathrm{em}} \tag{1.2}$$

This breaking can be achieved by introducing a *spin* $0$ scalar field $\Phi$ that transforms as a doublet under the $SU(2)_L$ with $U(1)_Y$ hypercharge $+1$. This complex scalar doublet is defined as

$$\Phi = \begin{pmatrix} \phi^+ \\ \phi^0 \end{pmatrix} . \tag{1.3}$$

The scalar potential involving the scalar doublet, which also contains self-interaction term for the doublet, is written as

$$V(\Phi) = \mu^2 \Phi^\dagger \Phi + \lambda (\Phi^\dagger \Phi)^2 . \tag{1.4}$$

The self-interaction of $\Phi$ is such that gauge invariance is broken spontaneously. The vacuum expectation value (vev) $v$ of the neutral component of doublet is expressed in terms of the mass parameter $\mu$ and the self-interaction strength $\lambda$ and is given by

$$v = \sqrt{\frac{-\mu^2}{\lambda}} . \tag{1.5}$$

for $\mu^2 < 0$ and $\lambda > 0$.

If the scalar field is shifted with respect to the above vev, then, written in terms of the shifted field, the gauge invariance of the theory appears to be broken. The $U(1)_{em}$ invariance, however, remains unbroken, since the non-zero vev pertains only to the neutral part of the scalar field, which has no electromagnetic interactions.

The resulting mass spectrum consists of massive fermionic and gauge fields as well as a neutral scalar particle known as *Higgs boson*, which has recently been discovered at the Large Hadron Collider (LHC), CERN, Geneva and has mass$\sim 125$ GeV.

Masses of the gauge bosons are obtained from the Lagrangian

$$\mathcal{L}_\Phi = (D^\mu \Phi)^\dagger D_\mu \Phi - V(\Phi), \tag{1.6}$$

where $D_\mu$ is defined by

$$D_\mu = \partial_\mu - ig_1 \frac{Y}{2} B_\mu - ig_2 \frac{\sigma^a}{2} W_\mu^a - ig_3 \frac{\lambda^b}{2} G_\mu^b, \tag{1.7}$$

where $g_1,\ g_2$ and $g_3$ are the gauge couplings for $\mathrm{U}(1)_Y$, $\mathrm{SU}(2)_L$ and $\mathrm{SU}(3)_c$ groups respectively. The masses of gauge bosons are obtained as

- $m_\gamma = 0$
- $m_W = \frac{1}{2} g_2 v$
- $m_Z = \frac{1}{2} v \sqrt{g_1^2 + g_2^2}$

The weak mixing angle $\theta_W$, also called Weinberg angle, which gives the relationship between the masses of $W$ and $Z$ bosons, is defined as

$$\theta_W \equiv \tan^{-1}\left(\frac{g_1}{g_2}\right). \tag{1.8}$$

The massless vector fields that corresponds to photon couples with matter fields with electromagnetic coupling constant *'e'*, the electric charge. This is related to the $SU(2)_L$ and $U(1)_Y$ couplings in the following way

$$g_2 sin\theta_W = g_1 cos\theta_W = e \tag{1.9}$$

and lastly, the $\rho$-parameter, which measures the relative strengths of neutral and charged current interactions in the theory, is given by

$$\rho = \frac{m_W^2}{m_Z^2 cos^2\theta_W} \approx 1. \tag{1.10}$$

Masses of fermions are generated via gauage invariant Yukawa interactions between scalar and fermionic fields :

$$\mathcal{L}_{\text{Yuk}} = \sum_{i,j=\text{generation}} \left( -Y_{ij}^u \bar{Q}_i \tilde{\Phi} u_j - Y_{ij}^d \bar{Q}_i \Phi d_j - Y_{ij}^l \bar{L}_i \Phi e_j + \text{h.c.} \right), \tag{1.11}$$

where $\tilde{\Phi} = i\sigma_2\Phi^*$ and $Q$ and $L$ represents the quark and lepton doublets respectively and $Y^u,\ Y^d,\ Y^l$ are the Yukawa coupling matrices for the up-quark, down-quark and charged leptons respectively. After the field $\Phi$ gets the vev $v$, the Yukawa Lagrangian takes the form of $m_\psi \bar{\psi}_L \psi_R$ with the mass matrices,

$$m^u_{ij} \propto vY^u_{ij},\ \ m^d_{ij} \propto vY^d_{ij},\ \ m^l_{ij} \propto vY^l_{ij}. \tag{1.12}$$

These mass matrices are in flavor basis and are to be diagonalized to get the mass basis. These Yukawa couplings are free parameters in SM and are fixed by the masses of the corresponding fermions. It should be noted that neutrinos do not have any mass term due to the absence of their right-handed partners.

The predictions of the SM have been tested to a high degree of precision experiments carried out at high-energy colliders like the LEP, Tevatron and currently at the LHC, as well as in low-energy experiments of flavor physics. In almost all cases, experimental observations are in accordance with the predictions of SM. The long elusive Higgs boson has also been discovered at the LHC [10, 11]. Apart from a few discrepancies (e.g., the anomalous magnetic moment of muon) the SM is the most consistent model of particle physics till date. This has established SM as a starting point, as far as building fundamental theoretical models of Nature is concerned. In spite of the huge success of SM, however, there are some observations that encourage us to go beyond the SM. In the next section we point out some of those observations.

## 1.4 Need for new physics beyond SM

In the following we outline some observations which indicate that the SM suffers from some drawbacks and is not a complete theory to describe the particle domain.

- There are many free parameters ($\sim 20$) in SM, which can only be fixed through experiments. All the masses, couplings and mixing parameters in the quark sector are described by these free parameters of the theory and there is no explanation as to why the parameters have such values.

- The structure of fermionic sector in SM remains unexplained. The masses of the SM fermions range from sub-eV (for neutrinos) to over hundred GeV (for top quark). There is no satisfactory fundamental explanation for this huge hierarchy in masses of fermions. The fermions also come in three 'generations', with higher generation

having higher mass. Such a replication is not predicted or explained by anything within the SM.

The mixing in the quark sector also has a generational structure, i.e, the largest mixing occurs between the generations one and two, followed by mixing of two and three and finally, mixing between one and three, which are the feeblest ones. SM does not explain this pattern.

- It is important to ensure that tree-level values of the various SM parameters are stable. The inclusion of higher order terms in general leads to radiative corrections that modify the couplings and masses via the renormalization procedure. Any quadratic correction to the mass for gauge bosons are tamed by the gauge symmetry. For fermions chiral symmetry does this task, leaving only a weak, logarithmic dependence. However, the Higgs boson being a scalar does not have any such way out to cancel quadratic corrections and its mass would be driven to the scale of new physics. For example, correction due to top quark contribution, shifts the mass of Higgs from its tree level value by,

$$\Delta m_H^2 = -\frac{|Y_t|^2}{4\pi^2}\Lambda_{cutoff}^2 \tag{1.13}$$

where $\Lambda_{cutoff}$ is some cut off scale up to which SM is well-behaved and beyond which some new physics comes in and $Y_t$ is the top-quark Yukawa coupling, due to which the correction is largest. Now, if $\Lambda_{cutoff} \sim M_{pl}$, where $M_{pl}$ is the Planck scale ($\sim 10^{19}$ GeV), then corrections to Higgs mass squared reach upto $10^{38} GeV^2$. Therefore, in order to maintain a Higgs mass consistent with experimental measurements, we need to add counter-terms to the Higgs mass squared, so that the divergences cancel out. This obviously requires a large fine-tuning of the parameters involved. This is called the *Fine-tuning/ Naturalness/ Hierarchy problem*.

This so called Hierarchy problem has motivated several new physics scenarios, the most popular one being the existence of *Supersymmetry (SUSY)*, which relates bosonic and fermionic degree of freedom.

- Unification of the electroweak and strong couplings, is the so called *Grand Unified Theories (GUT)*, cannot be achieved within the SM framework. The running of these couplings are such that they do not exactly unify at any given energy scale, if their evolution all the way up is controlled by SM interactions alone.

- Gravity, one of the four fundamental forces of Nature, which becomes important near Planck scale, is not included in SM. SM may at best be treated as an effective theory up to Planck scale and new physics should appear at that scale. One of the alternatives is *String theory*, which hope to predict a quantized description of gravity.

- The first evidence for Dark Matter (DM) came from the measurement of rotation curves of galaxies. The rotation curves were found to fit with the hypothesis that visible part of the galaxy was immersed in a halo of invisible matter i.e Dark Matter. In fact, the Universe consists of only $4.9\%$ of visible matter and the rest consists of DM and Dark Energy. There is no such particle in SM which can fit in properly to explain this DM riddle.

- SM can not explain the observed baryon asymmetry of the Universe, namely, why we have more matter than anti-matter. This will perhaps require a level of CP-violation, which is not present in the SM.

- Lastly, one of the most important findings suggesting the existence of physics beyond the SM is the evidence for non-zero neutrino masses and mixings, observed in the form of neutrino oscillation. In SM, a neutrino is massless because of the absence of the corresponding right-handed partner. In principle, neutrino masses can be easily accommodated in the SM framework by postulating the existence of right-handed heavy sterile neutrinos. But, the extreme smallness of neutrino mass, which are many orders of magnitude smaller than all the fermion masses, calls for a deeper understanding. Also, the bi-large mixing pattern of neutrinos, as evident from oscillation data, is very different from what is noticed in the quark sector. This suggest some new underlying mechanism. The question as to, why there is such a large difference between mass of neutrino and that of the charged lepton belonging to the same $SU(2)_L$ multiplet is still a mystry. If neutrinos are found to be Majorana particles, then lepton number would be violated by their mass-term, which might give us a hint of physics beyond the SM. Several models for explaining the neutrino mass and mixing have been put forward, starting from seesaw mechanisms, largely motivated by high-scale grand unified theories, to low-scale models like SUSY with lepton number violation. But the questions remain yet to be answered.

We have mentioned some of the shortcomings of SM. Clearly, we need some theory beyond SM (BSM) to address these loop-holes. With this motivation we proceed to study

some BSM models based on seesaw mechanism, which might become helpful in understanding and overcoming some of the incompletenesses of the SM.

# Chapter 2

# Neutrino Physics

## 2.1 Neutrino masses and mixing

Neutrinos are the most elusive of the known fundamental particles. They are neutral, spin-half fermions and they do not possess any color charge. As far as it is known, they only interact with charged fermions and massive gauge bosons through weak interactions. For this weakly interacting nature, neutrinos can be observed and studied experimentally only if there are very intense neutrino sources and availability of large detectors.

The history of neutrinos dates back to the early 1930's, but they were first observed only in the 1950's in the experiments carried out by Reines and Cowan [12]. In 1962, experiments at Brookhaven National Laboratory made a surprising discovery that neutrinos produced in association with muons do not behave the same way tas those produced in association with electrons. A second type of neutrino (the muon neutrino) was discovered in these experiments [13]. The evidence for third neutrino flavor eigenstate i.e the tau neutrino ($\nu_\tau$) was obtained only in 2001, when the *DONUT* ("Direct Observation of Nu Tau") experiment at Fermilab [14] managed to record a handful of $\nu_e + X \rightarrow \nu_\tau + Y$ events. For a long time, it was believed that neutrinos are massless, making them drastically different from other SM spin-half counterparts like the charged leptons ($e, \mu, \tau$) and the quarks ($u, d, s, c, t, b$), which have mass. This myth has been broken in the late 1990's, through the strong indication of non-zero neutrino masses through oscillation phenomena, which opened the floodgate to many fresh questions in neutrino physics.

Various experiments with solar [15–20], atmospheric [21, 22], accelerator [23–25] and reactor [26–31] neutrinos have established beyond doubt, the phenomena of neutrino oscillation. More explicitly, a neutrino produced in a well-defined flavor state (say, a muon neutrino $\nu_\mu$) has a non-zero probability of being detected in a different flavor state (say

$\nu_e$ i.e electron neutrino). This probability of flavor-transition between flavor eigenstates depends on the neutrino energy and the distance travelled between the source and the detector. The simplest and only consistent explanation of almost all neutrino data collected till date is a phenomenon referred to as *"neutrino mass-induced flavor oscillation"*. These neutrino oscillations, in turn imply that neutrinos have non-degenerate masses and neutrino flavor eigenstates are different from neutrino mass eigenstates, that is to say, this indicates *lepton mixing*.

So, if the neutrino masses are distinct and lepton mixing takes place, a neutrino flavor eigenstate can be produced as a superposition of neutrino mass eigenstates via weak interaction i.e a neutrino $\nu_\alpha$, with a well-defined flavor, has non-zero probability to be measured as a neutrino of a different flavor, say, $\nu_\beta$, where $\alpha, \beta = e, \mu, \tau$. The oscillation probability between the two flavor states are denoted as $P_{\alpha\beta}$ and it depends on the propagation distance (L), neutrino energy (E) and mass-squared differences between neutrinos, ($\Delta m^2_{ij} \equiv m^2_i - m^2_j; i, j = 1, 2, 3$). $P_{\alpha\beta}$ also depends on the lepton mixing matrix, known as Pontecorvo-Maki-Nakagawa-Sakata (PMNS) matrix $U$. $U$ relates the neutrino flavor eigenstates ($\nu_e, \nu_\mu, \nu_\tau$) with neutrino mass eigenstates ($\nu_1, \nu_2, \nu_3$) in the following way

$$\begin{pmatrix} \nu_e \\ \nu_\mu \\ \nu_\tau \end{pmatrix} = \begin{pmatrix} U_{e1} & U_{e2} & U_{e3} \\ U_{\mu 1} & U_{\mu 2} & U_{\mu 3} \\ U_{\tau 1} & U_{\tau 2} & U_{\tau 3} \end{pmatrix} \begin{pmatrix} \nu_1 \\ \nu_2 \\ \nu_3 \end{pmatrix} \tag{2.1}$$

To explain the neutrino data till date, it is customary to parametrize PMNS matrix $U$, with the three mixing angles $\theta_{12}, \theta_{13}, \theta_{23}$ and one complex phase $\delta$. In terms of these parameters the matrix U is represented as (where 'c', 's' stand for cosine and sine of the angles respectively),

$$U = \begin{pmatrix} c_{12}c_{13} & s_{12}c_{13} & s_{13}e^{-i\delta} \\ -s_{12}c_{23} - c_{12}s_{23}s_{13}e^{i\delta} & c_{12}c_{23} - s_{12}s_{23}s_{13}e^{i\delta} & s_{23}c_{13} \\ s_{12}s_{23} - c_{12}c_{23}s_{13}e^{i\delta} & -c_{12}s_{23} - s_{12}c_{23}s_{13}e^{i\delta} & c_{23}c_{13} \end{pmatrix} \tag{2.2}$$

In addition one may have two more CP-violating phases, $\xi$ and $\eta$, in the neutrino sector if neutrinos are of Majorana type. These phases show up in very special situations. To relate the mixing coefficients to experimentally observed effects, it's very important to indicate the *'ordering'* of neutrino mass eigenstates. In literature, this is done in the following way : $m^2_2 > m^2_1$ and $\Delta m^2_{21} < |\Delta m^2_{32}|$. So, there are practically three mass-related oscillation observables : $\Delta m^2_{21}$ (positive-definite), $|\Delta m^2_{32}|$ and the sign of $\Delta m^2_{32}$. A positive (negative) sign for $\Delta m^2_{32}$ implies $m^2_3 > m^2_2$ ($m^2_3 < m^2_2$) and refers to what is called *normal (inverted)*

neutrino mass hierarchy. We list below the best fit values of various neutrino oscillation parameters obatined from global analysis of experiments [32]

$$\Delta m^2_{21} = 7.54 \times 10^{-5} eV^2, |\Delta m^2_{32}| = 2.47(2.46) \times 10^{-3} eV^2 \tag{2.3}$$

$$sin^2\theta_{12} = 0.307, sin^2\theta_{23} = 0.39, sin^2\theta_{13} = 0.0241(0.0244), \tag{2.4}$$

where the values (values in brackets) correspond to $m_1 < m_2 < m_3$ ($m_3 < m_1 < m_2$).It should be noted that this 'bi-large' mixing pattern is very different from that in the quark sector, raising questions about some different physics origin. But, at the same time, virually no information regarding $\delta$ nor for the other two CP-violating phases $\xi$ and $\zeta$ are available. The same can be said about the sign of $\Delta m^2_{32}$. The absolute values of neutrino masses are not known yet, we only know the differences between mass squared values. From these information, the possibility that the lightest neutrino is virtually massless ($< 10^{-3} eV$), can't be ruled out. There lies another possibility that, all neutrino masses are practically the same ($m_1 \sim m_2 \sim m_3 \sim 0.1 eV$). Clearly, experiments and searches outside the arena of neutrino oscillations are very much required to obtain an estimation of absolute values of neutrino masses.

Several questions regarding neutrino sector still remain unanswered. For example, questions like –*what is the ordering of neutrino masses ?, Is there CP violation in the lepton sector ?, Are neutrinos Dirac or Majorana particles?, What is the absolute mass scale for the neutrinos?, Are there indications of new physics in existing experimental data? and lastly, is some physics beyond the SM responsible for the neutrino mass and mixing?* are still open [33]. Various brilliant experiments have been performed, some are still ongoing and future experiments are being designed to obtain more information which will eventually help to answer these questions. Some of these experiments are listed in the next section.

## 2.2 Experiments with neutrino

We briefly discuss below some of the experiments which helped to obtain the present picture of neutrino masses and mixing :

- **Atmospheric Neutrinos :** Atmospheric neutrinos are produced when cosmic rays (mostly protons) hit the atmosphere and produce a shower of pions. The pions then decay into muons ($\mu$) and muon-neutrinos ($\nu_\mu$). The muons further decay into

electrons, electron-neutrinos and muon-antineutrinos. Considering the events from both electron-type and muon-type, it is possible to define the ratio 'R' as [34] :

$$R \equiv \frac{(\mu/e)}{(\mu/e)_{MC}} \tag{2.5}$$

where 'MC' denotes the Monte-Carlo predictions. The denominator is the theoretical estimation for $(\mu/e)$ ratio assuming that neutrino interactions are governed by SM and they are massless. If there is no neutrino oscillation, R must be 1. Several experiments were performed to study atmospheric neutrino oscillation and thus this ratio. Among these experiments NUSEX [35, 36], Frejus [37–40], Soudan and Soudan-II [41–44], MACRO [45–47] were calorimeter-like detectors, while Kamiokande [48–54], Super-Kamiokande [55–60], IMB [61–63] were water Cherenkov detectors. All these showed a deviation from calculated value for 'R' and thus confirmed neutrino oscillation in atmosphere. These data indicate that there is either a depletion of muon-neutrinos or an excess of electron-neutrinos due to some non-standard property of neutrinos. Any confusion about the evidence of this atmospheric neutrino anomaly subsided after the Super-Kamiokande experiment measured the atmospheric neutrino flux and they are now considered to be standard results [64]

$$\Delta m^2_{\nu_\mu \nu_\tau} \simeq (1.5 - 3) \times 10^{-3} eV^2 \tag{2.6}$$

$$sin^2 2\theta_{\nu_\mu \nu_\tau} > 0.9 - 1 \tag{2.7}$$

The most appealing solution for the atmospheric neutrino anomaly is to assume that the muon-type neutrinos oscillate into tau-type neutrinos keeping the electron-neutrino flux unaltered. The observed data from Kamiokande as well as Super-Kamiokande experiments support this hypothesis.

- **Solar Neutrinos :** Thermonuclear reactions that take place inside the core of the Sun and produce both photons and neutrinos. A very big step towards experimental neutrino physics was obtained when an experiment lead by Ray Davis at the Homestake mine South Dakota [65], obtained evidence for a solar electron-type neutrino flux. The Homstake experiment was followed by three other experiments. Among these three experiments, the Kamiokande (Japan) was a large water-Cerenkov experiment as already mentioned above and the other two were

GALLEX (Italy) [16] and SAGE (USSR/Russia) [18], both of which were radiochemical experiments. The last two experiments detected neutrinos via inverse $\beta$ - decay of Gallium. These three experiments provided complementary information about solar neutrinos. Kamiokande experiment [66–70] was capable of detecting neutrinos in real time and determine their energy where as the other two experiments have no such capabilities but they have a lower energy detection threshold.

All these experiments detected solar electron-type neutrino fluxes to be much below the values predicted by SM calculations. This was referred to as *'solar neutrino puzzle'*. New light on the solar neutrino puzzle was reflected by the SNO experiment [71] results. The hypothesis that supports the data is that although Sun produces only electron-neutrinos, some of these $\nu_e$'s get converted into other neutrino flavors i.e neutrino oscillation takes place. Clearly, this is not possible if we stick to the SM framework for neutrinos in which they are massless. One must go beyond SM to understand this phenomenon. The best fit data for solar neutrinos are as follows [71]

$$\Delta m^2_{Solar} \simeq 1.2 \times 10^{-5} - 3.1 \times 10^{-4} eV^2 \tag{2.8}$$

$$sin^2 2\theta_{Solar} \simeq 0.58 - 0.95 \tag{2.9}$$

- **LSND experiment** : The LSND (Los Alamos Liquid Scintillation Detector) experiment [72] also confirmed neutrino oscillation. In this experiment neutrino oscillations from a stopped muon as well as from a muon in pion decay have been observed. The mass squared values and mixing parameters that best fit the data with $90\%$ Confidence Level from this experiments are given by [72]

$$\Delta m^2_{LSND} \simeq 0.2 - 10.0 eV^2 \tag{2.10}$$

$$sin^2 2\theta_{LSND} \simeq 0.003 - 0.03 \tag{2.11}$$

We see that, both the mass-squared differences in equation (2. 3) are much smaller than $\Delta m^2_{LSND}$. This is sometimes referred to as LSND anomaly. Furthermore, KARMEN experiment [73] at the Rutherford laboratory strongly constrained the allowed parameter space of LSND data. The MiniBooNE experiment [74, 75] at Fermilab is also probing the LSND parameter range to a further extent. None of the proposed

solutions to explain the LSND anomaly seem completely satisfactory. It is said that, if LSND observations are confirmed by MiniBooNE experiment, then there is a good possibility that a novel physical phenomenon is waiting to be uncovered.

- **K2K experiment** : After the Super-Kamiokande experiment with atmospheric neutrinos was performed, **K2K** experiment [23, 76] was designed to confirm these results. The evidence for neutrino oscillation in Super-Kamiokande was obtained by performing experiments on neutrinos produced high in the upper atmosphere of the earth. In this case, the exact number and energy of the produced neutrinos are uncertain because of the lack of information on the exact energy spectrum and flux of the cosmic rays hitting earth's atmosphere. The K2K (KEK to Super-Kamiokande) experiment is the first long-baseline neutrino oscillation experiment which uses artificially produced and controlled neutrino beam. In this experiment, instead of relying on neutrinos produced in the upper atmosphere, neutrinos are produced in KEK accelerator facility in Japan. Neutrinos produced in such a way, are then detected by the Super-Kamiokande detectors.

- **KamLAND experiment** : The **KamLAND** (Kamioka Liquid-scintillator Anti-Neutrino Detector) experiment [26, 27, 77, 78] in Japan, stands to be the first experiment to find indisputable evidence for neutrino mass using a terrestrial source of anti-neutrinos. KamLAND detects hundreds of anti-neutrinos per year from nuclear reactors located few hundred kilometers away, which is considered as a superb improvement over previous attempts by any other detector. Since 2002, KamLAND has observed anti-neutrino deficit as well as energy spectral distortion, thus confirming neutrino oscillations and non-zero neutrino masses. The KamLAND experiment determined a precise value for the neutrino oscillation parameters $\Delta m^2_{21}$ and $\theta_{12}$ at $3\sigma$ level, given by [78] :

$$\Delta m^2_{21} = 7.59^{+0.21}_{-0.21} \times 10^{-5} eV^2 \tag{2.12}$$

$$tan^2\theta_{12} = 0.47^{+0.06}_{-0.05} \tag{2.13}$$

  This is considered as one of the profound discoveries in neutrino physics.

- **Daya Bay experiment** : The **Daya Bay** experiment [30, 31, 79, 80] is another very important neutrino oscillation experiment with the goal to measure the $\theta_{13}$ mixing angle, using anti-neutrinos produced by the reactors at the Daya Bay Nuclear Power

Plant via the inverse beta decay process. Correct measurement of $\theta_{13}$ angle is very crucial, since its magnitude has implications for CP-violation in the leptonic sector. Previously, the most sensitive limit on the value of $\theta_{13}$ was provided by the **CHOOZ** reactor experiment [28] : $\theta_{13} < 0.17$. The goal of Daya Bay experiment is a measurement of $sin^2\theta_{13}$ upto $0.01$ or better, which is an order of magnitude better sensitivity than the CHOOZ limit. The experimental set-up at Daya Bay uses larger detectors to increase statistics and detectors are placed deeper underground to suppress background to achieve improved precision measurements over previous experiments.

- **SNO+ experiment** : An upadated version of the SNO experiment with solar neutrinos has been designed and named as **SNO+** [81]. The primary goal of SNO+ is a search for the Neutrinoless double $\beta$ decay process ($0\nu\beta\beta$). Additionaly SNO+ aims to measure reactor anti-neutrino oscillations, low-energy solar neutrinos, geo-neutrinos and to search for exotic physics. The SNO+ is kilo-tonne scale liquid scintillator detector, which detects neutrinos when they interact with electrons and nuclei in the detector and produce charged particles, which in turn produce flashes of light while passing through the scintillator.

  Apart from these experiments mentioned above there are various other experiments like, MINOS [82,83], IceCube [84], NO$\nu$A [85,86], RENO [29], Double CHOOZ [28], JUNO [87], Icarus [88], CNGS [89], LBNE [90], T2K [91], CHIPS [92], RENO-50 [93] and so on, which are trying provide more information and bounds regarding the neutrino masses and mixing.

- **Neutrinoless double $\beta$ decay process ($0\nu\beta\beta$) :** The question whether the neutrinos are Dirac or Majorana particles is one of the important experimental questions. The answer to this question will have a profound impact on the theoretical description of neutrinos. For interesting articles on neutrinoless double $\beta$ decay process, please see the incomplete references [94–111]. Also, oscillation experiments described above, only depend on the mass-squared differences of neutrino mass eigenstates and mixing angles. Therefore, to have a compact picture of absolute neutrino mass scale, we need other experiments. Given the current bounds on neutrino masses and mixing, one such experiment, where the lepton number is violated by Majorana neutrino, is neutrinoless double $\beta$ decay process ($0\nu\beta\beta$). For a nucleus with atomic number 'Z', the $0\nu\beta\beta$ process is represented as : $Z \longrightarrow (Z+2) + e^- + e^-$. Clearly this violates

lepton number by 2 units. The amplitude for $0\nu\beta\beta$ process is proportional to [112] :

$$A_{0\nu\beta\beta} \propto \Sigma_i U_{ei}^2 \frac{m_i}{E} \equiv \frac{m_{\beta\beta}}{E} \tag{2.14}$$

where $U_{ei}$ are the elements of PMNS mixing matrix, E is the energy of the process and $m_{\beta\beta}$ (commonly referred to as $m_{ee}$) is the effective neutrino mass for the process. It's important to note that $A_{0\nu\beta\beta}$ is directly proportional to the neutrino mass. This indicates that, value of $m_{ee}$, not only depends on the mass squared differences and mixing angles but also crucially depends on the magnitude of the masses. That's why searches for $0\nu\beta\beta$ process set bounds on the overall scale of neutrino mass. Also, as mentioned above, $0\nu\beta\beta$ signifies lepton number violation and thus indicates the existence of Majorana-type neutrinos. Till now, there is no firm experimental evidence to confirm or overrule this idea. Of course, experimental evidence for $0\nu\beta\beta$ process would establish the Majorana nature of neutrinos and thus would favor theoretical models, such as seesaw mechanisms, which tries to explain the smallness of neutrino mass by assuming neutrinos as Majorana particles. Within the neutrino community it is expected that a sharp peak at the $\beta\beta$ end point would give a quantitative estimation of $0\nu\beta\beta$ decay rate and ultimately provide a measure of effective Majorana mass $m_{\beta\beta}$. Some years ago, a controversial analysis of the Heidelberg-Moscow data [113] announced a positive hint for $0\nu\beta\beta$. Their claim was that $m_{ee}$ lies between $0.2 - 0.6eV$, but the questions on absolute scale of neutrino masses still remain open.

Another important indication on absolute scale of neutrino mass is expected to come from the end point searches of tritium decay [114]. This experiment measures the parameter $m_\nu \equiv \sqrt{\Sigma_i |U_{ei}|^2 m_i^2}$. We see that this experiment uses a different combination of mass and mixing parameters than the $0\nu\beta\beta$ process. The KATRIN experiment [115] has been proposed for a high sensitive search for absolute scale of $m_\nu$. It is expected that KATRIN will be able to reach a sensitivity of $0.3eV$.

## 2.3 Motivations for physics beyond the SM

By now it is confirmed that neutrinos have non-zero but very tiny masses compared all other fundamental fermion masses in the SM. Two striking features regarding the neutrino masses really worth noticing that — (i) neutrino masses are at least six orders of magnitude smaller than the electron (lightest charged fermion) mass and (ii) there is a 'mass-gap' between the electron mass and the largest allowed value of neutrino mass.

Neither we know the reasons for neutrino masses being so small, nor we know why there is such a large gap between mass of neutrino and other charged leptons. In addition to this, there is also the possibility that the massive neutrinos may turn out to be of Majorana-nature, unlike any other particle in SM framework. As already mentioned, determination of the nature of neutrinos i.e Dirac or Majorana-type will have tremendous impact on the understanding of neutrino physics and particle physics in general. This might not only uncover the origin of neutrino masses but will also indicate that conservation of lepton number is not really a sacred principle of nature. We have also discussed in the previous section that the most promising way to unravel this puzzle is to look for neutrinoless double beta decay processes.

At this point, various searches and theoretical models are being proposed to find out actually what kind of augmented, new physics scenarios beyond SM leads to non-zero neutrino masses. There are many possible ways to modify the SM so that small neutrino mass can be accommodated in the framework, with each probable way differing from one another. Many theoretical models are allowed by the existing data that can hope to descibe small neutrino masses. Therefore, the main point is to find out how the correct model for neutrino mass generation can be identified from this jigsaw of models. Perhaps the answer to this question lies with the upcoming neutrino experiments in the next decades.

The non-zero neutrino mass has profound theoretical significance. In the SM framework, masses of all elementary particles are generated when the neutral component of Higgs field accqires a vev via electroweak symmetry breaking. Thus the mass scales of these particles are determined by this vev, $v \simeq 246$ GeV. Non-zero neutrino masses may turn out to be the first signature of a new mass scale, completely unrelated to the to electroweak symmetry breaking scale. Alternatively, this may also indicate that the electroweak symmetry breaking is actually more complex than dictated by SM.

Apart from this, the pattern of neutrino mixing is also puzzling. A glance at the absolute values of the entries of quark mixing matrix i.e CKM matrix shows that the quark mixing matrix is almost proportional to the identity matrix and the small values of off-diagonal elements there follows a hierarchial pattern. But the entries of lepton mixing matrix i.e PMNS matrix are given by [33]

$$|U| \simeq \begin{pmatrix} 0.8 & 0.5 & 0.2 \\ 0.4 & 0.6 & 0.7 \\ 0.4 & 0.6 & 0.7 \end{pmatrix} \tag{2.15}$$

This shows that the PMNS matrix is far from diagonal and follows no hierarchial pattern. Several proposals have been put forward and researches are going on to understand the possible relationship, if any, between the quark and lepton mixing matrix and to find out the ordering principle, if any, responsible for the observed pattern of neutrino masses and lepton mixing. As already pointed out in the previous section, several experiments that involve precision neutrino oscillation measurements, are being proposed and carried out to address this flavor puzzle. Improved understanding of neutrino interactions – beyond the current paradigm is very much needed. Experimental set-ups on neutrino scattering are expected to be extremely helpful in this regard.

So, from the the experimental observations and facts described in the above paragraphs it must be realized that, we need to seek beyond the paradigm of SM, both theoretically and experimentally, to be able to find out solutions to the neutrino riddle. With this motivation, we present a reference to some of the neutrino mass generation schemes existing in the literature.

## 2.4 Models of neutrino mass generation

There exists numerous models that descibe neutrino mass generation consistent with the existing data. It goes beyond the scope of this dissertation to describe them all. Therefore, we discuss only some of these models briefly here :

- **Adding a right-handed neutrino to SM** : The simplest possible extension of SM which generates non-zero neutrino mass is one where a right-handed neutrino is added to the SM [116]. In this case both the left-handed ($\nu_L$) and right-handed ($\nu_R$) components are present in the scenario and they can form a mass term. This mass is similar to the mass terms of other charged leptons and quarks and the mass scale is therefore governed by the electroweak symmetry breaking scale. The neutrino mass term in this case is given by : $m_\nu = \frac{Y_\nu v}{\sqrt{2}}$, where $Y_\nu$ is the corresponding yukawa coupling. So, we see that to obtain sub-eV range neutrino mass, $Y_\nu$ has to be $\simeq 10^{-12}$ or less. But, the occurance of such a tiny coupling constant in the theory is very unnatural and a robust theory must give an explanation behind such smallness.

- **The seesaw mechanisms :** The basic principle behind the seesaw mechanism is that some extra fermionic or scalar fields are added to the SM. These extra fields are assumed to have relatively large mass scale compared to the electroweak scale. In some models the new physics scale is considered to be of the order of $10^{12}$ GeV

or greater. These BSM fields with relatively higher mass scale in turn generates small Majorana neutrino masses through the new Yukawa couplings with SM lepton fields.

There are three varieties of seesaw mechanism that are commonly used to generate small neutrino masses and they are called Type I, Type II and Type III seesaw mechanism [118–120]. In the case of Type I seesaw, one can add at least two fermionic singlets $N_i$ (right-handed neutrinos) and the neutrino masses read as: $m_\nu^I \simeq \frac{h_\nu^2 v^2}{M_N}$. Where $h_\nu$ is Dirac Yukawa coupling, $v \simeq 246$ GeV, the SM Higgs vev and $M_N$ is the right-handed neutrino mass. Small neutrino masses can be generated by properly adjusting the parameters $h_\nu$ and $M_N$. Type II seesaw is the case, where the scalar sector of the SM is extended by adding at least one $SU(2)_L$ Higgs triplet $\Delta$ with hypercharge 2. In this scenario neutrino masses are obtained as: $m_\nu^{II} \simeq Y_\nu v_\Delta$, with $v_\Delta$ as the vev of the neutral component of the triplet and $Y_\nu$ is yukawa coupling constant. The triplet vev and the Yukawa coupling can be adjusted to give the neutrino mass $\simeq$ sub-eV. But we have to keep in mind while choosing the value for triplet vev, that it has to satisfy the $\rho$ - parameter constraint presented in Chapter 1 of this dissertation. In Type III seesaw mechanism, by adding at least two extra matter fields (which are normally taken as fermionic triplets) with zero hypercharge, small neutrino masses can be generated as : $m_\nu^{III} \simeq \frac{\Gamma_\nu^2 v^2}{M_\Sigma}$, where $\Gamma_\nu$ is Dirac Yukawa coupling, v, the SM Higgs vev, $M_\Sigma$ is mass of the fermionic triplets. A detailed discussion on seesaw mechanism is presented in the next chapter.

- **Inverse seesaw mechanism :** Another realization of seesaw mechanism is the so-called 'Inverse Seesaw mechanism (ISS)' [122]. In this case, small neutrino masses arise as a result of new physics at the TeV scale, which may be probed at the collider experiments like the LHC. In the ISS framework, three right-handed neutrinos ($N_{iR}$) and three extra singlet neutral fermions($S_{iL}$) are added to the SM. In addition to these singlet fields, three left-handed neutrinos ($\nu_{iL}$) already exist in the SM. So, there are altogether six singlet fields in the framework now and ISS can be realized through the Lagrangian [123] :

$$\mathcal{L}_{ISS} = -Y_\nu^{ij} \bar{L}_i \tilde{\Phi} N_{Rj} - \bar{S}_{Lj} M_R^{ij} N_{Ri} - \frac{1}{2} \mu_S^{ij} (\bar{S}_{Li})^c S_{Lj} + h.c \tag{2.16}$$

This Lagrangian can be re-written as :

$$\mathcal{L}_{ISS} = -\bar{\nu}_{iL} m_D^{ij} N_{Rj} - \bar{S}_{Lj} M_R^{ij} N_{Ri} - \frac{1}{2} \mu_S^{ij} (\bar{S}_{Li})^c S_{Lj} + h.c \tag{2.17}$$

Where $L$ is the left-handed lepton doublet, $\Phi$ is SM Higgs doublet, $\tilde{\Phi} = i\sigma_2\Phi^*$ with $\sigma_2$ being the corresponding Pauli matrix, $Y_\nu$ is the $3 \times 3$ neutrino Yukawa coupling matrix, $M_R$ is a lepton number conserving complex $3 \times 3$ mass matrix, $m_D$ is a $3 \times 3$ Dirac mass matrix given by $m_D = Y_\nu v$ with Higgs vev $v = 246$ GeV and $\mu_S$ is a complex $3 \times 3$ symmetric Majorana mass matrix, that violates lepton number conservation by two units. Setting $\mu_S$ to zero, would restore the conservation of lepton number and thus would increase the symmetry of the model.

After electroweak symmetry breaking, in the basis $(\nu_L, S_L, N_L^c)$, the $9 \times 9$ neutrino matrix is obtained as

$$\mathcal{M}_\nu = \begin{pmatrix} 0 & m_D^T & 0 \\ m_D & 0 & M_R^T \\ 0 & M_R & \mu_S \end{pmatrix} \tag{2.18}$$

This mass matrix is symmetric and complex, so it can be diagonalized by a $9 \times 9$ unitary matrix $U_\nu$ in the following way

$$U_\nu^T \mathcal{M}_\nu U_\nu = Diag(m_1, m_2, ...m_9) \tag{2.19}$$

This produces three light and six heavy mass eigenstates. In the limit, $\mu_S \ll m_D \ll M_R$, the mass matrix $\mathcal{M}_\nu$ can be diagonalized in blocks and produces the $3 \times 3$ light neutrino mass matrix as

$$\mathcal{M}_{light} \simeq m_D^T (M_R^T)^{-1} \mu_S M_R^{-1} m_D \tag{2.20}$$

This matrix is then diagonalized using the PMNS matrix to generate masses for three light neutrinos as

$$U_{PMNS}^T \mathcal{M}_{light} U_{PMNS} = Diag(m_{\nu_1}, m_{\nu_2}, m_{\nu_3}) \tag{2.21}$$

Here $m_{\nu_1}, m_{\nu_2}, m_{\nu_3}$ are masses of three light neutrinos. The standard neutrinos with mass at sub-eV scale can be obtained for $m_D$ at electroweak scale, $M_R$ at TeV scale and $\mu_S$ at the keV scale.

- **Radiative corrections :** Lastly, in some models involving higher dimensional operators, small neutrino mass is generated via radiative corrections of new coupling constants at loop level. For a deeper understanding on these models, please see the incomplete references [124–129].

As mentioned above, apart from these techniques there exist a number of theoretical models in literature that describe tiny neutrino masses consistent with present data. In the next section, we turn to describe in brief the textures for neutrino masses that fit experimental data very well and make an attempt to predict the pattern of neutrino masses.

## 2.5 Texture zeros of neutrino mass matrices

We have seen that the structure of neutrino mass matrices is very important for future study of the underlying symmetries and resulting dynamics. From mixing matrix i.e PMNS matrix $U$ and the mass eigenvalues, it is possible to write down the allowed neutrino mass matrix for any arbitrary mass pattern assuming that the neutrinos are of Majorana nature. One such way, inspired by the studies of quark mixing matrices, is to consider mass matrices with zeros in it and at the same time, search for appropriate symmetries that will establish the viability of zero entries. The usefulness of such an approach is that, because of the presence of fewer parameters in the mass matrices it may be possible to obtain relations between different observables such as masses and mixing angles, that have higher predictiveness and can be tested in experiments. Such family of neutrino mass matrix textures, with independent zero entries in it, are referred to as *'zero textures'*.

The simplest symmetries that can be imposed in the context of texture zeros, are considered to be Abelian in nature. Given a mass matrix with texture zeros, it is almost always possible to find an extended scalar sector and suitable Abelian symmetries, such that the texture zeros originate as a result of symmetry requirements on the SM fields and extended sector fields. In that sense, texture zeros always can be associated with Abelian symmetries. The most simple scenario in this case takes place when the charged lepton matrix is diagonal, signifying six texture zeros in it. At the same time, by assuming that neutrinos are Majorana fermions, some texture zeros can be placed in the symmetric Majorana mass matrices of neutrinos. For an extensive review of 'texture-zeros', please see [130–132] and references therein.

The most popular among these texture zero approaches is the idea of *'two-zero-textures'* i.e the case where the symmetric Majorana neutrino mass matrices have two independent zero entries. This situation was first studied by Frampton, Glashow and Marfatia in 2002 [133]. Out of fifteen possible two-zero-textures, only seven are found to be consistent

with the bounds imposed by neutrino experimental data. They are listed below :

$$Case\ A_1 : M_\nu \sim \begin{pmatrix} 0 & 0 & \times \\ 0 & \times & \times \\ \times & \times & \times \end{pmatrix} \quad , \quad Case\ A_2 : M_\nu \sim \begin{pmatrix} 0 & \times & 0 \\ \times & \times & \times \\ 0 & \times & \times \end{pmatrix} \tag{2.22}$$

$$Case\ B_1 : M_\nu \sim \begin{pmatrix} \times & \times & 0 \\ \times & 0 & \times \\ 0 & \times & \times \end{pmatrix} \quad , \quad Case\ B_2 : M_\nu \sim \begin{pmatrix} \times & 0 & \times \\ 0 & \times & \times \\ \times & \times & 0 \end{pmatrix} \tag{2.23}$$

$$Case\ B_3 : M_\nu \sim \begin{pmatrix} \times & 0 & \times \\ 0 & 0 & \times \\ \times & \times & \times \end{pmatrix} \quad , \quad Case\ B_4 : M_\nu \sim \begin{pmatrix} \times & \times & 0 \\ \times & \times & \times \\ 0 & \times & 0 \end{pmatrix} \tag{2.24}$$

$$Case\ C : M_\nu \sim \begin{pmatrix} \times & \times & \times \\ \times & 0 & \times \\ \times & \times & 0 \end{pmatrix} \tag{2.25}$$

It can be easily seen that the seven allowed two-zero textures can be divided into three classes, with each class having their own typical implications on neutrino data [133]. For example, textures within class A have, $M_{ee} = 0$, which implies that neutrinoless double beta decay ($0\nu\beta\beta$) is forbidden at least at tree-level for textures of this class. Class C (which is a single - element class) alone allows both the $\mu\mu$ and $\tau\tau$ elements to be zero at the same time.

Class A textures also imply that the angle $\theta_{12}$ can turn out to be relatively large. On the contrary, textures of class B allow the $0\nu\beta\beta$ process. According to class C, the $0\nu\beta\beta$ decay is likely to be observable and the angle $\theta_{12}$ must be large enough to permit a search for CP-violation. Various efforts have been made to give reasonable structures of neutrino mass matrices by reconciling two-zero textures and experimental neutrino data. Among the viable cases classified by Frampton *et. al.*, only $A_1$ and $A_2$ predict $\theta_{13}$ to be different from zero at $3\sigma$. At the best fit value $A_1$ and $A_2$ predict, $0.024 \geq sin^2\theta_{13} \geq 0.012$ and $0.014 \leq sin^2\theta_{13} \leq 0.032$ respectively. The cases $B_1, B_2, B_3$ and $B_4$ predict nearly maximal CP-violation i.e $cos\delta \approx 0$. This is an important result predicted by two-zero texture of Majorana neutrino mass matrix in the light of MINOS, T2K and K2K experimental results, which gave hints for a large $\theta_{13}$ value [134]. Fritzsch *et. al.* [135] discusses an interesting observation that given the values of three flavor mixing angles $(\theta_{12}, \theta_{23}, \theta_{13})$ and two neutrino mass-squared differences $(\Delta m^2_{12}, \Delta m^2_{23})$, it is in principle possible to fully determine three CP-violating phases $(\delta, \zeta, \xi)$ and three neutrino masses. Recently, Meloni

*et. al.* [136] analyzed some of the two zero textures of neutrino masses in the light of the Planck data, that put a quite stringent upper bound on the sum of the active neutrino masses : $\Sigma \equiv \Sigma_i m_{\nu_i} < 0.23$ eV with $95\%$ CL. They have shown that, texture $C$ is not compatible with the normal ordering of the neutrino mass eigenstates. The process of analyzing predictions from two-zero textures of neutrino mass matrices and examining them in the light of ever increasing experimental data is still going on. For some more interesting articles on 'two-zero textures' and 'zero-textures' in general, please see the incomplete reference [137–143]. It can be said without hesitation that two-zero textures and texture zero approach in general, serve as a guideline to provide a viable model of neutrino mass structure.

# Chapter 3

# Seesaw mechanism

## 3.1 Introduction to seesaw

We have already mentioned seesaw mechanism briefly in the previous chapter. Here we present a more elaborate discussion of the seesaw feameworks, which generate Majorana masses for neutrinos. Such a mass term is generally of the form

$$\mathcal{L}_m = \frac{1}{2} m_L \bar{\nu_L} (\nu_L)^c \tag{3.1}$$

where $\nu_L$ is a left-handed neutrino field and $(\nu_L)^c = C\bar{\nu_L}^T, C = i\gamma^2\gamma^0$ being the charge conjugation operator. Such Majorana masses are possible since both the neutrino and the anti-neutrino have zero electric charge. Majorana masses for neutrinos are then not forbidden by electric charge conservation. However, such masses for neutrinos violates lepton number conservation by two units. Also, $\nu_L$ possesses non-zero isospin and hypercharge. So in the SM framework, assuming only Higgs doublets, such Majorana mass terms for left-handed neutrinos are forbidden by gauge invariance. The idea of the seesaw mechanism is to generate such terms effectively, after heavy external fields are integrated out. Ultra-small neutrino maases then can be justified in terms of 'big' mass parameters of these heavy fields.

There are three different realizations of seesaw mechanism. They are all based upon the fact that, according to group theory, two doublets can be decomposed into a triplet and a singlet ($2 \otimes 2 \equiv 3 \oplus 1$) combination. Thus the left-handed lepton doublet and the Higgs doublet of SM can couple either to a triplet or a singlet field. The three seesaw mechanisms outlined here bring such 'big' mass parameters from three different sectors, each of them going beyond the SM in its own way.

## 3.2 Type I seesaw : Fermion singlets

To understand the principle of type I seesaw mechanism [118], let's start with the neutrino mass matrix once more. We assume that right-handed neutrinos ($\nu_R$) are present in the scenario in addition to the usual left-handed neutrinos ($\nu_L$) of the SM. Therefore, it is now possible to construct a Dirac mass term for the neutrinos as follows

$$\mathcal{L}_{Mass}^{Dirac} = m_D \bar{\nu}_R \nu_L + h.c \tag{3.2a}$$

$$= \frac{1}{2}(m_D \bar{\nu}_R \nu_L + m_D (\bar{\nu}_L)^c (\nu_R)^c) + h.c\,. \tag{3.2b}$$

In general Majorana type mass terms are also possible for neutrinos, since they have zero electric charge. The Majorana mass term for left and right-handed neutrinos are written as

$$\mathcal{L}_{Mass}^{L} = \frac{1}{2} m_L (\bar{\nu}_L)^c \nu_L + h.c \tag{3.3a}$$

$$\mathcal{L}_{Mass}^{R} = \frac{1}{2} m_R (\bar{\nu}_R)^c \nu_R + h.c \tag{3.4a}$$

where 'L' and 'R' stands for left and right-handedness respectively. Let us define a vector field $n_L$ such that

$$n_L = \begin{pmatrix} \nu_L \\ (\nu_R)^c \end{pmatrix},\ (\bar{n}_L)^c = ((\bar{\nu}_L)^c \bar{\nu}_R) \tag{3.5}$$

where $(n_L)^c$ is the charge conjugate field of $n_L$. Then the total mass lagrangian for neutrinos can be written as

$$\mathcal{L}_{Mass}^{total} = \mathcal{L}_{Mass}^{Dirac} + \mathcal{L}_{Mass}^{L} + \mathcal{L}_{Mass}^{R} \tag{3.6}$$

$$= \frac{1}{2}(\bar{n}_L)^c M n_L \tag{3.7}$$

The mass matrix $M$, whose diagonalisation gives the physical neutrino masses is given by

$$M = \begin{pmatrix} m_L & m_D \\ m_D^T & m_R \end{pmatrix} \tag{3.5}$$

The positive mass eigenstates of this matrix are

$$m_{1,2} = \frac{1}{2}(m_L + m_R \pm \sqrt{(m_L - m_R)^2 + 4m_D^2}) \tag{3.6}$$

In the seesaw scenario the added right-handed neutrinos are assumed to have higher mass well above the electroweak symmetry breaking (EWSB) scale, while the Dirac mass $m_D$ (like other charged fermions) is considered to be of the order of EWSB scale. Therefore, in this scenario, $m_R \gg m_D$. On diagonalisation of $M$, the eigenvalues corresponding to the neutrino mass eigenstates are obtained as

$$m_1 \simeq \frac{m_D^2}{m_R} \tag{3.7}$$

$$m_2 \simeq m_R \tag{3.8}$$

It is clear from these equations that, now we have a right-handed neutrino with mass scale $\Lambda_N = m_R$, which also may be the scale of some new physics and at the same time a very light neutrino, with mass suppressed by $\frac{m_D}{\Lambda_N}$. This new mass scale is often taken to be close to the grand unification scale to explain the proposed sub-eV masses of the three left-handed neutrinos. In fact, heavier the new right-handed neutrino, the lighter is the left-handed neutrino. This is the underlying basic principle of seesaw mechanism.

Formally, in type I seesaw, right-handed heavy $SU(2)$ singlet fermion fields ($N_R$) with zero hypercharge are added to the SM fields to produce non-zero neutrino masses. The left-handed lepton doublets then couple to the Higgs field and the newly introduced right-handed fermion fields to produce the Majorana mass terms for the neutrinos. The extra piece of lagrangian for this new heavy right-handed fields is given by [121]

$$\mathcal{L}^{New} = i\bar{N}_R \partial\!\!\!/ N_R - [\frac{1}{2}\bar{N}_R M_N N_R^c + \bar{l}_L \tilde{\Phi} Y_N^\dagger N_R + h.c] \tag{3.9}$$

where the first two terms represent the kinetic term and Majorana mass term for the right-handed fermion fields and the third one is the Yukawa interaction term. $l_L$ and $\Phi$ are the left-handed lepton doublet and Higgs field respectively. The vev of Higgs field is denoted by 'v'.

The left-handed neutrino mass term can be estimated from the above lagrangian. The lagrangian can be solved to get the equation of motion. Expansion of the propagator gives a factor $\frac{i}{\not{p} - M_N}$, which for low momenta $p$ can be approximated by $\frac{(-i)}{M_N}$, with $M_N$ as the mass of heavy right-handed fermion fields. Then integrating out the heavy fields using the equation of motion, namely,

$$\frac{\partial \mathcal{L}^{New}}{\partial N_R} = 0 \tag{3.10}$$

one obtains the effective dimension 5 operator [121]

$$\delta L^{d=5} = \frac{1}{2} c^{d=5}_{\alpha\beta} (\bar{l^c}_{L\alpha} \tilde{\Phi}^*)(\tilde{\Phi}^\dagger l_{L\beta}) + h.c \tag{3.11}$$

The coefficient $c^{d=5}$ is given by [121]

$$c^{d=5} = Y_N^T \frac{1}{M_N} Y_N \tag{3.12}$$

After electroweak symmetry breaking, the neutrino mass is obtained by inserting the Higgs vev 'v' and is expressed as [121]

$$m_\nu = \frac{v^2}{2} c^{d=5} = Y_N^T \frac{v^2}{2M_N} Y_N \tag{3.13}$$

From this relation, light Majorana neutrino mass can be generated by properly adjusting the value of the parameters $Y_N$ and $M_N$.

## 3.3 Type II seesaw : Scalar triplets

In this case [119] the scalar sector of the SM is extended by adding at least one $SU(2)$ scalar triplet $\Delta(\Delta_1, \Delta_2, \Delta_3)$ with hypercharge 2. The electromagnetic charged states for the triplet can be obtained from the couplings to the leptons

$$\begin{aligned} \bar{\tilde{l_L}}(\tau \cdot \Delta) l_L &= (-(\bar{e_L})^c (\bar{\nu_L})^c) \begin{pmatrix} \Delta_3 & \Delta_1 - i\Delta_2 \\ \Delta_1 + i\Delta_2 & -\Delta_3 \end{pmatrix} \begin{pmatrix} \nu_L \\ e_L \end{pmatrix} \\ &= -(\bar{e_L})^c \Delta_3 \nu_L - (\bar{e_L})^c (\Delta_1 - i\Delta_2) e_L + (\bar{\nu_L})^c (\Delta_1 + i\Delta_2) \nu_L - (\bar{\nu_L})^c \Delta_3 e_L \end{aligned} \tag{3.14}$$

Since $e_L$ and $(\bar{e_L})^c$ have charge -1 and $\nu_L, (\bar{\nu_L})^c$ have no charge, the charged states of the triplet are given by [121]

$$\Delta^{++} \equiv \frac{1}{\sqrt{2}}(\Delta_1 - i\Delta_2),\ \Delta^+ \equiv \Delta_3,\ \Delta^0 \equiv \frac{1}{\sqrt{2}}(\Delta_1 + i\Delta_2) \tag{3.15}$$

The Yukawa interaction term of the new triplet, which violates lepton number by two units, is represented as

$$\mathcal{L}_{yuk} = Y_\Delta \bar{\tilde{l_L}} (\tau \cdot \Delta) l_L \tag{3.16}$$

where $\bar{\tilde{l_L}} = (-(\bar{e_L})^c (\bar{\nu_L})^c)$, $\tau$'s are the Pauli matrices and $Y_\Delta$ is the Yukawa coupling matrix. The rest of the part of the lagrangian of the triplet field containing the scalar potential

terms is given by [121] ,

$$\begin{aligned}\mathcal{L}_\Delta = M_\Delta^2 \Delta^\dagger\Delta + \frac{1}{2}\lambda_2(\Delta^\dagger\Delta)^2 + \lambda_3(\Phi^\dagger\Phi)(\Delta^\dagger\Delta) + \\ \frac{1}{2}\lambda_4(\Delta^\dagger T^i\Delta)^2 + \lambda_5(\Delta^\dagger T^i\Delta)(\Phi^\dagger\tau^i\Phi) + \\ (\mu_\Delta\tilde{\Phi}^\dagger(\tau\cdot\Delta)^\dagger\Phi + h.c)\end{aligned} \tag{3.17}$$

Here, $T^i$'s are the generators of the triplet representation of $SU(2)$

$$T_1 = \begin{pmatrix}0 & 0 & 0\\ 0 & 0 & -i\\ 0 & i & 0\end{pmatrix}. T_2 = \begin{pmatrix}0 & 0 & i\\ 0 & 0 & 0\\ -i & 0 & 0\end{pmatrix}, T_3 = \begin{pmatrix}0 & -i & 0\\ i & 0 & 0\\ 0 & 0 & 0\end{pmatrix} \tag{3.18}$$

In principle, one can start with gauge invariant as well as lepton number conserving triplet Yukawa interactions by assigning lepton number $L = -2$ to the scalar triplet. $L$ could then be broken spontaneously once $\Delta^0$ acquires a vev [144]. However, that would have led to a massless $SU(2)$ triplet Goldstone boson with unsuppressed coupling with the $Z$ boson. The consequence is a much larger contribution to the invisible decay width of the $Z$ than is permitted by the LEP data. Therefore, explicit $L$-violation is phenomenologically preferable in this scheme. A way to generate the triplet vev is through the trilinear interaction term in the scalar potential. In this case, minimization of the scalar potential produces a vev ($v_\Delta$) for the neutral component of the triplet $\Delta^0$, when the Higgs doublet $\Phi$ acquires a vev and is given by [116]

$$v_\Delta \equiv \frac{\mu_\Delta v^2}{M_\Delta^2} \tag{3.19}$$

It can be seen that, triplet vev can be made small by choosing a large value for the mass of the triplet field or by choosing the coefficient of the trilinear term to be vary small. Keeping a small value for the triplet vev ($v_\Delta$) is crucial in this model since it is directly related to neutrino masses through the Yukawa coupling term. Another important reason to keep the triplet vev small is to respect the $\rho$-parameter constraint, which restricts [145]

$$\rho = 1.0008^{+0.0017}_{-0.0007} \tag{3.20}$$

Since the neutral component of triplet $\Delta^0$ couples to the $W$ and $Z$-bosons, its vev contributes to their masses. Instead of the SM relations, we now have [34]

$$M_W^2 = \frac{1}{4}g_2^2(v^2 + 2v_\Delta^2) \tag{3.21}$$

$$M_Z^2 = \frac{1}{4}(g_1^2 + g_2^2)(v^2 + 4v_\Delta^2) \tag{3.22}$$

so that, expression for $\rho$-parameter now reads as [34],

$$\rho \equiv \frac{M_W^2}{M_Z^2 cos^2\theta_W} = \frac{1 + 2v_\Delta^2/v^2}{1 + 4v_\Delta^2/v^2} \tag{3.23}$$

Then using the constraint on $\rho$-parameter, we obtain an upper bound for the allowed value of $v_\Delta$ as [34],

$$\frac{v_\Delta}{v} < 0.07 \tag{3.24}$$

Majorana masses of neutrinos are generated when the neutral component of the triplet $\Delta^0$ acquires vev and the relation between the neutrino mass, Yukawa coupling and triplet vev is expressed as :

$$M_\nu^{ij} = v_\Delta Y_\Delta^{ij} \tag{3.25}$$

Here the coupling $Y_\Delta^{ij}$ decide the pattern of neutrino mixing, in analogy to the right-handed neutrino mass matrix in type I seesaw. The distinctive feature of type II seesaw lies in a different vev being responsible for neutrino masses, as compared to the other fermion masses. Thus the essence of this scenario is $v_\Delta \ll v$, thanks to the character of the scalar potential.

## 3.4 Type III seesaw : Fermion triplets

Type III sesaw [120] is very much similar to the type I seesaw mechanism. In the type III seesaw framework at least two heavy $SU(2)$ right-handed fermion triplets are added instead of fermion singlet fields. This is because at least two non-vanishing neutrino masses have to be generated in order to explain the oscillation data. The fermion triplet fields $\Sigma$ ($\Sigma_1, \Sigma_2, \Sigma_3$) have zero hypercharge. The Majorana mass term as well as the dynamics of the fields is governed by the lagrangian [121]

$$\mathcal{L}_\Sigma = i\bar{\Sigma_R}\not{D}\Sigma_R - [\frac{1}{2}\bar{\Sigma_R}M_\Sigma\Sigma_R^c + \bar{\Sigma_R}Y_\Sigma(\tilde{\Phi}^\dagger\tau l_L) + h.c] \tag{3.26}$$

The covariant derivative of the above equation is given by

$$D_\mu = \partial_\mu - ig_1\frac{Y}{2}B_\mu - ig_2\frac{T^a}{2}W_\mu^a, \tag{3.27}$$

Where, $T^a$'s are the $3 \times 3$ generators of $SU(2)$ introduced in the previous section. $Y_\Sigma$ is the Yukawa coupling and $l_L, \Phi$ are the SM lepton and Higgs doublets. The relation between the $SU(2)$ components of $\Sigma$ and the electric charge eigenstates are as follows [121]

$$\Sigma^{\pm} \equiv \frac{\Sigma_1 \mp i\Sigma_2}{\sqrt{2}},\ \Sigma^0 \equiv \Sigma_3 \tag{3.28}$$

In the case of type III seesaw also, the Lagrangian can be solved to get equation of motion for the fields. Following the same procedure as in the case of type I seesaw mechanism, after expanding the propagator and integrating out the heavy fields, the effective five dimensional operator is obtained as [121]

$$\delta\mathcal{L}^{d=5} = \frac{1}{2} c^{d=5}_{\alpha\beta} (\bar{l^{c}_{L\alpha}} \tau \Phi)(\tilde{\Phi}^{\dagger} \tau l_{L\beta}) + h.c \tag{3.29}$$

where the coefficient is [121]

$$c^{d=5} = Y_\Sigma^T \frac{1}{M_\Sigma} Y_\Sigma \tag{3.30}$$

Majorana neutrino masses are obtained when the Higgs field acquires a vev and is given by [121]

$$m_\nu = \frac{v^2}{2} Y_\Sigma^T \frac{1}{M_\Sigma} Y_\Sigma \tag{3.31}$$

It has been already pointed out that type III seesaw is very much similar to type I seesaw mechanism. We comment on some general features of these two models for neutrino mass generation. In both the cases, the effect of heavy new degrees of freedom (singlet and triplet fields in the case of type I and type III respectively) in low energy phenomena can be manifested by adding higher-dimensional operators to the SM. It is well known that, given the SM gauge symmetries and particle content, only one type of dimension-five operator is allowed and its generic form is given by [117]

$$\frac{1}{\Lambda}(L\Phi)(L\Phi) + h.c \equiv \frac{v^2}{\Lambda}\nu\nu + h.c \tag{3.32}$$

All other operators that can be constructed are of dimension six or higher. In the above relation $L$ and $\Phi$ are SM lepton and Higgs doublets respectively, 'v' is vev of the neutral component of Higgs and reflects the fact that neutrino mass is generated through this operator after electroweak symmetry is broken. The most interesting general feature of the seesaw models is the existence of a new physics scale $\Lambda$, which can be identified with the mass scale of heavy fermion triplet(singlet) $M_\Sigma$ ($M_N$) of type III (type I) seesaw mechanism. For $\Lambda \sim 10^{15}$ GeV or GUT scale, it is possible to obtain sub-eV range masses

for light neutrinos in agreement with the current experimental data. Such a high value of this new mass scale certainly motivates a possibility that the higher dimensional operator is indeed generated by some new physics beyond SM.

Of all the three seesaw scenarios described above, the works presented in this thesis are based on type II and type III seesaw framework.

## 3.5 Two-zero texture and the inadequacy of a single triplet

In the previous chapter we have seen that strong evidence has been accumulated in favour of neutrino oscillation from the solar, atmospheric, reactor and accelerator neutrino experiments over the last few years. A lot, however, is yet to be known, including the mass generation mechanism and the absolute values of the masses, in addition to mass-squared differences which affect oscillation rates. Also, a lot of effort is on to ascertain the nature of neutrino mass hierarchy, including the signs of the mass-squared differences. We have also pointed out that a gateway to information of the above kinds is the light neutrino mass matrix, in a basis where the charged lepton mass matrix is diagonal. In this context we have discussed a possibility that frequently enters into such investigations is one where the mass matrix has some zero entries, perhaps as the consequence of some built-in symmetry of lepton flavours. At the same time such 'zero textures' lead to a higher degree of predictiveness and inter-relation between mass eigenvalues and mixing angles by virtue of having fewer free paramaters. We have also pointed out that two-zero textures have a rather wide acceptability. It has been hinted in [146] that none of the seven possible two-zero-texture cases can be achieved by assuming only one scalar triplet. We write the allowed seven two-zero textures for the $3 \times 3$ symmetric Majorana mass matrix of the light neutrinos, denoted by $M_\nu$ once more for the sake of completeness :

$$Case\ A_1 : M_\nu \sim \begin{pmatrix} 0 & 0 & \times \\ 0 & \times & \times \\ \times & \times & \times \end{pmatrix} \quad , \quad Case\ A_2 : M_\nu \sim \begin{pmatrix} 0 & \times & 0 \\ \times & \times & \times \\ 0 & \times & \times \end{pmatrix} \tag{3.33}$$

$$Case\ B_1 : M_\nu \sim \begin{pmatrix} \times & \times & 0 \\ \times & 0 & \times \\ 0 & \times & \times \end{pmatrix} \quad , \quad Case\ B_2 : M_\nu \sim \begin{pmatrix} \times & 0 & \times \\ 0 & \times & \times \\ \times & \times & 0 \end{pmatrix} \tag{3.34}$$

$$Case\ B_3 : M_\nu \sim \begin{pmatrix} \times & 0 & \times \\ 0 & 0 & \times \\ \times & \times & \times \end{pmatrix} \quad , \quad Case\ B_4 : M_\nu \sim \begin{pmatrix} \times & \times & 0 \\ \times & \times & \times \\ 0 & \times & 0 \end{pmatrix} \tag{3.35}$$

$$Case\ C : M_\nu \sim \begin{pmatrix} \times & \times & \times \\ \times & 0 & \times \\ \times & \times & 0 \end{pmatrix} \tag{3.36}$$

These textures are defined in a basis where the charged lepton mass matrix is diagonal. In the context of Type-II seesaw the Yukawa couplings of scalar triplets $\Delta_k$ are given by [147] :

$$\mathcal{L}_Y = \frac{1}{2} \sum_{k=1}^{2} y_{ij}^{(k)} L_i^T C^{-1} i\tau_2 \Delta_k L_j + \text{h.c.}, \tag{3.37}$$

where $i, j = e, \mu, \tau$ , $C$ is the charge conjugation matrix, the $y_{ij}^{(k)}$ are the symmetric Yukawa coupling matrices of the triplets $\Delta_k$. From the above Lagrangian, the neutrino mass matrix is obtained as [147]

$$\mathcal{M}_{ij}^{\nu} = w_k y_{ij}^{k} \tag{3.38}$$

with $w_k$ s being the vev of the triplets. Among the neutrino mass terms, some are allowed, while others are not, as the consequence of a particular texture. This fact can be associated with a conserved global $U(1)$ symmetry, under which all fields have some charge. Under this symmetry, the lepton doublets $L_i$ and the scalar triplet $\Delta_k$ transform as [147]

$$L_i \longrightarrow p_i L_i \quad \text{and} \quad \Delta_k \longrightarrow p_0 \Delta_k \tag{3.39}$$

with phase factors $|p_i|, |p_0|$ = 1. An examination of each of the allowed textures reveals that the three phase factors for different lepton flavors i.e, $p_e, p_\mu, p_\tau$ have to be different from each other. The Higgs doublet transforms trivially under the horizontal symmetry, thus enabling the charged-lepton mass matrix to be diagonal. Now, let us look at the consequence of such a symmetry when just one triplet is present. We shall see that this assuption leads us to a contradiction.

In all the seven possible two-texture-zero cases, the $\mu\tau$ element of $\mathcal{M}_\nu$ is non-zero. Thus, the corresponding Yukawa coupling element $y_{\mu\tau}$ must be non-zero, and the resulting interaction term must conserve the $U(1)$ charge. This implies [147]

$$p_0 p_\mu p_\tau = 1 \tag{3.40}$$

We first examine the Cases $B_1, B_2, B_3, B_4$ and $C$. For these five cases, $y_{ee} \neq 0$. Therefore, upon applying the symmetry operation we have,

$$p_0 p_e^2 = 1 \tag{3.41}$$

The inequality of the $U(1)$ charges for the different neutrino flavour eigenstates then results in $y_{e\mu}$ picking up a phase factor [147] :

$$p_0 p_e p_\mu = \frac{p_\mu}{p_e} \neq 1 \tag{3.42}$$

This leads to the conclusion

$$y_{e\mu} = 0. \tag{3.43}$$

Proceeding in the same way with the $e\tau$ element of Yukawa coupling, we obtain

$$p_0 p_e p_\tau = \frac{p_\tau}{p_e} \neq 1 \tag{3.44}$$

which again implies

$$y_{e\tau} = 0 \tag{3.45}$$

On the other hand, it is seen that in none of the cases $B_1, B_2, B_3, B_4$ and $C$ , the Yukawa couplings $y_{e\mu}$ and $y_{e\tau}$ are both zero. Thus none of these five textures is viable when only one triplet is present in the scenario.

We next address the two remaining cases, namely $A_1$ and $A_2$ . For both of these, one has $y_{\mu\mu} \neq 0$ . Thus we have agin after the symmetry operation,

$$p_0 p_\mu^2 = 1 \tag{3.46}$$

However, that would again mean [147]

$$p_0 p_\mu p_\tau = \frac{p_\tau}{p_\mu} \neq 1 \tag{3.47}$$

This in turn destroys the viablity of these two texture as well. Thus one is forced to conclude that none of the seven possible two-zero-texture cases can be achieved by an abelian horizontal symmetry assuming only one scalar triplet. But, when two or more triplets are present, then there will be more freedom in terms of the charges possessed by them, and the phase factor relations will be less constraining. Thus the contradictions that appear with a single triplet can be avoided, so that at least some of the seven possible two-zero textures are allowed. Therefore it is important to examine the phenomenological consequences of an augmented triplet sector if Type-II seesaw has to be consistent with two-zero textures. We proceed in that direction in the following chapters.

# Chapter 4

# Doubly charged scalar decays in a type II seesaw scenario with two Higgs triplets

## 4.1 Introduction

It is by and large agreed that the Large Hadron Collider (LHC) experiments have discovered the Higgs boson predicted in the standard electroweak theory, or at any rate a particle with close resemblance to it [10, 11]. At the same time, driven by both curiosity and various physics motivations, physicists have been exploring the possibility that the scalar sector of elementary particles contains more members than just a single $SU(2)$ doublet. A rather well-motivated scenario often discussed in this context is one containing at least one complex scalar $SU(2)$ triplet of the type $(\Delta^{++}, \Delta^{+}, \Delta^{0})$. We have already seen how a small vacuum expectation value of the neutral member of the triplet, constrained as it is by the $\rho$-parameter, can lead to Majorana masses for neutrinos, driven by $\Delta L = 2$ Yukawa interactions of the triplet. Such mass generation does not require any right-handed neutrino, and this is the quintessential principle of the type II seesaw mechanism [119, 148, 149].

A phenomenologically novel feature of this mechanism is the occurrence of a doubly-charged scalar. Its signature at TeV scale colliders is expected to be seen, if the triplet masses are not too far above the electroweak symmetry breaking scale. The most conspicuous signal consists in the decay into a pair of same-sign leptons, i.e. $\Delta^{++} \to \ell^{+}\ell^{+}$. The same-sign dilepton invariant mass peaks resulting from this make the doubly-charged scalar show up rather conspicuously. Alternatively, the decay into a pair of same-sign $W$ bosons, i.e. $\Delta^{++} \to W^{+}W^{+}$, is dominant in a complementary region of the parameter space, which — though more challenging from the viewpoint of background elimination — can unravel a doubly-charged scalar [150].

In this chapter, we shall discuss the situation where a third decay channel, namely a doubly-charged scalar decaying into a singly-charged scalar and a $W$ of the same sign, is dominant or substantial. Such a decay mode is usually suppressed, since the underlying $SU(2)$ invariance implies relatively small mass splitting among the members of a triplet. However, when several triplets of similar nature are present and mixing among them is allowed, a transition of the above kind is possible between two scalar mass eigenstates. Apart from being interesting in itself, several scalar triplets naturally occur in models for neutrino masses and lepton mixing based on the type II seesaw mechanism. In particular, it has been hinted that in such a scenario realization of viable neutrino mass matrices with two texture zeros [133,151],using symmetry arguments [152], requires two or three scalar triplets [146]. Here, we take up the case of two coexisting triplets. We demonstrate that in such cases one doubly-charged state can often decay into a singly-charged state and a $W$ of identical charge. This is not surprising, because each of the two erstwhile studied decay modes is controlled by parameters that are rather suppressed. In the case of $\Delta^{++} \to \ell^+\ell^+$, the amplitude is proportional to the $\Delta L = 2$ Yukawa coupling, while for $\Delta^{++} \to W^+W^+$, it is driven by the triplet vacuum expectation value (vev). The restrictions from neutrino masses as well as precision electroweak constraints make both of these rates rather small. On the other hand, in the scenario with two scalar triplets with charged mass eigenstates $H_k^{++}$ and $H_l^+$ ($k, l = 1, 2$), the decay amplitude for $H_1^{++} \to H_2^+W^+$, if kinematically allowed, is controlled by the $SU(2)$ gauge coupling. Therefore, if one identifies regions of the parameter space where it dominates, one needs to devise new search strategies at the LHC [154], including ways of eliminating backgrounds.

We note that the mass parameters of the two triplets, on which no phenomenological restrictions exist, are *a priori* unrelated and, therefore, as a result of mixing between the two triplets, the heavier doubly-charged state can decay into a lighter, singly-charged state and a real $W$ over a wide range of the parameter space. In that range it is expected that this decay channel dominates for the heavier doubly-charged state. By choosing a number of benchmark points, we demonstrate that this is indeed the case. In the next subsection we begin by presenting a summary of the model with a single triplet and explain why the decay $\Delta^{++} \to \Delta^+W^+$ is disfavoured there.

## 4.2 The scenario with a single triplet

In this section we perform a quick recapitulation of the scenario with a single triplet field, in addition to the usual Higgs doublet $\phi$, using the notation of [155]. The Higgs triplet

$\Delta = (\Delta^{++}, \Delta^{+}, \Delta^{0})$ is represented by the $2 \times 2$ matrix

$$\Delta = \begin{pmatrix} \Delta^{+} & \sqrt{2}\Delta^{++} \\ \sqrt{2}\Delta^{0} & -\Delta^{+} \end{pmatrix}. \tag{4.1}$$

The vevs of the doublet and the triplet are given by

$$\langle\phi\rangle_0 = \frac{1}{\sqrt{2}} \begin{pmatrix} 0 \\ v \end{pmatrix} \quad \text{and} \quad \langle\Delta\rangle_0 = \begin{pmatrix} 0 & 0 \\ w & 0 \end{pmatrix}, \tag{4.2}$$

respectively. Thus, the triplet vev is obtained as $\langle\Delta^0\rangle = w/\sqrt{2}$ . The only doublet-dominated physical state that survives after the generation of gauge boson masses is a neutral scalar $H$.

The most general scalar potential involving $\phi$ and $\Delta$ can be written as [155]

$$\begin{aligned} V(\phi,\Delta) \;=\; & a\,\phi^\dagger\phi + \frac{b}{2}\,\mathrm{Tr}\,(\Delta^\dagger\Delta) + c\,(\phi^\dagger\phi)^2 + \frac{d}{4}\left(\mathrm{Tr}\,(\Delta^\dagger\Delta)\right)^2 \\ & + \frac{e-h}{2}\phi^\dagger\phi\,\mathrm{Tr}\,(\Delta^\dagger\Delta) + \frac{f}{4}\,\mathrm{Tr}\,(\Delta^\dagger\Delta^\dagger)\,\mathrm{Tr}\,(\Delta\Delta) \\ & + h\phi^\dagger\Delta^\dagger\Delta\phi + \left(t\,\phi^\dagger\Delta\tilde{\phi} + \text{h.c.}\right), \end{aligned} \tag{4.3}$$

where $\tilde{\phi} \equiv i\tau_2\phi^*$. For simplicity, we assume both $v$ and $w$ to be real and positive, which requires $t$ to be real as well. In other words, all CP-violating effects are neglected in this analysis.

The choice $a < 0$, $b > 0$ ensures that the primary source of spontaneous symmetry breaking lies in the vev of the scalar doublet. We assume the following orders of magnitude for the parameters in the potential:

$$a,\, b \sim v^2; \quad c,\, d,\, e,\, f,\, h \sim 1; \quad |t| \ll v. \tag{4.4}$$

Such a choice is motivated by

(a) proper fulfillment of the electroweak symmetry breaking conditions,

(b) the need to have $w \ll v$ small due to the $\rho$-parameter constraint,

(c) the need to keep doublet-triplet mixing low in general, and

(d) the urge to ensure perturbativity of all quartic couplings.

The mass Lagrangian for the singly-charged scalars in this model is given by

$$\mathcal{L}_S^{\pm} = -(H^-, \phi^-)\mathcal{M}_+^2 \begin{pmatrix} H^+ \\ \phi^+ \end{pmatrix} \tag{4.5}$$

with

$$\mathcal{M}_+^2 = \begin{pmatrix} (q + h/2)v^2 & \sqrt{2}v(t - wh/2) \\ \sqrt{2}v(t - wh/2) & 2(q + h/2)w^2 \end{pmatrix} \quad \text{and} \quad q = \frac{|t|}{w}. \tag{4.6}$$

It is interesting to note that the determinant of this mass matrix will vanish only if $t$ is negative. The field $\phi^+$ is the charged component of the doublet scalar field of the Standard Model (SM). One of the eigenvalues of this matrix is zero corresponding to the Goldstone boson which gives mass to the $W$ boson. The mass-squared of the singly-charged physical scalar is obtained as

$$m_{H^+}^2 = \left(q + \frac{h}{2}\right)(v^2 + 2w^2), \tag{4.7}$$

whereas the corresponding expression for the doubly-charged scalar is

$$m_{\Delta^{++}}^2 = (h + q)v^2 + 2fw^2. \tag{4.8}$$

Thus, in the limit $w \ll v$, we obtain

$$m_{\Delta^{++}}^2 - m_{H^+}^2 \simeq \frac{h}{2}v^2. \tag{4.9}$$

It is obvious from equation 4.9 that a substantial mass splitting between $\Delta^{++}$ and $H^+$ is in general difficult. This is clear from Figure 4.1 where we plot the mass difference between the two states for different values of $h$. Sufficient splitting, so as to enable the decay $\Delta^{++} \to H^+W^+$ to take place with appreciable branching ratio, will require $h \simeq 1$, $m_{\Delta^{++}} \lesssim 250\,\text{GeV}$ and a correspondingly smaller $m_{H^+}$. The limits from LEP and Tevatron disfavour triplet states with such low masses. Thus one concludes that the phenomenon of the doubly-charged scalar decaying into a singly-charged one and a $W$ is very unlikely.

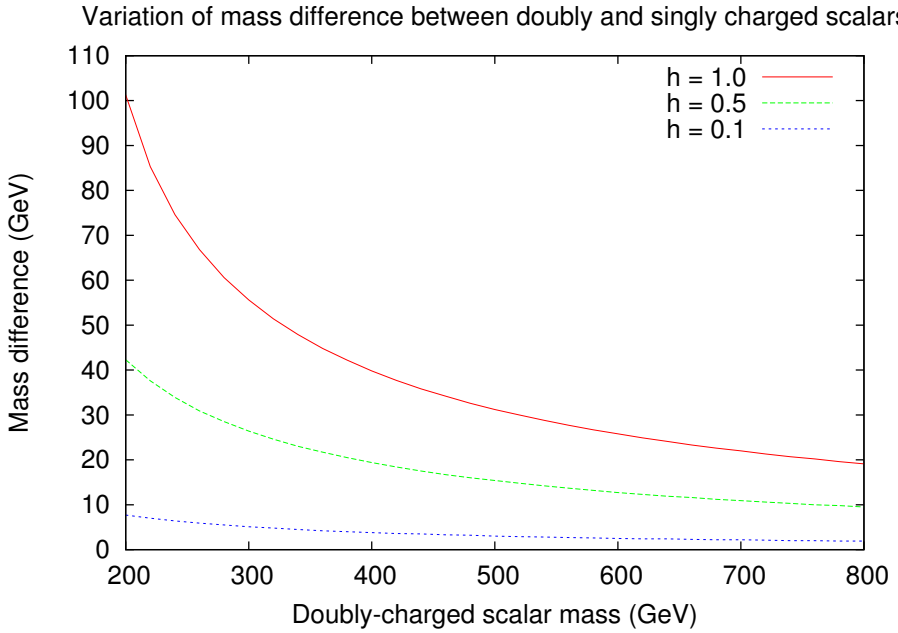


Figure 4.1: Variation of mass difference between the doubly and singly-charged scalars, for various values of the parameter $h$.

## 4.3 A two Higgs triplet scenario

There may, however, be some situations where a single triplet is phenomenologically inadequate. This happens, for example, when one tries to impose texture zeros in the neutrino mass matrix within a type II seesaw framework by using Abelian symmetries. It has been discussed in the previous chapter how a two-zero texture becomes inconsistent with this framework if a single scalar triplet is present. Having this is in mind, we venture into a model consisting of one complex doublet and two $Y = 2$ triplet scalars $\Delta_1$, $\Delta_2$, both written as 2×2 matrices:

$$\Delta_1 = \begin{pmatrix} \delta_1^+ & \sqrt{2}\delta_1^{++} \\ \sqrt{2}\delta_1^0 & -\delta_1^+ \end{pmatrix} \quad \text{and} \quad \Delta_2 = \begin{pmatrix} \delta_2^+ & \sqrt{2}\delta_2^{++} \\ \sqrt{2}\delta_2^0 & -\delta_2^+ \end{pmatrix}. \tag{4.10}$$

The vevs of the scalar triplets are given by

$$\langle\Delta_1\rangle_0 = \begin{pmatrix} 0 & 0 \\ w_1 & 0 \end{pmatrix} \quad \text{and} \quad \langle\Delta_2\rangle_0 = \begin{pmatrix} 0 & 0 \\ w_2 & 0 \end{pmatrix}. \tag{4.11}$$

The vev of the Higgs doublet is given by equation (4.2).

The scalar potential in this model involving $\phi$, $\Delta_1$ and $\Delta_2$ can be written as [156]

$$\begin{aligned} V(\phi,\Delta_1,\Delta_2) = & \\ & a\,\phi^\dagger\phi + \frac{1}{2}\,b_{kl}\,\mathrm{Tr}\,(\Delta_k^\dagger\Delta_l) + c(\phi^\dagger\phi)^2 + \frac{1}{4}\,d_{kl}\left(\mathrm{Tr}\,(\Delta_k^\dagger\Delta_l)\right)^2 \\ & + \frac{1}{2}\,(e_{kl}-h_{kl})\,\phi^\dagger\phi\,\mathrm{Tr}\,(\Delta_k^\dagger\Delta_l) + \frac{1}{4}\,f_{kl}\,\mathrm{Tr}\,(\Delta_k^\dagger\Delta_l^\dagger)\,\mathrm{Tr}\,(\Delta_k\Delta_l) \\ & + h_{kl}\,\phi^\dagger\Delta_k^\dagger\Delta_l\phi + g\,\mathrm{Tr}\,(\Delta_1^\dagger\Delta_2)\,\mathrm{Tr}\,(\Delta_2^\dagger\Delta_1) + g'\,\mathrm{Tr}\,(\Delta_1^\dagger\Delta_1)\,\mathrm{Tr}\,(\Delta_2^\dagger\Delta_2) \\ & + \left(t_k\,\phi^\dagger\Delta_k\tilde{\phi} + \mathrm{h.c.}\right), \end{aligned} \tag{4.12}$$

where summation over $k,l = 1,2$ is understood. This potential is not the most general one, as we have omitted some of the quartic terms. This is justified in view of the scope of this thesis, as laid out in the introduction. Moreover, due to the smallness of the triplet vevs, the quartic terms are not important numerically for the mass matrices of the scalars.

As in the case with a single triplet, we illustrate our main point here taking all the vevs $v, w_1, w_2$ as real and positive, and with real values for $t_1, t_2$ as well. Again, the following orders of magnitude for the parameters in the potential are assumed:

$$a,\ b_{kl} \sim v^2; \quad c,\ d_{kl},\ e_{kl},\ h_{kl},\ f_{kl},\ g,\ g' \sim 1; \quad |t_k| \ll v. \tag{4.13}$$

We also confine ourselves to cases where $w_1, w_2 \ll v$, keeping in mind the constraint on the $\rho$-parameter.

In general, the scalar potential (4.12) can only be treated numerically. However, since the triplet vevs $w_k$ are small (we will have $w_k \lesssim 1\,\mathrm{GeV}$ in our numerical part), it should be a good approximation to drop the quartic terms in the scalar triplets. In the following we will discuss the vevs and the mass matrices of the doubly and singly-charged scalars in this approximation, so that our broad conclusions are transparent. However, the numerical results presented in section 4.4 are obtained using the full potential (4.12), including even the effects of the small triplet vevs. We find that the results are in very good accordance with the approximation.

For the sake of a convenient notation we define the following $2 \times 2$ matrices and vectors [156]:

$$B = (b_{kl}), \quad E = (e_{kl}), \quad H = (h_{kl}), \quad t = \begin{pmatrix} t_1 \\ t_2 \end{pmatrix}, \quad w = \begin{pmatrix} w_1 \\ w_2 \end{pmatrix}. \tag{4.14}$$

With this notation the conditions for a stationary point of the potential are given by [156]

$$\left(B + \frac{v^2}{2}\,(E-H)\right) w + v^2\,t = 0, \tag{4.15}$$

$$a + cv^2 + \frac{1}{2}w^T(E-H)w + 2\,t\cdot w = 0, \tag{4.16}$$

where we have used the notation $t \cdot w = \sum_k t_k w_k$. These two equations are exact if one neglects all terms quartic in the triplet vevs in $V_0 \equiv V(\langle\phi\rangle_0, \langle\Delta\rangle_0)$. In equation (4.16) we have already divided by $v$, assuming $v \neq 0$. Using equation (4.15), the small vevs $w_k$ are obtained as [156]

$$w = -v^2 \left( B + \frac{1}{2} v^2 (E - H) \right)^{-1} t. \tag{4.17}$$

Now we discuss the mass matrices of the charged scalars. A glance at the scalar potential equation (4.12)—neglecting quartic terms in the triplet scalars—reveals that the first two lines of $V$ make no difference between the singly and doubly-charged scalars. Thus, the difference in the respective mass matrices originates in the terms of the third line. The mass matrix of the doubly-charged scalars is obtained as [156]

$$\mathcal{M}^2_{++} = B + \frac{v^2}{2} (E + H) . \tag{4.18}$$

As for the singly-charged fields $\Delta^+_k$, one has to take into account of the fact that they can mix with $\phi^+$ of the Higgs doublet. Writing the mass term as [156]

$$-\mathcal{L}^{\pm}_S = \left(\delta^-_1, \delta^-_2, \phi^-\right) \mathcal{M}^2_+ \begin{pmatrix} \delta^+_1 \\ \delta^+_2 \\ \phi^+ \end{pmatrix} + \text{h.c.}, \tag{4.19}$$

equation (4.12) leads to [156]

$$\mathcal{M}^2_+ = \begin{pmatrix} B + \frac{v^2}{2} E & \sqrt{2} v \, (t - Hw/2) \\ \sqrt{2} v \, (t - Hw/2)^\dagger & a + cv^2 + \frac{1}{2} w^T (E + H) w \end{pmatrix} . \tag{4.20}$$

Obviously, this mass matrix has to have an eigenvector with eigenvalue zero which corresponds to the would-be-Goldstone boson. Indeed, using equations (4.15) and (4.16), we find [156]

$$\mathcal{M}^2_+ \begin{pmatrix} v_T \\ v/\sqrt{2} \end{pmatrix} = 0, \tag{4.21}$$

which serves as a consistency check.

Note that the matrix $B$ largely controls the mass of the triplet scalars and the order of magnitude of its elements (or of its eigenvalues) is expected to be a little above the electroweak scale, represented by $v \simeq 246\,\text{GeV}$. On the other hand, the quantities $t_k$ trigger the small triplet vevs, so they should be considerably smaller than the electroweak scale. Therefore, in a rough approximation one could neglect the $t_k$ and the triplet vevs in the

mass matrix $\mathcal{M}_+^2$. In that limit, also $a + cv^2 = 0$ and the charged would-be-Goldstone boson consists entirely of $\phi^+$, without mixing with the $\delta_k^+$.

The mass matrices (4.18) and (4.20) are diagonalized by [156]

$$U^\dagger \mathcal{M}_{++}^2 U = \text{diag}\,(M_1^2, M_2^2) \quad \text{and} \quad V^\dagger \mathcal{M}_+^2 V = \text{diag}\,(\mu_1^2, \mu_2^2, 0), \tag{4.22}$$

respectively, with [156]

$$\begin{pmatrix} \delta_1^{++} \\ \delta_2^{++} \end{pmatrix} = U \begin{pmatrix} H_1^{++} \\ H_2^{++} \end{pmatrix}, \quad \begin{pmatrix} \delta_1^{+} \\ \delta_2^{+} \\ \phi^{+} \end{pmatrix} = V \begin{pmatrix} H_1^{+} \\ H_2^{+} \\ G^{+} \end{pmatrix}. \tag{4.23}$$

We have denoted the fields with definite mass by $H_k^{++}$ and $H_k^+$, and $G^+$ is the charged would-be-Goldstone boson.

The gauge Lagrangian relevant for the decays considered is given by [156]

$$\begin{aligned} \mathcal{L}_{\text{gauge}} &= ig \sum_{k=1}^{2} \left[ \delta_k^- (\partial^\mu \delta_k^{++}) - (\partial^\mu \delta_k^-)\, \delta_k^{++} \right] W_\mu^- \\ &\quad - \frac{g^2}{\sqrt{2}} \sum_{k=1}^{2} w_k W_\mu^- W^{-\mu} \delta_k^{++} + \text{h.c.} \end{aligned} \tag{4.24}$$

Here $g$ is the $SU(2)$ gauge coupling constant. Inserting equation (4.23) into this Lagrangian allows us to compute the decay rates of $H_1^{++} \to H_2^+ W^+$ and $H_k^{++} \to W^+ W^+$ ($k = 1, 2$).

The $\Delta L = 2$ Yukawa interactions between the triplets and the leptons are [156]

$$\mathcal{L}_Y = \frac{1}{2} \sum_{k=1}^{2} h_{ij}^{(k)} L_i^T C^{-1} i\tau_2 \Delta_k L_j + \text{h.c.}, \tag{4.25}$$

where $C$ is the charge conjugation matrix, the $h_{ij}^{(k)}$ are the symmetric Yukawa coupling matrices of the triplets $\Delta_k$, and the $i, j$ are the summation indices over the three neutrino flavours.[1] The $L_i$ denote the left-handed lepton doublets.

The neutrino mass matrix is generated from equation (4.25) when the triplets acquire vevs [156]:

$$(M_\nu)_{ij} = h_{ij}^{(1)} w_1 + h_{ij}^{(2)} w_2. \tag{4.26}$$

This connects the Yukawa coupling constants $h_{ij}^{(1)}$, $h_{ij}^{(2)}$ and the triplet vevs $w_1$, $w_2$, once the neutrino mass matrix is written down for a particular scenario. In our subsequent calculations, we proceed as follows:

[1] We assume the charged-lepton mass matrix to be already diagonal.

First of all, the neutrino mass eigenvalues are fixed according to a particular type of mass spectrum. We illustrate our points by resorting to normal hierarchy of the neutrino mass spectrum and setting the lowest neutrino mass eigenvalue to zero. Furthermore, using the observed central values of the various lepton mixing angles, the elements of the neutrino mass matrix $M_\nu$ can be found by using the equation

$$M_\nu = U\hat{M}_\nu U^\dagger, \tag{4.27}$$

where $U$ is the PMNS matrix given by [145]

$$U = \begin{pmatrix} c_{12}c_{13} & s_{12}c_{13} & s_{13}e^{-i\delta} \\ -s_{12}c_{23} - c_{12}s_{23}s_{13}e^{i\delta} & c_{12}c_{23} - s_{12}s_{23}s_{13}e^{i\delta} & s_{23}c_{13} \\ s_{12}s_{23} - c_{12}c_{23}s_{13}e^{i\delta} & -c_{12}s_{23} - s_{12}c_{23}s_{13}e^{i\delta} & c_{23}c_{13} \end{pmatrix} \tag{4.28}$$

and $\hat{M}_\nu$ is the diagonal matrix of the neutrino masses. In equation (4.27) we have dropped possible Majorana phases. One can use the recent global analysis of data to determine the various entries of $U$ [32]. We have taken the phase factor $\delta$ to be zero for simplicity. Then, using the central values of all angles, including that for $\theta_{13}$ as obtained from the recent Daya Bay and RENO experiments [29, 30], the right-hand side of equation (4.25) is completely known, at least in orders of magnitude. The actual mass matrix thus constructed has some elements at least one order of magnitude smaller than the others, thus suggesting texture zeros.

For each of the benchmark points used in the next section, $w_1$ and $w_2$, the vevs of the two triplets, are determined by values of the parameters in the scalar potential. Of course, the coupling matrices $h^{(1)}$ and $h^{(2)}$ are still indeterminate. In order to evolve a working principle based on economy of free parameters, we fix the Yukawa coupling matrix $h^{(2)}$ by choosing one suitable value for all elements of the $\mu$–$\tau$ block and another value, a smaller one, for the rest of the matrix. That fixes all the elements of the other matrix. Although there is a degree of arbitrariness in such a method, we emphasize that it does not affect the generality of our conclusions, so long as we adhere to the wide choice of scenarios adopted in the next section, including both small and large values of the $\Delta L = 2$ Yukawa couplings.

## 4.4 Benchmark points and doubly-charged scalar decays

Our purpose is to investigate the expected changes in the phenomenology of doubly-charged scalars when two triplets are present. In general, the two scalars of this kind,

namely, $H_1^{++}$ and $H_2^{++}$ can both be produced at the LHC via the Drell-Yan process, which can have about 10% enhancement from the two-photon channel. They will, over a large region of the parameter space, have the following decays [156]:

$$H_1^{++} \rightarrow \ell_i^+ \ell_j^+, \tag{4.29}$$
$$H_1^{++} \rightarrow W^+ W^+, \tag{4.30}$$
$$H_1^{++} \rightarrow H_2^+ W^+, \tag{4.31}$$
$$H_2^{++} \rightarrow \ell_i^+ \ell_j^+, \tag{4.32}$$
$$H_2^{++} \rightarrow W^+ W^+, \tag{4.33}$$

with $\ell_i, \ell_j = e, \mu$ in equation (4.29). As we discussed in section 4.2, in the context of the single-triplet model the decay analogous to equation (4.31) is practically never allowed, unless the masses are very low. On the other hand, mixing between two triplets opens up situations where the mass separation between $H_1^{++}$ and $H_2^+$ kinematically allows the transition (4.31). Denoting the mass of $H_k^{++}$ by $M_k$ and that of $H_k^+$ by $\mu_k$ ($k = 1, 2$) and using the convention $M_1 > M_2$ and $\mu_1 > \mu_2$, this decay is possible if $M_1 > \mu_2 + m_W$, where $m_W$ is the mass of $W$ boson. We demonstrate numerically that this can naturally happen, by considering three distinct regions of the parameter space and selecting four benchmark points (BPs) for each region.

We have seen that, in a model with a single triplet, the doubly-charged Higgs decays into either $\ell_i^+ \ell_j^+$ or $W^+W^+$. The former is controlled by the $\Delta L = 2$ Yukawa coupling constants $h_{ij}$, while the latter is driven by the triplet vev $w$. Since neutrino masses are given by $M_\nu = hw$, large ($\simeq 1$) values of $h_{ij}$ imply a small vev $w$, and vice versa. Accordingly, assuming $h_{ij} \neq 0$, three regions in the parameter space can be identified, where one can have [156]

i) $\Gamma(\Delta^{++} \rightarrow \ell_i^+ \ell_j^+) \ll \Gamma(\Delta^{++} \rightarrow W^+W^+)$,

ii) $\Gamma(\Delta^{++} \rightarrow \ell_i^+ \ell_j^+) \gg \Gamma(\Delta^{++} \rightarrow W^+W^+)$,

iii) $\Gamma(\Delta^{++} \rightarrow \ell_i^+ \ell_j^+) \sim \Gamma(\Delta^{++} \rightarrow W^+W^+)$.

In the context of two triplets, we choose three different 'scenarios' in the same spirit, with similar relative rates of the two channels $H_k^{++} \rightarrow \ell_i^+ \ell_j^+$ and $H_k^{++} \rightarrow W^+W^+$. Four BPs are selected for each such scenario through the appropriate choice of parameters in the scalar potential. The resulting masses of the various physical scalar states are shown in tables 4.1 and 4.2. Although our study focuses mainly on the phenomenology of charged

scalars, we also show the masses of the neutral scalars. It should be noted that the lightest CP-even neutral scalar, which is dominated by the doublet, has mass around 125 GeV for each BP. It has also been checked that, here as well as in the situation discussed in the next chapter, the benchmark points used by us are consistent with the observed signal strengths of the 125 GeV scalar, within $1\sigma$ level [158].

All the twelve BPs (distributed among the three different scenarios) have $M_1$ sufficiently above $\mu_2$ to open up $H_1^{++} \to H_2^+ W^+$. The branching ratios in different channels are of course dependent on the specific BP. We list all the branching ratios for $H_1^{++}$ and $H_2^{++}$ in table 4.3, together with their pair-production cross sections at the LHC with $\sqrt{s} = 14\,\text{TeV}$.

The cross sections and branching ratios have been calculated with the help of the package FeynRules (version 1.6.0) [159,160], thus creating a new model file in CompHEP (version 2.5.4) [161]. CTEQ6L parton distribution functions have been used, with the renormalisation and factorisation scales set at the doubly-charged scalar mass. Using the full machinery of scalar mixing in this model, the decay widths into various channels have been obtained.

The results summarised in table 4.3 show that, for the decay of $H_1^{++}$, the channel $H_2^+ W^+$ is dominant for two of the four BPs in scenario 1 and all four BPs in scenarios 2 and 3. This, in the first place, substantiates our claim that one may have to look for a singly-charged scalar in the final state that opens up when more than one doublet is present. This is because, for the BPs where $H_1^{++} \to H_2^+ W^+$ dominates, the branching ratios for the other final states are far too small to yield any detectable rates.

## 4.5 Usefulness of $H_1^{++} \longrightarrow H_2^+ W^+$ at the LHC

Table 4.3 contains the rates for pair-production of the heavier as well as the lighter doubly-charged scalar at the 14 TeV run of the LHC. A quick look at these rates revals that for the heavier of the doubly-charged scalars, it varies from about 1.4 fb to 3.6 fb, for masses ranging approximately between 400 and 550 GeV. Therefore, as can be read off from table 4.3, for ten of our twelve BPs, an integrated luminosity of about $500\,\text{fb}^{-1}$ is likely to yield about $700$ to $1800$ events of the $H_2^+ W^+ H_2^- W^-$ type. Keeping in mind the fact that $H_2^+$ mostly decays in the channel $H_2^+ \to \ell^+ \bar{\nu}_\ell$, such final states should *prima facie* be observed at the LHC, although event selection strategies of a very special nature may be required to distinguish the $H_2^+$ from a $W^+$ decaying into $\ell^+ \nu_\ell$.

The primary advantage of focusing on the channel $H_1^{++} \longrightarrow H_2^+ W^+$ is that it helps one in differentiating between the two kinds of type II cases, namely those containing one and

two scalar triplets, respectively. In order to emphasize this point, we summarize below the result of a simulation in the context of the 14 TeV run of the LHC. For our simulation, the amplitudes have been computed using the package Feynrules (version 1.6.0), with the subsequent event generation through MadGraph (version 5.12) [162], and showering with the help of PYTHIA 8.0. CTEQ6L parton distribution functions have been used.

We compare the two-triplet case with the single-triplet case. In the first case, there are two doubly charged scalars, and one has contributions from both $H_1^{\pm\pm}$ and $H_2^{\pm\pm}$ to the leptonic final states following their Drell-Yan production. While the former, in the chosen benchmark points, decays into $H_1^{\pm}W^{\pm}$, the latter goes either to a same-sign $W$-pair or to same-sign dileptons. If one considers two, three and four-lepton final states with missing transverse energy (MET), there will be contributions from both of the doubly-charged scalars, with appropriate branching ratios, combinatoric factors and response to the cuts imposed. We have carried out our analysis with a set of cuts listed in table 4.4, which are helpful in suppressing the standard model backgrounds. Thus one can define the following ratios of events emerging after the application of cuts [156]:

$$r_1 = \frac{\sigma(4\ell + \text{MET})}{\sigma(3\ell + \text{MET})}, \qquad r_2 = \frac{\sigma(4\ell + \text{MET})}{\sigma(2\ell + \text{MET})}. \tag{4.34}$$

The values of these ratios for the three scenarios of BP 3 are presented in table 4.5. In each case, the ratios for the two-triplet case is presented alongside the corresponding single-triplet case, with the mass of the doubly charged scalar in the latter case being close to that of the lighter state $H_2^{\pm\pm}$ in the former case. Both of the situations where, in the later case, the doubly charged scalar decays dominantly into either $W^{\pm}W^{\pm}$ or $\ell^{\pm}\ell^{\pm}$ are represented in our illustrative results. One can clearly notice from the results (which apply largely to our other benchmark points as well) that both $r_1$ and $r_2$ remain substantially larger in the two-triplet case as compared to the single-triplet case. One reason for this is an enhancement via the combinatoric factors in the two-triplet case. However, the more important reason is that the $4\ell$ events survive the missing transverse energy (MET) cut with greater efficiency. In the single-triplet case, the survival rate efficiency is extremely small when $H^{\pm\pm}$ decays mainly into same-sign dileptons, the MET coming mostly from energy-momentum mismeasurement (as a result of lepton energy smearing) or initial and final-state radiation. In the two-triplet case, on the other hand, the decay $H_1^{++} \longrightarrow H_2^{+}W^{+}$ leaves ample scope for having MET in $W$-decays as well as in the decay $H_2^{+} \longrightarrow \ell^{+}\bar{\nu}_{\ell}$, thus leading to substantially higher cut survival efficiency. Thus, from an examination of such numbers as those presented in table 4.5, one can quite effectively use

| | Mass (GeV) | BP 1 | BP 2 | BP 3 | BP 4 |
|---|---|---|---|---|---|
| Scenario 1 | $H_1^{++}$ | 515.99 | 515.99 | 521.54 | 524.15 |
| | $H_2^{++}$ | 443.04 | 429.16 | 455.59 | 470.15 |
| | $H_1^+$ | 515.98 | 515.98 | 498.97 | 515.78 |
| | $H_2^+$ | 368.45 | 360.15 | 423.26 | 418.65 |
| Scenario 2 | $H_1^{++}$ | 526.78 | 525.00 | 429.13 | 464.31 |
| | $H_2^{++}$ | 414.18 | 401.63 | 392.45 | 407.20 |
| | $H_1^+$ | 520.26 | 519.86 | 414.48 | 459.23 |
| | $H_2^+$ | 343.28 | 334.97 | 339.02 | 340.63 |
| Scenario 3 | $H_1^{++}$ | 521.54 | 464.31 | 525.00 | 429.13 |
| | $H_2^{++}$ | 455.59 | 407.20 | 401.63 | 392.45 |
| | $H_1^+$ | 498.97 | 459.23 | 519.86 | 414.48 |
| | $H_2^+$ | 423.26 | 340.63 | 334.97 | 339.02 |

Table 4.1: Charged scalar masses.

the channel $H_1^{++} \longrightarrow H_2^+ W^+$ to distinguish a two-triplet case from a single-triplet case, provided the heavier doubly-charged state is within the kinematic reach of the LHC.

| | Mass (GeV) | BP 1 | BP 2 | BP 3 | BP 4 |
|---|---|---|---|---|---|
| Scenario 1 | $H^0_{1R}$ | 365.70 | 364.86 | 350.39 | 364.59 |
| | $H^0_{2R}$ | 193.89 | 194.00 | 256.09 | 245.96 |
| | $H^0_{3R}$ | 125.00 | 125.03 | 125.01 | 125.01 |
| | $H^0_{1I}$ | 364.98 | 364.85 | 350.39 | 364.59 |
| | $H^0_{2I}$ | 194.43 | 193.98 | 256.08 | 245.96 |
| Scenario 2 | $H^0_{1R}$ | 365.69 | 365.70 | 295.58 | 325.51 |
| | $H^0_{2R}$ | 173.97 | 173.96 | 173.98 | 173.96 |
| | $H^0_{3R}$ | 125.02 | 125.02 | 125.04 | 125.02 |
| | $H^0_{1I}$ | 365.69 | 365.70 | 295.59 | 325.52 |
| | $H^0_{2I}$ | 173.97 | 173.96 | 173.98 | 173.96 |
| Scenario 3 | $H^0_{1R}$ | 350.39 | 325.51 | 365.69 | 295.58 |
| | $H^0_{2R}$ | 256.08 | 173.96 | 173.98 | 173.96 |
| | $H^0_{3R}$ | 125.02 | 125.02 | 125.04 | 125.02 |
| | $H^0_{1I}$ | 350.39 | 325.51 | 365.69 | 295.58 |
| | $H^0_{2I}$ | 256.08 | 173.96 | 173.98 | 173.96 |

Table 4.2: Neutral scalar masses.

| | Data | BP 1 | BP 2 | BP 3 | BP 4 |
|---|---|---|---|---|---|
| Scenario 1 | BR($H_1^{++} \to H_2^+ W^+$) | 0.08 | 0.10 | 0.99 | 0.99 |
| | BR($H_1^{++} \to W^+ W^+$) | 0.92 | 0.90 | 0.01 | 0.004 |
| | BR($H_1^{++} \to \ell_i^+ \ell_j^+$) | $< 10^{-16}$ | $< 10^{-16}$ | $< 10^{-19}$ | $< 10^{-20}$ |
| | BR($H_2^{++} \to W^+ W^+$) | 0.99 | 0.99 | 0.99 | 0.99 |
| | BR($H_2^{++} \to \ell_i^+ \ell_j^+$) | $< 10^{-19}$ | $< 10^{-19}$ | $< 10^{-17}$ | $< 10^{-18}$ |
| | $\sigma(pp \to H_1^{++} H_1^{--})$ | 1.664 fb | 1.534 fb | 1.446 fb | 1.408 fb |
| | $\sigma(pp \to H_2^{++} H_2^{--})$ | 3.044 fb | 3.5 fb | 2.714 fb | 2.308 fb |
| Scenario 2 | BR($H_1^{++} \to H_2^+ W^+$) | 0.99 | 0.99 | 0.99 | 0.98 |
| | BR($H_1^{++} \to W^+ W^+$) | $< 10^{-21}$ | $< 10^{-21}$ | $< 10^{-17}$ | $< 10^{-20}$ |
| | BR($H_1^{++} \to \ell_i^+ \ell_j^+$) | 0.01 | 0.01 | 0.001 | 0.02 |
| | BR($H_2^{++} \to W^+ W^+$) | $< 10^{-18}$ | $< 10^{-18}$ | $< 10^{-14}$ | $< 10^{-18}$ |
| | BR($H_2^{++} \to \ell_i^+ \ell_j^+$) | 0.99 | 0.99 | 0.99 | 0.99 |
| | $\sigma(pp \to H_1^{++} H_1^{--})$ | 1.36 fb | 1.41 fb | 3.59 fb | 2.46 fb |
| | $\sigma(pp \to H_2^{++} H_2^{--})$ | 3.98 fb | 4.65 fb | 5.28 fb | 4.38 fb |
| Scenario 3 | BR($H_1^{++} \to H_2^+ W^+$) | 0.99 | 0.99 | 0.99 | 0.99 |
| | BR($H_1^{++} \to W^+ W^+$) | $< 10^{-12}$ | $< 10^{-10}$ | $< 10^{-11}$ | $< 10^{-9}$ |
| | BR($H_1^{++} \to \ell_i^+ \ell_j^+$) | $< 10^{-9}$ | $< 10^{-11}$ | $10^{-11}$ | $< 10^{-11}$ |
| | BR($H_2^{++} \to W^+ W^+$) | 0.0001 | 0.98 | 0.97 | 0.99 |
| | BR($H_2^{++} \to \ell_i^+ \ell_j^+$) | 0.99 | 0.02 | 0.03 | 0.01 |
| | $\sigma(pp \to H_1^{++} H_1^{--})$ | 1.45 fb | 2.46 fb | 1.41 fb | 3.59 fb |
| | $\sigma(pp \to H_2^{++} H_2^{--})$ | 2.71 fb | 4.38 fb | 4.65 fb | 5.28 fb |

Table 4.3: Decay branching ratios and production cross sections for doubly-charged scalars.

| |
|---|
| $\text{MET} > 70$ GeV |
| $\Sigma\lvert p_T^{\text{vis}}\rvert + \text{MET} > 500$ GeV |
| $\left\lvert p_T^{\text{lepton}} \right\rvert > 30$ GeV |
| $\lvert\eta_{\text{lep}}\rvert < 2.5$ |
| $\lvert\eta_{\text{jet}}\rvert < 4.5$ |

Table 4.4: Cuts used for determination of ratios of events $r_1$ and $r_2$. The subscript $T$ stands for 'transverse' and $\eta$ denotes the pseudorapidity.

| BP 3 | Ratio | Two triplets | One triplet |
|---|---|---|---|
| Scenario 1 | $r_1$ | 0.20 | 0.04 |
| | $r_2$ | 0.05 | 0.01 |
| Scenario 2 | $r_1$ | 0.44 | $< 10^{-6}$ |
| | $r_2$ | 0.21 | $< 10^{-9}$ |
| Scenario 3 | $r_1$ | 0.12 | $< 10^{-5}$ |
| | $r_2$ | 0.04 | $< 10^{-6}$ |

Table 4.5: Ratio of events $r_1$, $r_2$ for two-triplet and single-triplet scenario respectively for benchmark point 3.

## 4.6 Conclusions

In this chapter, we have argued, taking models with the type II seesaw mechanism for neutrino mass generation as a motivation, that it makes sense to consider scenarios with more than one scalar triplet. As the simplest extension, we have formulated in detail a model with two $Y = 2$ complex triplets of this kind. On taking into account the mixing of the triplets with each other (and also with the doublet, albeit with considerable restriction), and thus identifying all the mass eigenstates along with their various interaction strengths, we find that the heavier doubly-charged scalar decays dominantly into the lighter singly-charged scalar and a $W$ boson over a large region of the parameter space. It should be re-iterated that this feature is a generic one and is avoided only in very limited situations or in the case of unusually high values of the triplet Yukawa coupling. The deciding factor here is the decay being driven by the $SU(2)$ gauge coupling.

Thus the above mode is often the only way of looking for the heavier doubly-charged scalar state and thus for the existence of two scalar triplets. Our choice of benchmark points for reaching this conclusion spans cases where the $\Delta L = 2$ lepton couplings of

the triplets have values at the high (close to one) and low as well as the intermediate level, consistent with the observed neutrino mass and mixing patterns. In general, with the heavier triplet mass ranging up to more than 500 GeV, one expects about 700 to 1800 events of the type $pp \to H_2^+ W^+ H_2^- W^-$ at the 14 TeV run of the LHC, for an integrated luminosity of 500 fb$^{-1}$. We have also demonstrated that ratios of the numbers of two, three and four-lepton events with MET offer a rather spectacular distinction of the two-triplet case from one with a single triplet only.

For unsuppressed production of doubly charged scalars, the Drell - Yan pair production mode is useful, since no suppression by triplet vev's comes into play. On the other hand, the smallness of the triplet vev also makes the single production rate (via gauge boson fusion) of doubly charged scalar rather small [163]. Of course, for $H^{++}H^{--}$ production, there are possibilities of detecting a doubly charged Higgs at the colliders through the decays $H^{++} \to l^+l^+$ and $H^{++} \to W^+W^+$. In these cases it is interesting to note that the interplay of the two parameters, the triplet Yukawa coupling $h_{ll}$ and triplet vev $w$ actually govern the relative strengths of the two decays channels $H^{++} \to l^+l^+$ and $H^{++} \to W^+W^+$, as for the identification of the $H^{\pm\pm}$ signal. We would like to mention that the doubly charged scalars may be detected at the LHC for the $l^\pm l^\pm$ decay mode with $300 fb^{-1}$ integrated luminosity, upto a mass range of $1TeV$ even with a branching fraction $\sim 60\%$ into this channel. But, in spite of the distinctive nature of the signal produced by $H^{++} \to l^+l^+$ decay, their faking by a number of sources cannot be ruled out [163]. On the other hand, in the complementary region of parameter space, doubly charged scalars are most likely to be observed upto a mass of $700GeV$ in the $H^{++} \to W^+W^+$ decay mode. But, it is worth mentioning that signals from this decay mode are in general more background prone than the $l^+l^+$ decay mode [163]. The techniques used in [163] for the decay $H^{++} \to W^+W^+$ can be extended to the decay $H^{++} \to H^+W^+$ for background suppression.

# Chapter 5

# CP-violating phase in a two Higgs triplet scenario : some phenomenological implications

## 5.1 Introduction

We begin by recapitulating the theme explored in the last chapter. We have already seen that type-II seesaw models can generate Majorana neutrino masses without any right-handed neutrino(s) with the help of one or more Y=2 scalar triplets. The restriction of the vacuum expectation value (vev) of such a triplet, arising from the limits on the $\rho$-parameter (with $\rho = m_W^2/m_Z^2 \cos^2\theta$), is obeyed in a not so unnatural manner, where the constitution of the scalar potential can accommodate large triplet scalar masses vis-a-vis a small vev. In fact, this very feature earns such models classification as a type of 'seesaw'.

A lot of work has been done on the phenomenology of scalar triplets which, interestingly, also arise in left-right symmetric theories [164]. One can, however, still ask the question: is a single-triplet scenario self-sufficient, or does the replication of triplets (together with the single scalar doublet of the SM) bring about any difference in phenomenology? This question, otherwise a purely academic one, acquires special meaning in the context of some neutrino mass models which aims to connect the mass ordering with the values of the mixing angles, thereby achieving some additional predictiveness. We have mentioned in the previous chapters that a class of such models depend on texture zeros, where a number of zero entries (usually restricted to two) in the mass matrix enable one to establish the desired connection.

The existence of such zero entries require the imposition of some additional symmetry. We have pointed out that the simultaneous requirement of zero textures and the type-II

seesaw mechanism,however, turns out to be inconsistent. The inconsistency is gone for two or more triplets. This resurrects the relevance of the phenomenology of two-triplet, one doublet scalar sectors, this time with practical implications. We have studied such phenomenology in the previous chapter. An important conclusion of that study was that, whereas the doubly charged scalar in the single triplet scenario would decay mostly in the $\ell^\pm\ell^\pm$ or $W^\pm W^\pm$ modes, the decay channel $H_1^{++} \longrightarrow H_2^+ W^+$ acquires primacy over a large region of the parameter space. Some predictions on this in the context of the Large Hadron Collider were also shown. However, an added possibility with two triplet is the possibility of at least one CP-violating phase being there. This in principle can affect the phenomenology of the model, which is worth studying.

With this in view, we have analyzed in the present chaper the one-doublet, two-triplet framework, including CP-violating effects arising via a relative phase between the triplets. Thus, the vev of one triplet has been made complex and consequently, the coefficient of the corresponding trilinear term in the scalar potential has also been rendered complex.

Indeed, the introduction of a phase results in some interesting findings that were not present when the relative phase was absent. First of all, as a result of mixing between two triplets and presence of a relative phase between them, something on which no phenomenological restrictions exits, the heavier doubly charged scalar can dominantly decay into the lighter doubly charged scalar plus the SM-like Higgs boson i.e. $H_1^{++} \to H_2^{++} h$, over a larger range of parameter space. This can give rise to a spectacular signal in the context of LHC. Basically, as a final state, we obtain $H_1^{++} \to \ell^+\ell^+ h$ i.e a doubly charged scalar decaying into two same-sign leptons plus the SM-like Higgs. This decay often dominates over all other decay channels. When this decay is not present due to insufficient mass-difference between respective scalars, the decay $H_2^{++} \longrightarrow H_2^+ W^+$ mostly dominates, and its consequence was discussed in some detail in the previous chapter on the CP-conserving scenario.

Secondly, for some combination of parameters, the decays mentioned in the above paragraph are not possible with a vanishing or small phase, due to insufficient gap in masses between the respective scalars. However, if we continuously increase the value of the phase, keeping all the other parameters fixed, the mass differences between the scalars start to increase, so that the aforementioned channel finally opens up.

Thirdly, we have noticed in the previous chapter that the gauge coupling dominated decay $H_1^{++} \to H_2^+ W^+$ dominates over the Yukawa coupling dominated decay $\Delta^{++} \to \ell^+\ell^+$, even in those region of parameter space where we have chosen the Yukawa

coupling matrices to be sufficiently large ($\simeq 1$). On the other hand, the CP-violating phase suppresses the neutrino mass matrix elements for the same value of the triplet vacuum expectation values (vev). This in turn requires an increase in the corresponding Yukawa coupling matrix elements, since the vev's and Yukawa couplings are related by the expression for neutrino masses. The outcome of this whole process is that, for several BPs, the decay $H_1^{++} \to \ell^+\ell^+$ competes with the decay into $H_2^+W^+$.

Finally, the CP-conserving scenario marks out regions of the parameter space, where the branching ratios of the decays $H_1^{++} \longrightarrow \ell^+\ell^+$ and $H_1^{++} \to W^+W^+$ are of comparable, though subdominant, rates. As the phase picks up, the same vev causes a hike in Yukawa coupling, as discussed above. In such situations, the decay $H_1^{++} \to \ell^+\ell^+$ mostly dominates over the $W^+W^+$ mode.

Since, to the best of our knowledge, very little has been written on CP-violating phase(s) in two-triplet scenarios, we introduce the issue in a minimalistic manner, introducing one such phase. The presence of additional phases can of course subject the allowed parameter space to new possibilities. We postpone their discussion for a further study.

We begin by presenting a summary of the scenario with a single triplet with complex vev in the next section.

## 5.2 A single scalar triplet with a CP-violating phase

We first give a glimpse of the scenario with a single triplet $\Delta = (\Delta^{++}, \Delta^+, \Delta^0)$, over and above the usual Higgs doublet $\phi$, using the notation of [155]. $\Delta$ is equivalently denoted by the $2 \times 2$ matrix

$$\Delta = \begin{pmatrix} \Delta^+ & \sqrt{2}\Delta^{++} \\ \sqrt{2}\Delta^0 & -\Delta^+ \end{pmatrix}. \tag{5.1}$$

The vev's of the doublet and the triplet are expressed as

$$\langle\phi\rangle_0 = \frac{1}{\sqrt{2}} \begin{pmatrix} 0 \\ v \end{pmatrix} \quad \text{and} \quad \langle\Delta\rangle_0 = \begin{pmatrix} 0 & 0 \\ v_T & 0 \end{pmatrix}, \tag{5.2}$$

respectively. The only doublet-dominated physical state that survives after the generation of gauge boson masses is a neutral scalar $h$.

The most general scalar potential including $\phi$ and $\Delta$ can be written as [155]

$$\begin{aligned} V(\phi,\Delta) \;=\; & a\,\phi^\dagger\phi + \frac{b}{2}\,\mathrm{Tr}\,(\Delta^\dagger\Delta) + c\,(\phi^\dagger\phi)^2 + \frac{d}{4}\left(\mathrm{Tr}\,(\Delta^\dagger\Delta)\right)^2 \\ & + \frac{e-h}{2}\phi^\dagger\phi\,\mathrm{Tr}\,(\Delta^\dagger\Delta) + \frac{f}{4}\,\mathrm{Tr}\,(\Delta^\dagger\Delta^\dagger)\,\mathrm{Tr}\,(\Delta\Delta) \\ & + h\phi^\dagger\Delta^\dagger\Delta\phi + \left(t\,\phi^\dagger\Delta\tilde{\phi} + \mathrm{h.c.}\right), \end{aligned} \tag{5.3}$$

where $\tilde{\phi} \equiv i\tau_2\phi^*$ and $\tau_2$ is the Pauli matrix. All parameters in the Higgs potential are real except $t$ which is complex in general. By performing a global $U(1)$ transformation, $v$ can always be chosen real and positive. Because of the $t$-term in the potential there is no second global symmetry to make $v_T$ real. As already mentioned, $t$ can also be complex and, therefore, it can be written as $t = |t|\,e^{i\alpha}$ and $v_T = we^{i\gamma}$ with $w \equiv |v_T|$. Minimization of the scalar potential with respect to the phase of $v_T$ i.e $\gamma$, gives the relation between the phases as $\alpha + \gamma = \pi$. [1]

The choice $a < 0$, $b > 0$ ensures that the dominant source of spontaneous symmetry breaking is the scalar doublet. It is further assumed, following [155], that

$$a,\, b \sim v^2; \quad c,\, d,\, e,\, f,\, h \sim 1; \quad |t| \ll v. \tag{5.4}$$

Such a choice is motivated by the following considerations as mentioned in the previous chapter

- The need to fulfill the electroweak symmetry breaking conditions,
- To have $w \ll v$ sufficiently small, as required by the $\rho$-parameter constraint,
- To keep doublet-triplet mixing low in general, and
- To ensure that all quartic couplings are perturbative.

The mass terms for the singly-charged scalars can be expressed in a compact form as

$$\mathcal{L}_S^{\pm} = -(H^-, \phi^-)\mathcal{M}_+^2 \begin{pmatrix} H^+ \\ \phi^+ \end{pmatrix} \tag{5.5}$$

with

$$\mathcal{M}_+^2 = \begin{pmatrix} (q + h/2)v^2 & \sqrt{2}v(t^* - v_T h/2) \\ \sqrt{2}v(t - v_T^* h/2) & 2(q + h/2)w^2 \end{pmatrix} \quad \text{and} \quad q = \frac{|t|}{w}. \tag{5.6}$$

[1] For an analogous situation with two Higgs doublets, see, for example [165].

Keeping aside the charged Goldstone boson, the mass-squared of the singly-charged physical scalar is obtained as

$$m_{H^+}^2 = \left(q + \frac{h}{2}\right)(v^2 + 2w^2), \tag{5.7}$$

while the doubly-charged scalar mass is expressed as

$$m_{\Delta^{++}}^2 = (h+q)v^2 + 2fw^2. \tag{5.8}$$

Thus, in the limit $w \ll v$,

$$m_{\Delta^{++}}^2 - m_{H^+}^2 \simeq \frac{h}{2}v^2. \tag{5.9}$$

Therefore, a substantial mass splitting between $\Delta^{++}$ and $H^+$ is in general difficult. This tends to disfavour the $H^+W^+$ decay channel of $\Delta^{++}$, as compared to $\ell^+\ell^+$ and $W^+W^+$, as already been pointed out in the previous chapter.

## 5.3 Two scalar triplets and a CP-violating phase

We write down the expressions for the triplets and the scalar potential involving them once more for the sake of completeness. The $Y = 2$ triplet scalars $\Delta_1$, $\Delta_2$, both written as 2×2 matrices [147]:

$$\Delta_1 = \begin{pmatrix} \delta_1^+ & \sqrt{2}\delta_1^{++} \\ \sqrt{2}\delta_1^0 & -\delta_1^+ \end{pmatrix} \quad \text{and} \quad \Delta_2 = \begin{pmatrix} \delta_2^+ & \sqrt{2}\delta_2^{++} \\ \sqrt{2}\delta_2^0 & -\delta_2^+ \end{pmatrix}. \tag{5.10}$$

The vev's of the scalar triplets are given by [147]

$$\langle\Delta_1\rangle_0 = \begin{pmatrix} 0 & 0 \\ w_1 & 0 \end{pmatrix} \quad \text{and} \quad \langle\Delta_2\rangle_0 = \begin{pmatrix} 0 & 0 \\ w_2 & 0 \end{pmatrix}. \tag{5.11}$$

The vev of the Higgs doublet is as usual given by equation (5.2).

The scalar potential in this model involving $\phi$, $\Delta_1$ and $\Delta_2$ is given by [147],

$$\begin{aligned} V(\phi, \Delta_1, \Delta_2) = \\ & a\,\phi^\dagger\phi + \frac{1}{2}\,b_{kl}\,\mathrm{Tr}\,(\Delta_k^\dagger\Delta_l) + c(\phi^\dagger\phi)^2 + \frac{1}{4}\,d_{kl}\left(\mathrm{Tr}\,(\Delta_k^\dagger\Delta_l)\right)^2 \\ & + \frac{1}{2}\,(e_{kl} - h_{kl})\,\phi^\dagger\phi\,\mathrm{Tr}\,(\Delta_k^\dagger\Delta_l) + \frac{1}{4}\,f_{kl}\,\mathrm{Tr}\,(\Delta_k^\dagger\Delta_l^\dagger)\,\mathrm{Tr}\,(\Delta_k\Delta_l) \\ & + h_{kl}\,\phi^\dagger\Delta_k^\dagger\Delta_l\phi + g\,\mathrm{Tr}\,(\Delta_1^\dagger\Delta_2)\,\mathrm{Tr}\,(\Delta_2^\dagger\Delta_1) + g'\,\mathrm{Tr}\,(\Delta_1^\dagger\Delta_1)\,\mathrm{Tr}\,(\Delta_2^\dagger\Delta_2) \\ & + \left(t_k\,\phi^\dagger\Delta_k\tilde{\phi} + \mathrm{H.c.}\right), \end{aligned} \tag{5.12}$$

where summation over $k, l = 1, 2$ is understood.

In the previous chapter, all the vev's as well the parameters in the potential were assumed to be real. As has already been mentioned, this need not be the situation in general. To see the phenomenology including CP-violation, we make a minimal extension of the simplified scenario by postulating *one* CP-violating phase to exist. This entails a complex vev for any one triplet (in our case we have chosen it to be $\Delta_1$). At the same time, there is a complex phase in the coefficient $t_1$ of the trilinear term in the potential. Thus one can write $t_1 = |t_1|\, e^{i\beta}$ and $w_1 = |w_1|\, e^{i\alpha}$.

Using considerations very similar to those for the single-triplet model, we have taken

$$a,\, b_{kl} \sim v^2; \quad c,\, d_{kl},\, e_{kl},\, h_{kl},\, f_{kl},\, g,\, g' \sim 1; \quad |t_k| \ll v. \tag{5.13}$$

We have chosen to restrict ourselves to cases where $w_1, w_2 \ll v$, keeping in mind the constraint on the $\rho$-parameter.

As in the previous chapter, we use the smallness of the triplet vev's $w_k$, and drop the quartic terms in the scalar triplets during the diagonalisation of the mass matrices. This enables one to use approximate analytical expressions, which makes our broad conclusions somewhat transparent. However, the numerical results presented in section 5.4 are obtained using the full potential (5.12), including the effects of the triplet vev's.

For convenience we define the following matrices and vectors [147]:

$$B = (b_{kl}), \qquad E = (e_{kl}), \qquad H = (h_{kl}), \tag{5.14}$$

$$t = \begin{pmatrix} |t_1| cos\beta \\ t_2 \end{pmatrix}, t' = \begin{pmatrix} |t_1| sin\beta \\ 0 \end{pmatrix}, w = \begin{pmatrix} |w_1| cos\alpha \\ w_2 \end{pmatrix}, w' = \begin{pmatrix} |w_1| sin\alpha \\ 0 \end{pmatrix}. \tag{5.15}$$

In terms of the parameters defined in equations 5.14 and 5.15, the conditions for a stationary point of the potential are [147]

$$\left(B + \frac{v^2}{2}(E - H)\right) w + v^2\, t = 0, \tag{5.16}$$

$$a + cv^2 + \frac{1}{2} w^T (E - H) w + 2\, t \cdot w + 2t' \cdot w' + \frac{1}{2} w'^T (E - H) w' = 0, \tag{5.17}$$

$$(b_{11} + \frac{v^2}{2}(e_{11} - h_{11}))|w_1| sin\alpha - v^2 |t_1| sin\beta = 0, \tag{5.18}$$

using the notation $t \cdot w = \sum_k t_k w_k$. These three equations are exact if one neglects all terms quartic in the triplet vev's in $V_0 \equiv V(\langle\phi\rangle_0, \langle\Delta\rangle_0)$. In equation (5.17) we have already

divided by $v$, assuming $v \neq 0$. The small vev's $w_k$ are thereafter obtained as [147]

$$w = -v^2 \left( B + \frac{1}{2} v^2 (E - H) \right)^{-1} t. \tag{5.19}$$

And from equation (5.18) the phase of $t_1$ can be expressed as [147]

$$sin\beta = \frac{v^{-2}(b_{11} + \frac{v^2}{2}(e_{11} - h_{11}))|w_1| sin\alpha}{|t_1|} \tag{5.20}$$

This re-iterates the fact that the phases $t_1$ and $w_1$ are related to each other. It is also evident from (5.20) that the value of the angle $\alpha$ has to be $n\pi$ where $n = 0, 1, 2, 3....$ when the phase $\beta$ is absent.

Next we discuss the mass matrices of charged scalars. The mass matrix of the doubly-charged scalars is obtained as [147]

$$\mathcal{M}^2_{++} = B + \frac{v^2}{2} (E + H) . \tag{5.21}$$

It is interesting to note that if we drop those quartic terms for simplification from our scalar potential, then our doubly charged mass matrix remains the same as in the previous chapter. This gives the impression that the relative phase between triplets does not affect the doubly charged mass matrix if we drop the quartic terms in the potential. But in our numerical calculation, where we have taken the full scalar potential including the quartic terms, we find such a dependence, arising obviously from the quartic terms. This will be discussed further in the next section.

As for the singly-charged fields $\Delta^+_k$, one has to consider their mixing with $\phi^+$, the would-be Goldstone boson of the Standard Model. We write the mass term as [147]

$$-\mathcal{L}^{\pm}_S = \left(\delta^-_1, \delta^-_2, \phi^-\right) \mathcal{M}^2_+ \begin{pmatrix} \delta^+_1 \\ \delta^+_2 \\ \phi^+ \end{pmatrix} + \text{h.c.}, \tag{5.22}$$

equation (5.12) leads to [147]

$$\mathcal{M}^2_+ = \begin{pmatrix} B + \frac{v^2}{2} E & \sqrt{2} v \left(t - Hw/2\right) \\ \sqrt{2} v \left(t - Hw/2\right)^\dagger & a + cv^2 + \frac{1}{2} w^T (E + H) w + \frac{1}{2} w'^T (E + H) w' \end{pmatrix}. \tag{5.23}$$

This mass matrix must have a zero eigenvalue, corresponding to the Goldstone boson. Indeed, on substituting the minimization equations (5.16), (5.17) and (5.18), we find that [147]

$$Det(\mathcal{M}^2_+) = 0, \tag{5.24}$$

which ensures a consistency check.

As in the previous chapter, the mass matrices (5.21) and (5.23) are diagonalized by [147]

$$U_1^\dagger \mathcal{M}_{++}^2 U_1 = \text{diag}\,(M_1^2, M_2^2) \quad \text{and} \quad U_2^\dagger \mathcal{M}_{+}^2 U_2 = \text{diag}\,(\mu_1^2, \mu_2^2, 0), \tag{5.25}$$

respectively, with [147]

$$\begin{pmatrix} \delta_1^{++} \\ \delta_2^{++} \end{pmatrix} = U_1 \begin{pmatrix} H_1^{++} \\ H_2^{++} \end{pmatrix}, \quad \begin{pmatrix} \delta_1^{+} \\ \delta_2^{+} \\ \phi^{+} \end{pmatrix} = U_2 \begin{pmatrix} H_1^{+} \\ H_2^{+} \\ G^{+} \end{pmatrix}. \tag{5.26}$$

We have denoted the fields with definite mass by $H_k^{++}$ and $H_k^{+}$; and $G^+$ is the charged Goldstone boson.

We also outline the neutral sector of the model, which now cannot be separated into CP-even and CP-odd sectors. Thus the mass matrix for the neutral sector of the present scenario turns out to be a $6 \times 6$ matrix , including mixing between real and imaginary parts of the complex neutral fields. The symmetric neutral mass matrix is denoted by $\mathcal{M}_{neut}$. So, the mass term for the neutral part can be written as [147] :

$$-\mathcal{L}_S^0 = (N_{01}, N_{02}, N_{03}, N_{04}, N_{05}, N_{06})\, \mathcal{M}_{neut}^2 \begin{pmatrix} N_{01} \\ N_{02} \\ N_{03} \\ N_{04} \\ N_{05} \\ N_{06} \end{pmatrix} + \text{h.c.}, \tag{5.27}$$

Where $N_{0n}$'s are the neutral states in flavor basis. This mass matrix is diagonalized by [147]

$$U_3^\dagger \mathcal{M}_{neut}^2 U_3 = \text{diag}\,(M_{01}^2, M_{02}^2, M_{03}^2, M_{04}^2, M_h^2, 0) \tag{5.28}$$

with [147]

$$\begin{pmatrix} N_{01} \\ N_{02} \\ N_{03} \\ N_{04} \\ N_{05} \\ N_{06} \end{pmatrix} = U_3 \begin{pmatrix} H_{01} \\ H_{02} \\ H_{03} \\ H_{04} \\ h \\ G_0 \end{pmatrix}. \tag{5.29}$$

Where $h$ is identified with the SM-like Higgs boson and $G_0$ is the neutral Goldstone boson.

It is interesting to note that once we remove the phases of coefficient of trilinear term in scalar potential and the vev of triplet $H_1^{++}$ by setting $\alpha = \beta = 0$ , then the mixing between the CP-even and CP-odd scalars vanishes and we get back the usual separate $3 \times 3$ matrices for these two sectors. This also serves as a consistency check for the model.

The $\Delta L = 2$ Yukawa interactions of the triplets are [147]

$$\mathcal{L}_Y = \frac{1}{2} \sum_{k=1}^{2} y_{ij}^{(k)} L_i^T C^{-1} i\tau_2 \Delta_k L_j + \text{h.c.}, \tag{5.30}$$

where $C$ is the charge conjugation matrix, the $y_{ij}^{(k)}$ are the symmetric Yukawa coupling matrices of the triplets $\Delta_k$, and the $i, j$ are the summation indices over the three neutrino flavours. The charged-lepton mass matrix is diagonal in this basis.

The neutrino mass matrix is generated from $\mathcal{L}_Y$ as [147]

$$(M_\nu)_{ij} = y_{ij}^{(1)} |w_1| cos\alpha + y_{ij}^{(2)} w_2. \tag{5.31}$$

This relates the Yukawa coupling constants $y_{ij}^{(1)}$, $y_{ij}^{(2)}$ and the real part of the triplet vev's, namely, $|w_1|cos\alpha$ and $w_2$.

The neutrino mass eigenvalues are fixed according to a particular type of mass spectrum. In this chapter also, we illustrate our points, without any loss of generality, in the context of normal hierarchy, setting the lowest neutrino mass eigenvalue to zero. Again, the elements of the neutrino mass matrix $M_\nu$ can be found by using

$$M_\nu = U^\dagger \hat{M}_\nu U, \tag{5.32}$$

where $U$ is the PMNS matrix already defined in the previous chapter. $\hat{M}_\nu$ is the diagonal matrix of the neutrino masses. We have followed the same procedure, as described in the previous chapter, to compute the elements of $U$. Also, the phase $\delta$ has been set to zero. For $\theta_{13}$, we have used the results from the Daya Bay and RENO experiments [29,30].

All terms on the right-hand side of equation (5.30) are approximately known, which is sufficient for predicting phenomenology in the 100 GeV - 1 TeV scale.. The actual mass matrix thus constructed, on numerical evaluation, approximately reflects a two-zero texture which is one of the motivations of this study.

For each benchmark point used in the next section, $w_1$ and $w_2$ get determined by values of the other parameters in the scalar potential. Of course, the coupling matrices $y^{(1)}$ and $y^{(2)}$ are still indeterminate in this case also. We fix the matrix elements of $y^{(2)}$ and $y^{(1)}$ following the same method used in the previous chapter and it has already been mentioned there that our broad conclusions do not depend on this 'working rule'.

Of couse, the success of a two-triplet scenario in the context of a seesaw mechanism requires the electroweak vacuum to be (meta)stable till at least the seesaw scale. In general, the tendency of the top quark yukawa coupling to turn the doublet quartic couplings negative is resposible for the loss of stability. Additional scalar quartic couplings usually offsets this effect [166], and the present scenario is no exception. It been shown in [167] that one can ensure stability upto $10^{16-18}GeV$ with a single triplet. With the low-energy quartic couplings not too different from these and with one more triplet interacting with the doublet, the situation is even more optimistic. Moreover, the acceptence of a metastable electroweak vacuum can help the scenario even further.

## 5.4 Benchmark points and numerical predictions

The trademark signal of Higgs triplets is contained in the doubly charged components. In the current scenario, too, one would like to see the signatures of the two doubly charged scalars, especially the heavier one, namely $H_1^{++}$ whose decays have already been shown to contain a rather rich phenomenology.

The $H_1^{++}$, produced at the LHC via the Drell-Yan process can, in general, have two-body decays through the following channels [147]:

$$H_1^{++} \rightarrow H_2^{++}h, \tag{5.33}$$
$$H_1^{++} \rightarrow \ell_i^+\ell_j^+, \tag{5.34}$$
$$H_1^{++} \rightarrow W^+W^+, \tag{5.35}$$
$$H_1^{++} \rightarrow H_2^+W^+, \tag{5.36}$$
$$H_2^{++} \rightarrow \ell_i^+\ell_j^+, \tag{5.37}$$
$$H_2^{++} \rightarrow W^+W^+, \tag{5.38}$$

with $h$ is the SM-like Higgs and $\ell_i, \ell_j = e, \mu$.

The decay modes (5.33)and (5.36) are absent in the single-triplet model. On the other hand, mixing between two triplets opens up situations where the mass separation between $H_1^{++}, H_2^{++}$ and $H_1^{++}, H_2^+$ is sufficient to kinematically allow the transitions (5.33) and (5.36). The decay (5.33) opens up a spectacular signal, especially when $H_2^{++}$ mostly decays into two same sign leptons, leading to

$$H_1^{++} \rightarrow \ell_i^+\ell_j^+h \tag{5.39}$$

Let us denote the mass of SM Higgs by $M_h$, that of $H_k^{++}$ by $M_k$ and that of $H_k^+$ by $\mu_k$ ($k = 1, 2$). Then, in the convention $M_1 > M_2$, $\mu_1 > \mu_2$, the decays (5.33)and (5.36) are possible only if $M_1 > M_2 + M_h$ and $M_1 > \mu_2 + m_W$. We demonstrate numerically that this can naturally happen by considering three distinct regions of the parameter space and selecting four benchmark points (BPs) for each region. The relative phase between two triplets also a plays an important roll in these cases. In order to emphasise this, we have also chosen three different values of the phase, namely $\alpha = 30^\circ, 45^\circ$ and $60^\circ$ for each benchmark point. Thus we have considered 36 BPs alltogether, comprising three distinct regions of the parameter space and relative phases between triplets to justify our findings.

We have seen that, in a single-triplet model, the doubly-charged Higgs decays into either $\ell_i^+\ell_j^+$ or $W^+W^+$. The former is controlled by the $\Delta L = 2$ Yukawa couplings $y_{ij}$, while the latter is driven by $w$, the triplet vev. Neutrino masses are given by (5.31), implying large values of $y_{ij}$ for small $w$ and vice versa. Interestingly, the presence of triplet phase through the $cos\alpha$ term in this equation actually suppresses the effect of vev $w_1$ of the first triplet. This in turn implies that we get higher values for Yukawa coupling matrix entries $y_1^{ij}$ compared to the case where CP-violating effects are absent. In this chapter also, we have identified, for the chosen values of triplet phase, three regions in the parameter space, corresponding to [147]

i) $\Gamma(H_{1,2}^{++} \to \ell_i^+\ell_j^+) \ll \Gamma(H_{1,2}^{++} \to W^+W^+)$,

ii) $\Gamma(H_{1,2}^{++} \to \ell_i^+\ell_j^+) \gg \Gamma(H_{1,2}^{++} \to W^+W^+)$,

iii) $\Gamma(H_{1,2}^{++} \to \ell_i^+\ell_j^+) \sim \Gamma(H_{1,2}^{++} \to W^+W^+)$.

These are referred to as scenarios 1, 2 and 3 respectively in the subsequent discussion.

The masses of the various physical scalars and some of their phenomenological properties are shown in Tables 5.1-5.9. Although our study involves mainly the phenomenology of charged scalars, we have also listed the masses of neutral scalars. Values of the parameters occuring in the scalar potential have been used appropriately for obtaining these benchmark values of masses. Once more, there emerges a 125 GeV scalar whose interactions are consistent with the observed signal strengths at the LHC.

In the previous chapter, we had concentrated on those benchmark points in the parameter space, for which $H_1^{++} \to H_2^+W^+$ becomes a dominant decay mode. In the present chapter, we draw the reader's attention to an interesting complementary situation : one can have, in certain regions of the parameter space, $H_1^{++} \to H_2^{++}h$ as the dominant channel in $H_1^{++}$ decay. Since the triplet masses are free parameters, this can of course happen

without any 'theoretical design'. However. the presence of the CP-violating phase can also play an interesting role here. This is demonstated in Figure 5.1. To understand the situation, suppose the mass parameters in the potential are fixed in such a way that the decay $H_1^{++} \to H_2^{++}h$ is not possible for $\alpha = 0$. Now, if the CP-violating phase $\alpha$ is gradually increased from zero, keeping all other parameters fixed, then both the mass differences $m_{H_1^{++}} - m_{H_2^{++}}$ and $m_{H_1^{++}} - m_{H_2^{+}}$ start increasing rather sharply for $\alpha \gtrsim 60^\circ$. This is because the degree of doublet-triplet mixing for $\Delta_1$ in our parametrisation changes with $\alpha$. In such situations, as shown, for example, in Table 5.9, the quartic couplings cause the decay $H_1^{++} \to H_2^{++}h$ to dominate over $H_1^{++} \to H_2^{+}W^{+}$. Thus, other than the free parameters corresponding to the scalar masses, the CP-violating phase has a part to play in the phenomenology of a two-triplet scenario. One consequence of this will be discussed below.

Earlier, we neglected contributions from the quartic terms in our scalar potential in the approximate forms of the doubly and singly-charged mass matrices. However, the import of the phase is not properly captured unless one retains these terms. Thus it is only via a full numerical analysis of the potential retaining all terms that the above effect of the phase of the trilinear term becomes apparent.

It should also be noted that the cosine of the complex phase suppresses the contribution to neutrino masses. Consequently, for the same triplet vev, one requires larger values of the Yukawa interaction strengths. This makes the $l^+l^+$ decay mode of a doubly charged scalar more competitive with $W^+W^+$, as compared to the results presented in the previous chapter.

The branching ratios for a given scalar in different channels are of course dependent on the various parameters that characterise a BP. We list all the charged scalar masses in Tables 5.1, 5.4 and 5.7. Moreover, the neutral scalar masses are shown in Tables 5.2, 5.5 and 5.8 for three different values of triplet phase $\alpha$. The branching ratios for $H_1^{++}$ and $H_2^{++}$ for different triplet phases are listed in Tables 5.3,5.6 and 5.9, together with their pair-production cross sections at the LHC with $\sqrt{s} = 13\,\text{TeV}$. The cross sections and branching ratios have been calculated with the help of the package FeynRules (version 1.6.0) [159, 160], thus creating a new UFO model file in MadGraph5-aMC@NLO (version 2.3.3) [168]. Using the full machinery of scalar mixing in this model, the decay widths into various channels have been obtained.

From Tables 5.3, 5.6 and 5.9, we see that decay (5.39) dominates, when the masses of $H_1^{++}$ and $H_2^{++}$ are sufficiently separated. Also, when the phase space needed for this decay (5.39) is not available, the process (5.36) dominates over all other remaining decays.

Benchmark points when decay (5.36) mostly dominates for $H_1^{\pm\pm}$ have been discussed in detail in the previous chapter. Here we supplement those observations with some results for the case when decay (5.39) has an interesting consequence, as exemplitied by Figures 5.2 and 5.3.

Figure 5.2 specifically shows the effect of enhancement of the CP-violating phase. We have seen in Figure 5.1 that $m_{H_1^{++}} - m_{H_2^{++}}$ goes up for $\alpha \gtrsim 60^\circ$. With this in view, the plots in Figure 5.2 has been drawn for a case where both of the doubly-charged scalars have appreciable coupling to same-sign dileptons. In the left panel of Figure 5.2, where the phase is lower, one notices two such dilepton pair peaks. The leptons selected for this purpose satisfy: $\left|p_T^{\rm lepton}\right| > 20$ GeV, $|\eta_{\rm lep}| < 2.5$, $|\Delta R_{\ell\ell}| > 0.2$ and $|\Delta R_{\ell {\rm j}}| > 0.4$ where $\Delta R^2 = \Delta\eta^2 + \Delta\phi^2$. Each peak is the result of Drell-Yan pair production of the corresponding doubly-charged scalar and the presence of two triplets is clearly discernible from the peaks themselves. In the right panel of Figure 5.2, however, with $\alpha = 65^\circ$, one notices only the lower mass peak. This is because the decay $H_1^{++} \to H_2^{++}h$ then reigns supreme. As a result, one notices only lower mass peak, but events in association with an SM-like Higgs are noticeable. Thus the signature of two triplets shows an interesting dichotomy of LHC signsls, depending on the value of the CP-violating phase.

Figure 5.3 further elaborates the first of the above situations. The plots there bear testimony to the situation where two peaks are still visible. Table 5.10 contains the numerical values of the number of events around each peak, for five of our benchmark spectra, with varying phase. The numbers are illustrated for an integrated luminosity of $2500 fb^{-1}$. The number of events corresponding to a bin within $\pm 20 GeV$ of the invariant mass peak. From this, we clearly expect several hundred events around the lower mass peak and $60 - 140$ events around the higher one.

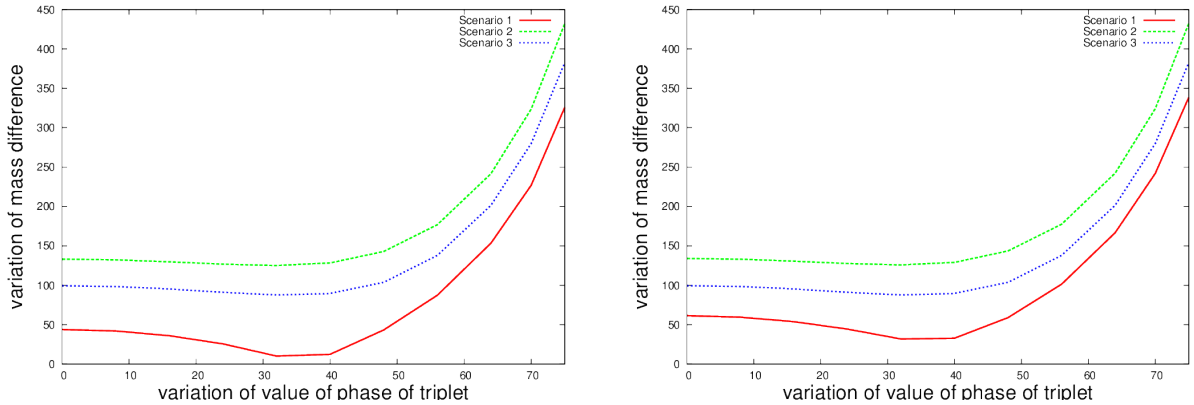


Figure 5.1: Variation of mass difference between (left panel) $\mathcal{H}_1^{++}$ and $\mathcal{H}_2^{++}$ and (right panel) $\mathcal{H}_1^{++}$ and $\mathcal{H}_2^{+}$ with phase of triplet $\alpha$ for BP 1 of scenario 1 and BP 3 of scenario 2 for $\alpha = 30°$, BP 4 of scenario 2 for $\alpha = 60°$

| $\alpha = 30°$ | Mass (GeV) | BP 1 | BP 2 | BP 3 | BP 4 |
|---|---|---|---|---|---|
| Scenario 1 | $H_1^{++}$ | 516.61 | 513.83 | 522.13 | 537.62 |
| | $H_2^{++}$ | 391.40 | 389.82 | 426.93 | 440.96 |
| | $H_1^{+}$ | 516.58 | 513.81 | 522.10 | 537.55 |
| | $H_2^{+}$ | 390.60 | 389.79 | 408.83 | 416.30 |
| Scenario 2 | $H_1^{++}$ | 526.00 | 529.85 | 477.38 | 485.76 |
| | $H_2^{++}$ | 397.61 | 390.10 | 389.10 | 389.33 |
| | $H_1^{+}$ | 525.94 | 529.80 | 477.34 | 485.70 |
| | $H_2^{+}$ | 393.79 | 390.01 | 389.00 | 389.28 |
| Scenario 3 | $H_1^{++}$ | 558.71 | 562.35 | 485.76 | 477.38 |
| | $H_2^{++}$ | 427.00 | 407.20 | 389.33 | 389.10 |
| | $H_1^{+}$ | 557.59 | 559.11 | 485.70 | 477.34 |
| | $H_2^{+}$ | 392.90 | 405.91 | 389.28 | 389.00 |

Table 5.1: Charged scalar masses for phase $\alpha = 30°$.

| $\alpha = 30^\circ$ | Mass (GeV) | BP 1 | BP 2 | BP 3 | BP 4 |
|---|---|---|---|---|---|
| Scenario 1 | $H_{01}$ | 730.57 | 726.65 | 738.36 | 760.19 |
| | $H_{02}$ | 730.49 | 726.62 | 738.32 | 760.15 |
| | $H_{03}$ | 552.30 | 551.25 | 551.40 | 552.65 |
| | $H_{04}$ | 552.15 | 551.20 | 551.34 | 552.56 |
| | $h$ | 125.16 | 125.18 | 125.20 | 125.15 |
| Scenario 2 | $H_{01}$ | 743.85 | 749.33 | 675.11 | 686.96 |
| | $H_{02}$ | 743.00 | 749.25 | 675.00 | 686.90 |
| | $H_{03}$ | 552.21 | 551.50 | 550.17 | 550.53 |
| | $H_{04}$ | 552.10 | 551.39 | 550.05 | 550.40 |
| | $h$ | 125.21 | 125.18 | 125.22 | 125.23 |
| Scenario 3 | $H_{01}$ | 787.10 | 789.25 | 687.00 | 676.15 |
| | $H_{02}$ | 787.00 | 789.10 | 686.90 | 676.08 |
| | $H_{03}$ | 541.16 | 542.00 | 552.21 | 549.90 |
| | $H_{04}$ | 541.07 | 541.91 | 552.00 | 549.75 |
| | $h$ | 125.23 | 125.26 | 125.13 | 125.16 |

Table 5.2: Neutral scalar masses for phase $\alpha = 30^\circ$.

| $\alpha = 30^\circ$ | Data | BP 1 | BP 2 | BP 3 | BP 4 |
|---|---|---|---|---|---|
| Scenario 1 | BR($H_1^{++} \to H_2^{++}h$) | $5.1 \times 10^{-3}$ | not allowed | not allowed | not allowed |
| | BR($H_1^{++} \to H_2^{+}W^{+}$) | 0.99 | 0.99 | 0.79 | 0.99 |
| | BR($H_1^{++} \to W^{+}W^{+}$) | $2.8 \times 10^{-3}$ | $6.5 \times 10^{-2}$ | 0.21 | $< 10^{-6}$ |
| | BR($H_1^{++} \to \ell_i^{+}\ell_j^{+}$) | $< 10^{-20}$ | $< 10^{-19}$ | $< 10^{-17}$ | $< 10^{-22}$ |
| | BR($H_2^{++} \to W^{+}W^{+}$) | 0.99 | 0.99 | 0.99 | 0.99 |
| | BR($H_2^{++} \to \ell_i^{+}\ell_j^{+}$) | $< 10^{-17}$ | $< 10^{-17}$ | $< 10^{-16}$ | $< 10^{-19}$ |
| | $\sigma(pp \to H_1^{++}H_1^{--})$ | 1.10 fb | 1.13 fb | 1.05 fb | 0.42 fb |
| | $\sigma(pp \to H_2^{++}H_2^{--})$ | 3.97 fb | 4.10 fb | 2.70 fb | 1.06 fb |
| Scenario 2 | BR($H_1^{++} \to H_2^{++}h$) | 0.84 | 0.96 | not allowed | not allowed |
| | BR($H_1^{++} \to H_2^{+}W^{+}$) | 0.13 | 0.03 | 0.76 | 0.42 |
| | BR($H_1^{++} \to W^{+}W^{+}$) | $< 10^{-19}$ | $< 10^{-19}$ | $< 10^{-18}$ | $< 10^{-20}$ |
| | BR($H_1^{++} \to \ell_i^{+}\ell_j^{+}$) | 0.03 | $8.9 \times 10^{-3}$ | 0.24 | 0.58 |
| | BR($H_2^{++} \to W^{+}W^{+}$) | $< 10^{-18}$ | $< 10^{-18}$ | $< 10^{-19}$ | $< 10^{-18}$ |
| | BR($H_2^{++} \to \ell_i^{+}\ell_j^{+}$) | 0.99 | 0.99 | 0.99 | 0.99 |
| | $\sigma(pp \to H_1^{++}H_1^{--})$ | 1.01 fb | 1.02 fb | 1.56 fb | 1.43 fb |
| | $\sigma(pp \to H_2^{++}H_2^{--})$ | 3.60 fb | 4.04 fb | 3.97 fb | 3.95 fb |
| Scenario 3 | BR($H_1^{++} \to H_2^{++}h$) | 0.99 | 0.99 | not allowed | not allowed |
| | BR($H_1^{++} \to H_2^{+}W^{+}$) | $2.1 \times 10^{-3}$ | $1.3 \times 10^{-2}$ | 0.99 | 0.99 |
| | BR($H_1^{++} \to W^{+}W^{+}$) | $< 10^{-13}$ | $< 10^{-13}$ | $< 10^{-9}$ | $< 10^{-10}$ |
| | BR($H_1^{++} \to \ell_i^{+}\ell_j^{+}$) | $< 10^{-10}$ | $< 10^{-10}$ | $< 10^{-6}$ | $< 10^{-7}$ |
| | BR($H_2^{++} \to W^{+}W^{+}$) | 0.03 | 0.01 | 0.04 | 0.02 |
| | BR($H_2^{++} \to \ell_i^{+}\ell_j^{+}$) | 0.97 | 0.99 | 0.96 | 0.98 |
| | $\sigma(pp \to H_1^{++}H_1^{--})$ | 0.77 fb | 0.74 fb | 1.45 fb | 1.58 fb |
| | $\sigma(pp \to H_2^{++}H_2^{--})$ | 3.61 fb | 2.75 fb | 3.95 fb | 3.98 fb |

Table 5.3: Decay branching ratios and production cross sections for doubly-charged scalars for phase $\alpha = 30^\circ$.

| $\alpha = 45^\circ$ | Mass (GeV) | BP 1 | BP 2 | BP 3 | BP 4 |
|---|---|---|---|---|---|
| Scenario 1 | $H_1^{++}$ | 542.27 | 539.35 | 549.85 | 566.55 |
| | $H_2^{++}$ | 406.60 | 405.20 | 438.46 | 450.96 |
| | $H_1^{+}$ | 542.22 | 539.20 | 548.73 | 564.92 |
| | $H_2^{+}$ | 405.90 | 405.07 | 422.28 | 428.94 |
| Scenario 2 | $H_1^{++}$ | 543.30 | 538.15 | 551.62 | 564.34 |
| | $H_2^{++}$ | 405.10 | 404.10 | 440.10 | 448.82 |
| | $H_1^{+}$ | 542.50 | 537.65 | 550.90 | 563.65 |
| | $H_2^{+}$ | 405.00 | 403.20 | 439.72 | 447.90 |
| Scenario 3 | $H_1^{++}$ | 545.82 | 540.32 | 550.90 | 567.80 |
| | $H_2^{++}$ | 409.80 | 405.00 | 439.50 | 452.45 |
| | $H_1^{+}$ | 544.71 | 539.46 | 550.15 | 565.90 |
| | $H_2^{+}$ | 409.00 | 404.75 | 425.38 | 432.80 |

Table 5.4: Charged scalar masses for phase $\alpha = 45^\circ$.

| $\alpha = 45^\circ$ | Mass (GeV) | BP 1 | BP 2 | BP 3 | BP 4 |
|---|---|---|---|---|---|
| Scenario 1 | $H_{01}$ | 766.78 | 762.75 | 774.79 | 797.22 |
| | $H_{02}$ | 766.60 | 762.11 | 774.23 | 797.00 |
| | $H_{03}$ | 573.00 | 572.50 | 575.50 | 576.17 |
| | $H_{04}$ | 572.65 | 572.00 | 575.15 | 575.95 |
| | $h$ | 125.15 | 125.22 | 125.19 | 125.13 |
| Scenario 2 | $H_{01}$ | 768.10 | 760.37 | 772.90 | 795.85 |
| | $H_{02}$ | 768.00 | 760.13 | 772.75 | 795.50 |
| | $H_{03}$ | 575.32 | 570.00 | 574.30 | 576.85 |
| | $H_{04}$ | 575.15 | 569.22 | 573.78 | 576.20 |
| | $h$ | 125.12 | 125.16 | 125.24 | 125.17 |
| Scenario 3 | $H_{01}$ | 771.10 | 758.52 | 778.10 | 798.37 |
| | $H_{02}$ | 770.85 | 758.00 | 777.85 | 798.00 |
| | $H_{03}$ | 577.31 | 568.75 | 578.29 | 577.21 |
| | $H_{04}$ | 577.00 | 568.13 | 578.00 | 577.00 |
| | $h$ | 125.18 | 125.21 | 125.13 | 125.16 |

Table 5.5: Neutral scalar masses for phase $\alpha = 45^\circ$.

| $\alpha = 45^\circ$ | Data | BP 1 | BP 2 | BP 3 | BP 4 |
|---|---|---|---|---|---|
| Scenario 1 | BR($H_1^{++} \to H_2^{++}h$) | 0.99 | 0.99 | not allowed | not allowed |
| | BR($H_1^{++} \to H_2^{+}W^{+}$) | $8.2 \times 10^{-4}$ | $9.1 \times 10^{-4}$ | 0.90 | 0.96 |
| | BR($H_1^{++} \to W^{+}W^{+}$) | $2.4 \times 10^{-5}$ | $1.7 \times 10^{-4}$ | 0.09 | 0.04 |
| | BR($H_1^{++} \to \ell_i^{+}\ell_j^{+}$) | $< 10^{-21}$ | $< 10^{-21}$ | $< 10^{-18}$ | $< 10^{-19}$ |
| | BR($H_2^{++} \to W^{+}W^{+}$) | 0.99 | 0.99 | 0.99 | 0.99 |
| | BR($H_2^{++} \to \ell_i^{+}\ell_j^{+}$) | $< 10^{-18}$ | $< 10^{-18}$ | $10^{-18}$ | $< 10^{-17}$ |
| | $\sigma(pp \to H_1^{++}H_1^{--})$ | 0.88 fb | 0.87 fb | 0.80 fb | 0.71 fb |
| | $\sigma(pp \to H_2^{++}H_2^{--})$ | 3.39 fb | 3.33 fb | 2.43 fb | 2.13 fb |
| Scenario 2 | BR($H_1^{++} \to H_2^{++}h$) | 0.99 | 0.99 | not allowed | not allowed |
| | BR($H_1^{++} \to H_2^{+}W^{+}$) | $4.5 \times 10^{-4}$ | $3.9 \times 10^{-4}$ | 0.64 | 0.88 |
| | BR($H_1^{++} \to W^{+}W^{+}$) | $< 10^{-20}$ | $< 10^{-21}$ | $< 10^{-19}$ | $< 10^{-20}$ |
| | BR($H_1^{++} \to \ell_i^{+}\ell_j^{+}$) | $3.1 \times 10^{-6}$ | $1.7 \times 10^{-4}$ | 0.36 | 0.12 |
| | BR($H_2^{++} \to W^{+}W^{+}$) | $< 10^{-19}$ | $< 10^{-18}$ | $< 10^{-18}$ | $< 10^{-19}$ |
| | BR($H_2^{++} \to \ell_i^{+}\ell_j^{+}$) | 0.99 | 0.99 | 0.99 | 0.99 |
| | $\sigma(pp \to H_1^{++}H_1^{--})$ | 0.93 fb | 0.89 fb | 0.86 fb | 0.75 fb |
| | $\sigma(pp \to H_2^{++}H_2^{--})$ | 2.55 fb | 3.35 fb | 2.46 fb | 2.18 fb |
| Scenario 3 | BR($H_1^{++} \to H_2^{++}h$) | 0.99 | 0.99 | not allowed | not allowed |
| | BR($H_1^{++} \to H_2^{+}W^{+}$) | $3.6 \times 10^{-5}$ | $1.4 \times 10^{-4}$ | 0.99 | 0.99 |
| | BR($H_1^{++} \to W^{+}W^{+}$) | $< 10^{-13}$ | $< 10^{-12}$ | $< 10^{-8}$ | $< 10^{-9}$ |
| | BR($H_1^{++} \to \ell_i^{+}\ell_j^{+}$) | $< 10^{-10}$ | $< 10^{-10}$ | $< 10^{-10}$ | $< 10^{-8}$ |
| | BR($H_2^{++} \to W^{+}W^{+}$) | 0.02 | 0.04 | 0.97 | 0.05 |
| | BR($H_2^{++} \to \ell_i^{+}\ell_j^{+}$) | 0.98 | 0.96 | 0.03 | 0.95 |
| | $\sigma(pp \to H_1^{++}H_1^{--})$ | 0.92 fb | 0.95 fb | 0.84 fb | 0.73 fb |
| | $\sigma(pp \to H_2^{++}H_2^{--})$ | 3.42 fb | 3.37 fb | 2.44 fb | 2.15 fb |

Table 5.6: Decay branching ratios and production cross sections for doubly-charged scalars for phase $\alpha = 45^\circ$.

| $\alpha = 60^\circ$ | Mass (GeV) | BP 1 | BP 2 | BP 3 | BP 4 |
|---|---|---|---|---|---|
| Scenario 1 | $H_1^{++}$ | 557.90 | 563.51 | 564.20 | 556.56 |
| | $H_2^{++}$ | 412.20 | 411.51 | 434.37 | 439.71 |
| | $H_1^{+}$ | 557.62 | 563.25 | 559.18 | 548.00 |
| | $H_2^{+}$ | 411.65 | 411.18 | 423.27 | 426.15 |
| Scenario 2 | $H_1^{++}$ | 558.20 | 565.20 | 566.40 | 554.30 |
| | $H_2^{++}$ | 411.90 | 413.61 | 436.56 | 438.12 |
| | $H_1^{+}$ | 558.00 | 564.50 | 565.90 | 553.65 |
| | $H_2^{+}$ | 410.75 | 412.85 | 435.85 | 435.32 |
| Scenario 3 | $H_1^{++}$ | 556.65 | 560.30 | 567.80 | 552.90 |
| | $H_2^{++}$ | 410.25 | 408.35 | 437.90 | 436.59 |
| | $H_1^{+}$ | 556.00 | 559.75 | 563.21 | 550.00 |
| | $H_2^{+}$ | 409.85 | 407.80 | 425.56 | 429.11 |

Table 5.7: Charged scalar masses for phase $\alpha = 60^\circ$.

| $\alpha = 60^\circ$ | Mass (GeV) | BP 1 | BP 2 | BP 3 | BP 4 |
|---|---|---|---|---|---|
| Scenario 1 | $H_{01}$ | 788.52 | 796.91 | 784.64 | 765.05 |
| | $H_{02}$ | 788.35 | 796.27 | 784.21 | 764.62 |
| | $H_{03}$ | 581.43 | 583.16 | 579.62 | 577.78 |
| | $H_{04}$ | 581.32 | 582.95 | 579.13 | 577.21 |
| | $h$ | 125.16 | 125.24 | 125.14 | 125.20 |
| Scenario 2 | $H_{01}$ | 790.21 | 793.82 | 786.52 | 762.90 |
| | $H_{02}$ | 790.00 | 793.11 | 786.09 | 762.42 |
| | $H_{03}$ | 579.32 | 580.16 | 582.32 | 574.21 |
| | $H_{04}$ | 579.00 | 579.92 | 582.00 | 573.86 |
| | $h$ | 125.15 | 125.10 | 125.21 | 125.09 |
| Scenario 3 | $H_{01}$ | 786.51 | 790.63 | 785.00 | 760.71 |
| | $H_{02}$ | 786.00 | 790.27 | 784.32 | 760.29 |
| | $H_{03}$ | 577.82 | 576.21 | 580.14 | 570.90 |
| | $H_{04}$ | 577.50 | 576.00 | 579.55 | 570.58 |
| | $h$ | 125.23 | 125.14 | 125.23 | 125.18 |

Table 5.8: Neutral scalar masses for phase $\alpha = 60^\circ$.

| $\alpha = 60^\circ$ | Data | BP 1 | BP 2 | BP 3 | BP 4 |
|---|---|---|---|---|---|
| Scenario 1 | BR($H_1^{++} \to H_2^{++}h$) | 0.99 | 0.98 | 0.99 | not allowed |
| | BR($H_1^{++} \to H_2^{+}W^{+}$) | $3.9 \times 10^{-4}$ | $2.6 \times 10^{-2}$ | 0.01 | 0.94 |
| | BR($H_1^{++} \to W^{+}W^{+}$) | $1.7 \times 10^{-5}$ | $8.9 \times 10^{-3}$ | $6.9 \times 10^{-5}$ | 0.05 |
| | BR($H_1^{++} \to \ell_i^{+}\ell_j^{+}$) | $< 10^{-21}$ | $< 10^{-20}$ | $< 10^{-21}$ | $< 10^{-19}$ |
| | BR($H_2^{++} \to W^{+}W^{+}$) | 0.99 | 0.99 | 0.99 | 0.99 |
| | BR($H_2^{++} \to \ell_i^{+}\ell_j^{+}$) | $< 10^{-18}$ | $< 10^{-18}$ | $< 10^{-19}$ | $< 10^{-14}$ |
| | $\sigma(pp \to H_1^{++}H_1^{--})$ | 0.79 fb | 0.71 fb | 0.72 fb | 0.84 fb |
| | $\sigma(pp \to H_2^{++}H_2^{--})$ | 3.22 fb | 3.15 fb | 2.48 fb | 2.51 fb |
| Scenario 2 | BR($H_1^{++} \to H_2^{++}h$) | 0.99 | 0.79 | 0.99 | not allowed |
| | BR($H_1^{++} \to H_2^{+}W^{+}$) | $3.2 \times 10^{-5}$ | 0.21 | $3.1 \times 10^{-3}$ | 0.88 |
| | BR($H_1^{++} \to W^{+}W^{+}$) | $< 10^{-21}$ | $< 10^{-21}$ | $< 10^{-21}$ | $< 10^{-21}$ |
| | BR($H_1^{++} \to \ell_i^{+}\ell_j^{+}$) | $2.1 \times 10^{-4}$ | $1.4 \times 10^{-4}$ | $3.7 \times 10^{-4}$ | 0.12 |
| | BR($H_2^{++} \to W^{+}W^{+}$) | $< 10^{-18}$ | $< 10^{-19}$ | $< 10^{-17}$ | $< 10^{-18}$ |
| | BR($H_2^{++} \to \ell_i^{+}\ell_j^{+}$) | 0.99 | 0.99 | 0.99 | 0.99 |
| | $\sigma(pp \to H_1^{++}H_1^{--})$ | 0.77 fb | 0.74 fb | 0.81 fb | 0.86 fb |
| | $\sigma(pp \to H_2^{++}H_2^{--})$ | 3.26 fb | 3.19 fb | 2.46 fb | 2.53 fb |
| Scenario 3 | BR($H_1^{++} \to H_2^{++}h$) | 0.99 | 0.90 | 0.99 | not allowed |
| | BR($H_1^{++} \to H_2^{+}W^{+}$) | $2.5 \times 10^{-4}$ | 0.10 | $1.2 \times 10^{-2}$ | 0.99 |
| | BR($H_1^{++} \to W^{+}W^{+}$) | $< 10^{-14}$ | $< 10^{-13}$ | $< 10^{-10}$ | $< 10^{-10}$ |
| | BR($H_1^{++} \to \ell_i^{+}\ell_j^{+}$) | $< 10^{-10}$ | $< 10^{-11}$ | $< 10^{-12}$ | $< 10^{-8}$ |
| | BR($H_2^{++} \to W^{+}W^{+}$) | 0.03 | 0.04 | 0.89 | 0.02 |
| | BR($H_2^{++} \to \ell_i^{+}\ell_j^{+}$) | 0.97 | 0.96 | 0.11 | 0.98 |
| | $\sigma(pp \to H_1^{++}H_1^{--})$ | 0.81 fb | 0.75 fb | 0.72 fb | 0.83 fb |
| | $\sigma(pp \to H_2^{++}H_2^{--})$ | 3.28 fb | 3.20 fb | 2.50 fb | 2.54 fb |

Table 5.9: Decay branching ratios and production cross sections for doubly-charged scalars for phase $\alpha = 60^\circ$.

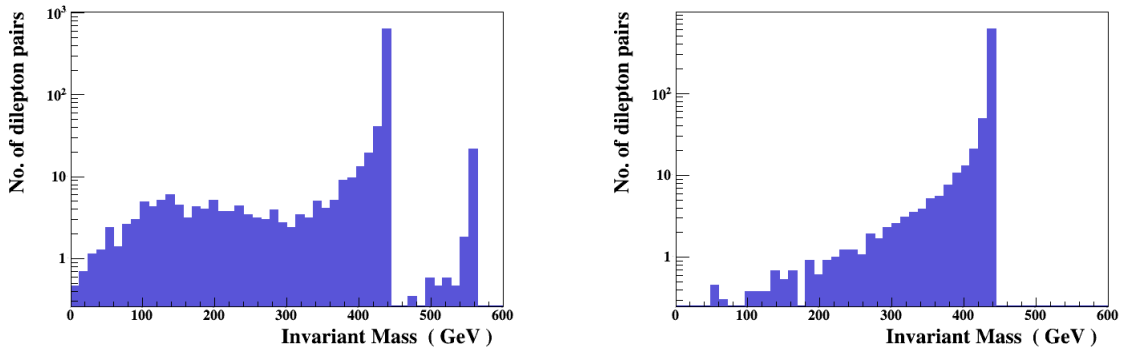


Figure 5.2: Invariant mass distribution of same sign di-leptons for (left panel) $\alpha = 60^{\circ}$ and (right panel) $\alpha = 65^{\circ}$ for BP 4 of Scenario 2

| Benchmark points, Scenario 2 | No. of events at the $H_2^{++}$ peak | No. of events at the $H_1^{++}$ peak |
|---|---|---|
| BP 3 for $\alpha = 30^{\circ}$ | 527 | 100 |
| BP 4 for $\alpha = 30^{\circ}$ | 520 | 139 |
| BP 3 for $\alpha = 45^{\circ}$ | 329 | 65 |
| BP 4 for $\alpha = 45^{\circ}$ | 287 | 60 |
| BP 4 for $\alpha = 60^{\circ}$ | 389 | 72 |

Table 5.10: Number of same-sign dilepton events generated at the LHC, for the benchmark points corresponding to Figure 3. The integrated luminosity is taken to be $2500 fb^{-1}$, for $\sqrt{s} = 13TeV$.

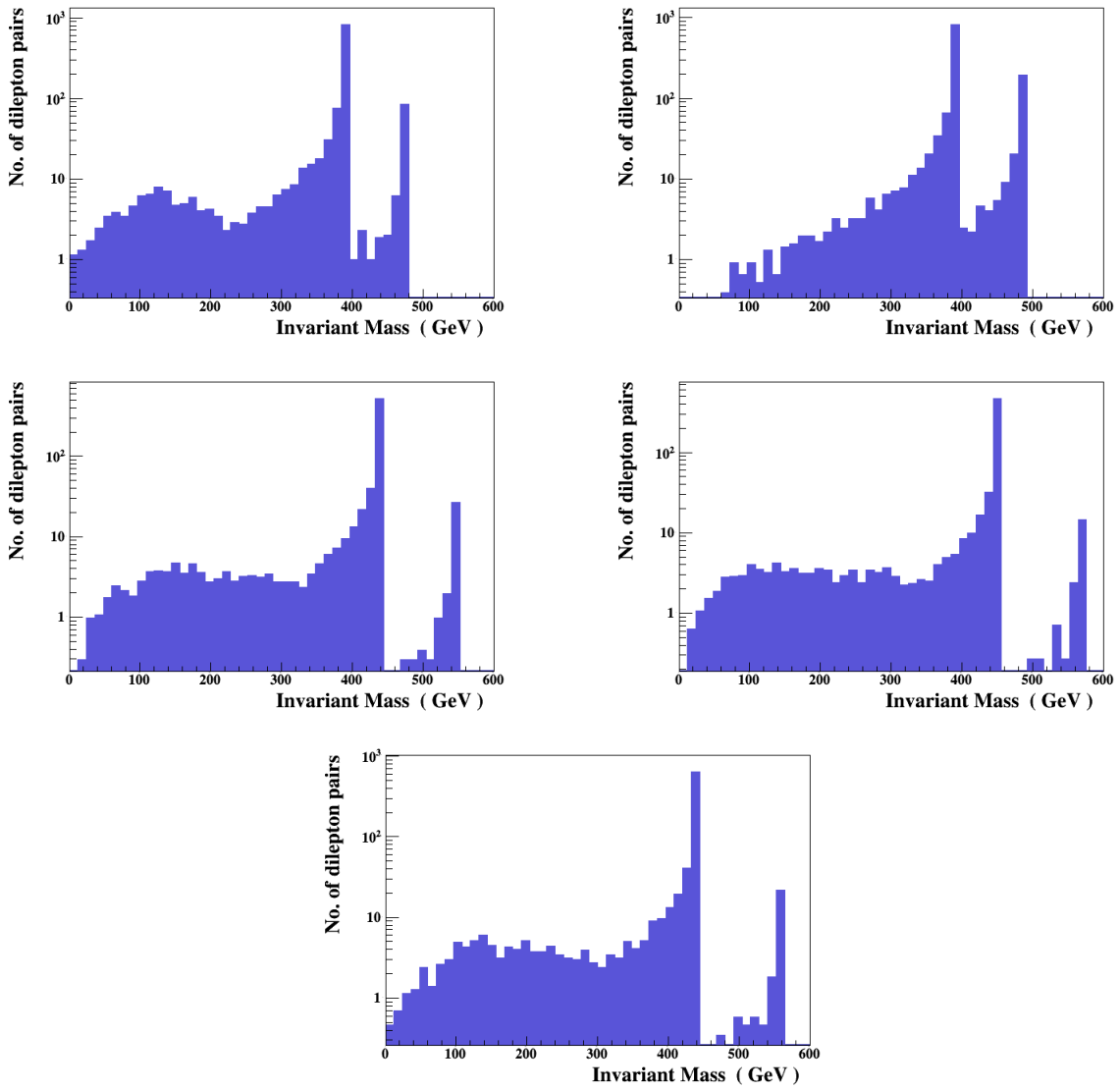


Figure 5.3: Invariant mass distribution of same sign di-leptons for chosen benchmark points. In the top (left panel) BP 3 and (right panel) BP 4 of Scenario 2 for $\alpha = 30°$. In the middle (left panel) BP 3 and (right panel) BP 4 of Scenario 2 for $\alpha = 45°$. In the bottom, BP 4 of Scenario 2 for $\alpha = 60°$.

## 5.5 Conclusions

We have considered a one-doublet, two-triplet Higgs scenario, with one CP-violating phase in the potential. It is noticed that a larger phase leads to bigger mass-separations between the two doubly-charged mass eigenstates, and also between the states $H_1^{++}$ and $H_2^+$. Consequently, this scenario admits a larger region of the parameter space, when the decay $H_1^{++} \to H_2^{++}h$ opens up. When it is allowed, this decay often overrides $H_1^{++} \to H_2^+W^+$. While the role of the latter decay as a characteristic signal of such models was discussed in our earlier work, we emphasize here that the former mode leads to another interesting signal, arising from $H_1^{++} \to \ell_i^+\ell_j^+h$. This would mean that the production of SM-like Higgs together with same-sign dileptons peaking at the mass of the lighter doubly-charged scalar. Such a signal, too, may give us a distinctive signature of a two-triplet scenario at the LHC.

# Chapter 6

# Dark matter

## 6.1 Introduction

Astrophysical observations during the past few decades produced evidences beyond doubt that most of the matter consisting our universe is non-luminous or dark. The existence of this dark matter (DM) is one of the strongest indications that there should be physics beyond the Standard Model (SM) of particle physics. Numerous indirect observations in the astronomical and cosmological scales [169] such as, accurate measurement of galactic rotation curves, measurements of orbital velocities of individual galaxies in clusters, cluster mass determination via gravitational lensing, precise measurements of the **Cosmic Microwave Background (CMB)** acoustic fluctuations, the abundance of light elements and the mapping of large-scale structures point to the presence of new elementary particles that interact only through the gravitational and (perhaps) weak forces. In addition cosmological simulations based on $\Lambda$**CDM** model [170] successfully predict the observed large-scale structures of the Universe. The Planck satellite mission [171] has published precise measurements of the CMB, which are in complete agreement with the predictions of $\Lambda$CDM model, describing a cosmos dominated by dark energy ($\Lambda$) and cold (i.e non-relativistic) dark matter (CDM). According to the $\Lambda$CDM model, which provides the only platform that can explain all observations till date, our universe is composed of $5\%$ atoms (known matter), $27\%$ dark matter and $68\%$ dark energy.

The first evidence for a dark matter dominance of the Coma galaxy cluster was indicated by astronomer Fritz Zwicky in 1933 [172]. Despite the advancement of our understanding of the amount and distribution of dark matter on various scales, we still don't have any answer to the most basic question – *What is the dark matter made of?* One possible answer is that, it is made of new particles and one must look beyond the standard

paradigm of particle physics to search for them. As a consequence, several more questions arise, like — *Does the dark matter consists of one particle species or involve many? What are the properties of these particles, such as their maases, interaction cross-sections, spin and other quantum numbers? Are these particles absolutely stable or very long-lived (i.e. have half-life longer than the age of the Universe)?* [173] All these are open questions waiting to be explored. In the next section we briefly point out some evidences for the existence of dark matter (DM).

## 6.2 Evidences for dark matter

In this section we will briefly discuss some of the compelling evidences that consolidate the presence of DM in the universe.

- **Galactic rotation curves :** It has been mentioned earlier that the evidence for DM was first discovered by Zwicky. Measurements of the velocity dispersion of galaxies in the Coma cluster led to the conclusion that they could not be bound to the cluster by the gravitational attraction of visible matter (stars, gas, dust) alone.

  Existence of DM was again pointed out in the 1970's by Rubin and others [174]. This is, perhaps, the most convincing evidence for DM till date. The evidence came from the observation that various luminous objects (stars, gas clouds, globular clusters or entire galaxies) move faster than the expectation, if they only felt the gravitational attraction of other visible objects. An important step in this regard was the measurement of galactic rotation curves. The rotational velocity $v$ of an object, as a function of the radius $r$ beyond the visible core of galaxy, indicates that the mass continues to grow with the radius. If all the mass of the galaxy $M$ is assumed to be concentrated at the core, an object of mass $m$ orbiting the galaxy would experience a gravitational force $F = GMm/r^2 = mv^2/r$, and $v = (GM/r)^{1/2}$ i.e $v(r) \propto 1/\sqrt{r}$. Instead, in most galaxies it has been found that $v$ becomes approximately constant up to the largest values of $r$ where the rotation curve can be measured. In our galaxy, $v \simeq 240km/s$ at the location of our solar system, with little change up to the largest observable radius. This observation can be explained by assuming the existence of a *dark halo*, with mass density $\rho(r) \propto 1/r^2$ i.e $M(r) \propto r$. This indicates that galaxies contain more mass than the total amount of masses in stars, gas and other visible objects.

- **Gravitational lensing and Bullet cluster :** Gravitational lensing is the bending (or lensing) of light due to the presence of massive objects. This is a general relativis-

tic phenomenon. Galaxy clusters being highly massive structures show this effect. Due to this effect, a background object seems brighter than it otherwise would appear (see, *e.g.*, [175, 176]). The dark matter present in the galaxy cluster, though not visible, contributes significantly to the total mass of the cluster. The best evidence to date for the existence of DM comes from the weak lensing observations of famous Bullet Cluster (1E0657-558), a unique cluster merger [177], where the lensing effect shows a large amount of dark matter. In addition to this, another property of DM comes out of this cluster merger, the DM halos have passed right through both the gas clouds and appear almost undisturbed after the collision. But the visible gas clouds of both clusters have undergone characteristic changes. It becomes evident from this, that the DM interacts with luminous matter as well as itself very weakly. Also the observation that the lensing effect extends beyond the central (visible) region of the cluster may be interpretated as a pointer to the non-baryonic nature of dark matter.

- **Other observations :** There are many other observations which establishes the existence of DM on a stronger footing. One of the most important phenomenon is the determination of cosmological parameters by the power spectrum of CMB aniosotropy. The best-fit values to the $\Lambda$CDM model gives matter density of the universe as $\Omega_M h^2 = 0.127^{+0.007}_{-0.013}$ and primordial baryon density of the universe as $\Omega_B h^2 = 0.0223^{+0.0007}_{-0.0009}$ [178]. The difference in these two densities clearly indicates that most of the matter component in the universe is not the atoms but something else, thus confirming the existence of DM. This also mandates that the DM is necessarily non-baryonic. Another important way to determine the baryon density of the universe is based on Big-Bang Nucleosynthesis (BBN). The baryon density is consistent with the data obtained from CMB power spectrum, $\Omega_B h^2 = 0.0216^{+0.0020}_{-0.0021}$ [179].

  A new technique to determine matter density $\Omega_M$ uses large-scale structure via the power spectrum in galaxy-galaxy correlation function. As a result of the acoustic oscillation in the baryon-photon fluid, the power spectrum also shows the "baryon oscillation" [180]. Independent of CMB results, they determined the matter density to be $\Omega_M h^2 = 0.130 \pm 0.010$. This is consistent with the CMB data and thus strongly advocates the need for non-baryonic dark matter.

## 6.3 Some properties of dark matter

The observations that give us evidence for DM also shed light on some of the obvious properties of DM. A theory hoping to solve the DM riddle is also guided by these requirements. We enlist below some of the properties of DM indicated by the experminents.

- The DM must be 'dark', i.e., it should have no (or extremely weak) interactions with photons. So it must be electrically neutral. If DM had either a small charge or a small electric or magnetic dipole moment, it would couple to the photon-baryon fluid and thus altering the features of the CMB as well as the matter power spectrum.

- The DM cannot be baryonic. The interaction between DM and baryons should also be weak. A consequence of non-baryonicity is color neutrality, meaning DM particles may not take part in strong interactions, otherwise that particle would just act as baryonic matter. As mentioned above, observations of baryonic acoustic oscillation (BAO) and CMB angular power spectrum disfavour the non-baryonic nature of DM.

- Weak interactions of DM particles are not excluded. But, coupling to the electroweak gauge bosons $W^{\pm}$ and $Z$ must be somewhat weaker than that of other SM particles. Otherwise, direct-detection experiments would already have found such interactions.

- The stability of at least the lightest DM particles must be high and this in turn predicts the DM self-interactions to be rather weak. The lack of impact of cosmic events that influence the baryonic matter distribution, such as the merger of the Bullet cluster, on the DM-distribution imply that the DM particles have to be highly collision-less. Even if the particles in the dark-sector have no coupling to the known SM particles, interactions between particles in the dark-sector eventually affect the structures of DM-halos. For hard-sphere elastic scattering, the constraints are at the level of cross-section per unit dark matter mass $\sigma/m_{\chi} \lesssim 1 cm^2/g$ obtained from observations of the structure of galaxy clusters [181].

- As already mentioned, the DM must be stable. To put it another way, DM must have lifetime larger than the age of the universe.

- Studies on the anisotropies of the CMB radiation spectrum requires the DM to be "cold" that is to say, something that was non-relativistic at the time of decoupling.

keV-range warm dark matter, too is not ruled out.

- DM can not be made up of SM particles as most of them are charged. Within the ambit of SM only neutrinos can be a potential DM candidate. Actually it does contribute in the relic density of DM to a small extent. But it can not be the CDM component, as neutrinos are expected to have masses in sub-eV range [182]. With this small mass it can not probably contribute significantly to the matter density of universe. From the Gunn-Tremaine bound [183] it appears that massive galactic halos can not be made up of neutrinos of mass $\leq 1$ MeV.

Thus it becomes evident that the SM can not accommodate a viable DM candidate. But it is also worth noting that although observations tend to imply that DM is non-baryonic, there are exotic baryonic objects e.g., white dwarfs, neutron stars, super-massive black holes which comprise MAssive Compact Halo Objects (MACHO) [184, 185], which may in principle still contribute partially to the DM content.

## 6.4 Candidates for dark matter

We outline below some potential candidates for DM :

- **WIMPs :** Weakly Interacting Massive Particles(WIMPs), denoted as $\chi$, are particles with mass roughly between 10 GeV and few TeV and cross-sections of approximately weak interaction strength. Within standard cosmology, their present relic density can be calculated reliably if the WIMPs were in thermal and chemical equilibrium with the SM particles after inflation. From particle physics perspective, the early universe was a high energy place where energy and mass could switch from one form to the other according to Einstein's equation $E = mc^2$. Pairs of particles and their antiparticles are being created and annihilated. However, as the universe expands, it cools and as a result, it loses the energy necessary to create particle-antiparticle pairs. For a particular particle, the creation process depends on the mass of the particle — the more is the mass, the more energy is required to produce them. As the temperature decreases the massive particle-antiparticle pairs "freeze out" earlier. After freezing out the remaining particle-antiparticle pairs can mutually annihilate leaving only energy. To avoid this fate, there must either be some asymmetry or the "cross section" - the probability for interacting - must be so low that particles and their antiparticles move in different directions without meeting

often enough to annihilate completely. This process leaves some relic density that depends on the properties of the particles.

To match the relic density necessary to make up the cosmic dark matter, the cross section required is about that of the weak nuclear force. A particle that interacts through the weak force but not the electromagnetic force will have the right relic density. Moreover, it won't interfere with BBN or the CMB. The hypothesized WIMPs fit the requirements for cosmologists' 'Cold Dark Matter'. This coincidence of scales - the relic density and the weak force interaction scale - is sometimes referred to as the "WIMP miracle" and was part of the motivation to adopt the WIMP as the leading candidate for cosmological dark matter.

- **Axion :** Although its not WIMP type DM, but axion is one of the leading non-baryonic cold DM candidates. The idea of axion, a light pseudoscalar boson, was put forward to solve the strong CP problem [186]. A number of astrophysical observations and laboratory experiments put bound on axion mass to be $\sim 10^{-9}$ eV. Even though the mass is so small they are still cold as their production is non-thermal. Some reviews and recent studies can be found in [187–193].

- **The lightest supersymmetric particle :** By far the most popular and extensively studied BSM scenario is Supersymmetry (SUSY). In supersymmetric theories every SM particle has its super-partner particle differing in spin by half a unit. In most versions of SUSY, there is a conserved discrete symmetry, R-parity, to fulfill the requirement of proton stability.It is defined as, $R = (-1)^{3(B-L)+2S}$. Here B and L is baryon and lepton number respectively and S is the spin of the particle. For SM particles R = 1 and for supersymmetric particles R = -1. In the minimal supersymmetric standard model (MSSM), four linearly independent, non-strongly interacting neutral spin 1/2 particles occur, and are called neutralinos. These are linear superpositions of the superpartners of the photon, the $Z$-boson and the two neutral scalars. The lightest neutralino is often the lightest SUSY particle (LSP) and is a good DM candidate. A number of references on neutralino CDM can be found in literature. Some of the studies on neutralino LSP can be found in references [194–197]. However, there are other variants of SUSY model where the DM candidate is not neutralino but some other supersymmetric particle (sneutrino or gravitino for example).

- **Inert Higgs Doublet Model :** Two Higgs doublet model (2HDM) is a simple extension of SM. In 2HDM there is one extra Higgs doublet in addition to the SM Higgs

doublet. This model is attractive because it is a minimal extension to SM which can accommodate additional source of CP violation which is needed to explain the baryon asymmetry of the universe. Also there are other motivations. In a version of 2HDM, named as inert (Higgs) doublet model (IDM) [198] an unbroken $Z_2$ symmetry ensures the stability of the lightest neutral scalar (or pseudoscalar) particle. A recent study of this DM candidate can be found in [199].

- **Universal Extra Dimension :** Another theory that produces a viable dark matter candidate is Universal Extra Dimensions (UED), in which the existence of additional compact spacelike dimension is postulated. The extra dimension is not visible because its compactification radius is too small to be observed. The dark matter candidate in UED theories is a stable particle known as the Lightest Kaluza- Klein Particle or LKP which is odd under a $Z_2$ symmetry called Kaluza-Klein parity. Various aspects of LKP as a dark matter has been discussed in [200–211].

- **Heavy neutrinos :** Another possible candidate for DM is heavy neutrino. SM neutrinos cannot constitute a significant part of DM because current upper limits on their masses imply that they would freely stream on scales of many megapersecs (Mpc) and hence wash out the density fluctuations observed at these scales. Cosmological simulations have shown, however, that a Universe dominated by neutrinos would not be in agreement with the observed clustering scale of galaxies [212].

  Sterile neutrinos are hypothetical particles which were originally introduced to explain the smallness of the neutrino masses [213]. In addition, they provide a viable dark matter candidate. Depending on their production mechanism, they would constitute cold or a warm dark matter candidate [214, 215]. However, the neutrino must be stable and it is not understood that why a massive neutrino should not be allowed to decay.

## 6.5 Calculation of dark matter relic density

After its production WIMPs ($\chi$) remain in thermal equilibrium and in abundance when the temperature of the universe is greater than the mass of the particle $m_\chi$. The equilibrium abundance (or density) of these particles is maintained by the annihilation of these particles with their anti-particles, $\bar{\chi}$ into other lighter particles (say X), i.e $\chi\bar{\chi} \longrightarrow X\bar{X}$ and vice versa $X\bar{X} \longrightarrow \chi\bar{\chi}$. But the temperature of the universe decreases gradually and when it becomes less than $m_\chi$, the equilibrium abundance drops. Clearly the annihilation

rate for $\chi\bar{\chi} \longrightarrow X\bar{X}$ will also drop. At the point when the annihilation rate falls below the expansion rate of the universe H, the interactions maintaining the thermal equilibrium 'freeze out'. Since the $\chi$ ' s are stable (i.e., they can not decay) then after the freeze out the abundance of them also become fixed and what remains afterward is just the *thermal relic* of WIMPs. In the next subsection we will describe the calculation of the relic density following standard equilibrium thermodynamics [216].

### 6.5.1 Standard calculation of relic density

The number density of the particle $\chi$, in thermal equilibrium of the early universe is given by,

$$n_{eq} = \frac{g}{(2\pi)^3} \int d^3p f(\vec{p}), \tag{6.1}$$

where $g$ is the internal degrees of freedom of $\chi$ and $f(\vec{p})$ is the phase space distribution function and is given by usual Fermi-Dirac (FD) or Bose-Einstein (BE) distribution,

$$f(\vec{p}) = \frac{1}{\exp\left(\frac{E-E_0}{T}\right) \pm 1}, \tag{6.2}$$

where '+' is for FD statistics and '-' for BE statistics and $E_0$ is a constant of the corresponding species.
In the relativistic limit ($T \gg m$) and $T \gg E_0$,

$$n_{eq} = \begin{cases} \left(\frac{\zeta(3)}{\pi^2}\right) gT^3 & \text{for BE statistics,} \\ \left(\frac{3\zeta(3)}{4\pi^2}\right) gT^3 & \text{for FD statistics,} \end{cases} \tag{6.3}$$

here $\zeta$ is the Riemanian zeta function. In the non-relativistic limit ($m \gg T$), both for FD and BE species, and we have,

$$n_{eq} = g\left(\frac{mT}{2\pi}\right)^{3/2} \exp\left(\frac{m-E_0}{T}\right). \tag{6.4}$$

The evolution with time (or temperature), of the number density of $\chi$ is given by the Boltzmann equation,

$$\frac{dn}{dt} = -3Hn - \langle\sigma v\rangle(n^2 - n_{eq}^2), \tag{6.5}$$

where

$$H = \frac{1}{a}\frac{da}{dt} \tag{6.6}$$

is the Hubble parameter ($a$ is the scale factor of the universe) and $\langle\sigma v\rangle$ is the thermally averaged annihilation cross section times relative velocity. The first term in the right-hand

side of equation. 6.5 accounts for the reduction of number density due to the expansion of the universe. The second term takes care of decrease (or increase) in $n$ due to the interaction of $\chi$ with other particles in the spectrum. After solving equation 6.5 we can calculate the contribution of $\chi$ in the energy density of the universe by defining the quantity, $\Omega_\chi$ as,

$$\Omega_\chi h^2 \equiv \frac{\rho_\chi}{\rho_c} = \frac{m_\chi n}{\rho_c}, \tag{6.7}$$

where $h$ is the Hubble parameter in the units of 100 km s$^{-1}$ Mpc$^{-1}$ and $\rho_c$ is the critical density of the universe and is given by,

$$\rho_c = \frac{3H^2}{8\pi G_N}. \tag{6.8}$$

At the point when the annihilation rate $\Gamma = n\langle\sigma v\rangle \lesssim H$, the annihilation of $\chi$s ceases and the relic abundance remains fixed afterward. At the freeze out temperature the annihilation cross section can be expanded in powers of squared relative velocity,

$$\sigma v = a + bv^2 + \ldots, \tag{6.9}$$

where the first term comes from the $s$-wave annihilation and the second from both $s$ and $p$-wave annihilation. A nice discussion on these types of annihilation cross section in the low velocity limit can be found in [217]. In most of the cases the first two terms in the expansion are enough to produce a fair estimate of the relic density. With proper approximations equation. 6.5 can be solved analytically and the relic density is given by [216, 218],

$$\Omega_\chi h^2 \approx \frac{1.04 \times 10^9/1\text{GeV}}{M_{\rm Pl}} \frac{x_F}{\sqrt{g_*(x_F)}} \frac{1}{a + \frac{3b}{x_F}}, \tag{6.10}$$

where $M_{\rm Pl}$ is the Planck mass and $g_*(x_F)$ is the total number of relativistic DOF at the freeze out temperature. Here $x_F$ ($= m/T_F$, $T_F$ being the freeze out temperature) is solved from the equation,

$$x_F = \ln\left(\frac{15}{8}\sqrt{\frac{5}{2}}\frac{g}{2\pi^3}\frac{mM_{\rm Pl}(a + 6b/x_F)}{\sqrt{g_*(x_F)x_F}}\right). \tag{6.11}$$

However, there are three important exceptions to the validity of the above mentioned prescription [219, 220],

- annihilation near mass thresholds (*i.e.*, kinematically forbidden channels at $T = 0$, but which can be significant at higher temperatures),

- coannihilations (*i.e.*, when particles which are slightly heavier than $\chi$ and affect the number density of $\chi$), and
- resonances in the annihilation cross section (*i.e.*, when $m_\chi$ is half the mass of the particle exchanged in the $s$-channel annihilation process).

Systematic treatment of finite temperature corrections takes care of the first case. But this marginally affects the relic density. The latter two cases depend significantly on the particle spectrum and thus on the parameters of the theory.

### 6.5.2 Coannihilation

In the particle spectrum of the theory if there are particles nearly degenerate with the relic particle then the freeze out of these particles occurs almost at the same epoch when the relic particle $\chi$ decouples and can affect the relic abundance of $\chi$. For example, consider there are $N$ particle species, $\chi_i$ $(i = 1, 2, \ldots, N)$ and $m_i < m_j$ if $i < j$, *i.e.*, $\chi_1$ is the lightest particle. The number density $n_i$ of each species $\chi_i$ will obey appropriate Boltzmann equations. Moreover, all the heavier particles ($\chi_i$ with $i > 1$) will ultimately decay to $\chi_1$. So from any number $N_i$ of $\chi_i$ particles we end up getting exactly $N_i$ number of $\chi_1$ at the end of the decay chain. Thus to determine the relic abundance of $\chi_1$ it is meaningful to study the evolution of the number density $n(= \sum_j n_j)$ instead of each number density separately. In this case the Boltzmann equation reduces to,

$$\frac{dn}{dt} = -3Hn - \langle \sigma_{\text{eff}} v \rangle (n^2 - n_{eq}^2). \tag{6.12}$$

The quantity $\sigma_{\text{eff}}$ is given by,

$$\sigma_{\text{eff}}(x) = \frac{1}{g_{\text{eff}}^2} \sum_{i,j=1}^{N} \sigma_{ij} F_i F_j \tag{6.13}$$

where

$$g_{\text{eff}}(x) = \sum_{i=1}^{N} F_i(x), \tag{6.14a}$$

$$F_i(x) = g_i (1 + \Delta_i)^{3/2} \exp(-x\Delta_i), \tag{6.14b}$$

with

$$\Delta_i = \frac{m_i - m_1}{m_1} \text{ and } x = \frac{m}{T}. \tag{6.15}$$

Here $\sigma_{ij} \equiv \sigma(\chi_i\chi_j \rightarrow \text{SM})$ and $g_i$ is the number of internal degrees of freedom of the species $\chi_i$ taking part in the annihilation or coannihilation process. In the non-relativistic limit we have, $\langle\sigma_{\text{eff}}v\rangle \sim a_{\text{eff}}(x) + b_{\text{eff}}(x)v^2 + \mathcal{O}(v^4)$. The approximate expression for the relic density will now become,

$$\Omega_\chi h^2 \approx \frac{1.04\times10^9/1\text{GeV}}{M_{\text{Pl}}}\frac{x_F}{\sqrt{g_*(x_F)}}\frac{1}{I_a+\frac{3I_b}{x_F}}, \tag{6.16}$$

where $I_{a,b}$ are given by,

$$I_a = x_F\int_{x_F}^{\infty} a_{\text{eff}}(x)x^{-2}dx, \tag{6.17a}$$

$$I_b = 2x_F^2\int_{x_F}^{\infty} b_{\text{eff}}(x)x^{-3}dx. \tag{6.17b}$$

The freeze out temperature is given by,

$$x_F = \ln\left(\frac{15}{8}\sqrt{\frac{5}{2}}\frac{g_{\text{eff}}(x_F)}{2\pi^3}\frac{m_1 M_{\text{Pl}}(a_{\text{eff}}(x_F)+6b_{\text{eff}}(x_F)/x_F)}{\sqrt{g_*(x_F)x_F}}\right). \tag{6.18}$$

We shall now briefly discuss some efforts for the search of DM in the next section.

## 6.6 Search for dark matter

Search for the DM particles has become one of the most exciting topics in Astroparticle physics and considerable progress has been achieved in experimental and theoretical research. Various efforts have been made and are still going on to explore the mystery of DM and presently they can be divided into three categories : indirect searches, accelerator searches and direct searches. Indirect methods employ space-based and terrestrial instruments to search for signals from products of WIMP annihilation, such as $\gamma$-rays or positrons. Accelerator searches such as those at the LHC look for WIMPs leading to missing reconstructed energy in the final states to get a hint of the DM mass. However, neither of these techniques is by itself capable of providing a robust statement on the nature of Dark Matter. Instead, it is direct observation of WIMPs in terrestrial experiments that can be a definitive way of detection. Meeting this challenge and detecting galactic WIMPs is recognised as one of the highest priorities in physics today.

### 6.6.1 Direct detection

Signature of dark matter in a direct detection experiment consists of recoil spectrum of single scattering events. Here, the aim is to identify nuclear recoil produced by the col-

lisions between the new particles and the detector's target nuclei. The elastic scattering of WIMPs with masses of $(10 - 1000)GeV/c^2$ would produce nuclear recoils in the range of $(1 - 100)keV$ [221]. To identify such low-energy interactions clearly, a detailed knowledge on the signal signatures, the particle physics aspects and nuclear physics modelling is mandatory. Furthermore, for the calculation of event rates in direct detection experiments, the dark matter density and the halo velocity distribution in the Milky Way are required. In the next paragraph we mention results of some direct detection experiments. For a deeper understanding on direct detection experiments, see [222].

The **CoGeNT** (Coherent Germanium Neutrino Technology) detector [223–225] began collecting data at the Soudan Underground Laboratory, Minnesota, in 2009. They have revealed a seasonal modulation consistent with the presence of WIMPs with masses $\simeq 7GeV/c^2$. The **CDMS** (Cryogenic Dark Matter Search) [226] and its successor the **CDMS II** experiment [227] use germanium and silicon bolometers to search for dark matter. The experiments are located at the Soudan Underground Laboratory. A combined analysis of all CDMS II detectors yields an upper limit on the WIMP-nucleon spin-independent cross-section of $3.8 \times 10^{-44}cm^2$ for a WIMP mass of $70GeV/c^2$. CDMS II performed additionally a study for an annual modulation of the event rate using data from October 2006 to September 2008 [228]. No evidence for an annual modulation was found and this data disfavours the modulation claim of the CoGeNT experiment. The successor of the CDMS II experiment is the **SuperCDMS** detector which employs an improved technology. SuperCDMS experiment focuses on dark matter masses below $30GeV/c^2$ and they have derived a limit on the cross-section for a $8GeV/c^2$ WIMP mass which is given by $1.2 \times 10^{-42}cm^2$ [229]. The results of SuperCDMS set most sensitive exclusion limits at low WIMP masses [230]. SuperCDMS is also the first direct detection experiment which derives limits on more general WIMP interactions calculated with a non-relativistic effective field theory [231]. The second generation of the SuperCDMS experiment will be located at SNOLAB. A similar detector concept is used by the **EDELWEISS** collaboration [232] which operates at Laboratoire Souterrain de Modane (LSM). The most sensitive limit can be derived at a WIMP mass of $90GeV/c^2$ and a cross-section of around $4 \times 10^{-44}cm^2$. Both the CDMS and the EDELWEISS experiments have performed axion searches also. In the **CRESST-II** experiment [233, 234] at Laboratori Nazionali del Gran Sasso (LNGS), an excess of events is observed, corresponding to a WIMP mass of $11.6GeV/c^2(4.2\sigma)$ or $25.3GeV/c^2(4.7\sigma)$ with a cross-section of $3.7 \times 10^{-41}cm^2$ or $1.6 \times 10^{-42}cm^2$ respectively. In future, the CRESST collaboration is aimed to focus on low mass WIMP. This would allow to search for WIMP masses down to $1GeV/c^2$. A possible next generation experiment,

**EURECA** (European Underground Rare Event Calorimeter Array) [235], is a joint effort mostly originating from the EDELWEISS, CRESST and ROSEBUD [236] collaborations. The final goal is to reach a sensitivity of $3 \times 10^{-46} cm^2$. In principle, a joint experiment between EURECA and SuperCDMS would be feasible, combining various technologies and exploiting their complementarity. From the **DarkSide** experiment [237] an exclusion limit is placed which is at $6.1 \times 10^{-44} cm^2$ at $100 GeV/c^2$ WIMP mass. The **XENON10** experiment obtained sensitivities at WIMP masses as low as $5 GeV/c^2$ [238]. The successor of XENON10, **XENON100** [239, 240], started operation at the LNGS laboratory in 2009. However, no evidence for dark matter was found. While interpreting the data as spin-independent interactions of WIMP particles, a best sensitivity of $2 \times 10^{-45} cm^2$ for $55 GeV/c^2$ WIMP mass was obtained. Furthermore, exploiting the low background rate of the experiment, various leptophilic dark matter models have been excluded [241]. To increase the sensitivity further, a next generation detector, **XENON1T** [242], is being constructed. The goal is to achieve two orders of magnitude improvement in sensitivity by reducing the background by a factor of $\sim 100$ compared to XENON100. In 2013, the **LUX** (Large Underground Xenon) experiment [243], installed at the Sanford underground laboratory in the US, released first data [244]. These results improved towards the results of XENON100 down to $7.6 \times 10^{-46} cm^2$ for a WIMP mass of $33 GeV/c^2$. This is currently the lowest limit for direct detection experiments for spin independent interactions for WIMP masses above $6 GeV/c^2$. The LUX and ZEPLIN collaborations have joined to build the multiton **LZ detector** [245] to increase the sensitivity on WIMP-matter cross-sections. Another experiment, **PandaX** [246], tested cross-sections down to $10^{-44} cm^2$ for a $45 GeV/c^2$ WIMP mass [247]. One of the first bounds on the dark matter cross-section from a detector using superheated fluids was achieved by the **SIMPLE** experiment which is operated at LSBB in France. A sensitivity to the spin-dependent WIMP-proton cross-section of $5.7 \times 10^{-39} cm^2$ at $35 GeV/c^2$ was achieved [248]. **PICO** detector [249] (formed from the **PICASSO** and **COUPP** experiments) shows the strongest exclusion limit on the spin-dependent WIMP-proton cross-section at $40 GeV/c^2$ of around $9 \times 10^{-40} cm^2$ at $90\% C.L.$ PICO is operated in the SNOLAB underground laboratory.

### 6.6.2 Indirect search

While direct detection experiments discussed in the previous section require dark matter to be present in the Earth's neighborhood, this is not generally necessary for indirect detection searches. In this case, it is assumed that WIMPs are their own anti-particles and

will annihilate in standard model particles after collisions occur between them. Possible annihilation scenarios include

$$\chi\chi \longrightarrow q\bar{q}, \ell\bar{\ell}, W^+W^-, ZZ. \tag{6.19}$$

These primary particles eventually decay into positrons, electrons, anti-protons, protons, neutrinos and $\gamma$-rays, which can be observed by suitable detectors. As it is generally not known which particles are preferentially generated in the WIMP annihilation, various channels are usually considered in the analysis independently. The Sun is a very interesting target for such searches, as it is expected to store WIMPs in its core while moving through the galactic halo. Results from the indirect detection of signals from WIMP annihilation in the Sun can be directly compared to the results from underground experiments [250].

An analysis from **Super-Kamiokande** places the first constraints from indirect searches on spin-dependent scattering cross sections below dark matter mass $\sim 10GeV/c^2$ [251]. A Monte Carlo study shows that no events have been observed, excluding spin-dependent WIMP-nucleon cross sections above $10^{-39}$ to $10^{-40}cm^2$. Similar results on WIMP annihilations in the Sun from other neutrino detectors have been observed from **IceCube** [252] and **ANTARES** [253] experiments. Both experiments did not detected any signal. In particular ANTARES, which is located in the northern hemisphere, mainly focuses on dark matter annihilation signals from the Galactic Centre. IceCube, which is a gigantic neutrino detector installed in the South Pole, is also searching for WIMP annihilation in the Galactic Center. Preliminary studies show that IceCube is sensitive to velocity-averaged annihilation cross sections of $\approx 10^{-21}$ to $10^{-22}cm^3s^{-1}$ for WIMP masses as low as $30GeV/c^2$ [254,255]. The 'smoking gun' signature for WIMP annihilation would be a line in the $\gamma$-spectrum of objects expected to have an high WIMP density, e.g., the Galactic Center or dwarf spheroidal galaxies. As WIMPs do not couple directly to photons, the processes $\chi\chi \longrightarrow \gamma\gamma$ or $\chi\chi \longrightarrow \gamma Z$ do not happen at tree-level. They appear only as largely suppressed second-order processes. Still, the two monoenergetic gammas would produce a sharp, distinct spectral feature at the dark matter mass ($m_\chi$), accompanied by a somewhat broader and lower peak from $\chi\chi \longrightarrow \gamma Z$ at reduced energies. The **FermiLAT** (Fermi satellite - Large Area Telescope) observed the $\gamma$-spectrum from 20 MeV to 300 GeV. In 2012, there has been a claim that a $\gamma$- line at $130GeV$ has been found in the LAT data at the Galactic Center [256, 257]. In an updated analysis the global significance at $130GeV$ was found to be only $1.6\sigma$ and this seemd to be too wide for the instrument's resolution. At this point, it is thought that more data is needed to varify

the situation. **PAMELA** experiment reported a rising fraction of positrons in the total $e^-e^+$-flux for energies above $\sim 5$ GeV [258, 259]. An excess of antiparticles, in particular positrons, is widely discussed as a promising signature for dark matter annihilation. Moreover, the **AMS-02** experiment recently confirmed the excess, which keeps increasing up to energies of $\sim 300$ GeV [260, 261], the current high-energy limit of the instrument. However, several difficulties with the interpretation of the positron excess observed by PAMELA and AMS-02 have been pointed out and at present these results are considered to be somewhat controvesial.

### 6.6.3 Accelerator search

WIMPs are very weakly interacting. So, they do not deposit any energy in the detectors and one needs to look at the total energy and momentum of an event in order to indentify such particles via a missing energy signal. In *pp*-collisions at the LHC, the initial longitudial momentum of the partons is unknown, hence only the missing energy in the transversal plane, $\not{E}_T$ can be used for the WIMP search. The ATLAS [10] and CMS [11] detectors at the LHC were designed to search for the Higgs particle, for new physics beyond the SM and as well as for precision tests of the Standard Model. Astrophysical uncertainties are not present in collider results. However, the very small time a particle spends in the detector offers a huge obstacle in the process of identifying DM particles from collider data alone.

As pair-production of WIMPs of the type $q\bar{q} \longrightarrow \chi\bar{\chi}$ where $\chi$ is the DM particle cannot be detected by the detectors, the most generic approach to search for WIMP production at a hadron collider is to search for pair-production associated with initial (or final) state radiation

$$q\bar{q} \longrightarrow \chi\bar{\chi} + X \tag{6.20}$$

with '$X$' being a $\gamma$, $Z$ or $W$-boson, or a gluon. Till now, the collider searches using monojets or mono-photons accompanied by $\not{E}_T$ remained fruitless [262–264]. To allow meaningful comparison with direct detection experiment some benchmark scenarios have been proposed (see e.g, [265–267] and references therein). Assuming that the WIMP is a Dirac fermion and that the mediator couples to all quarks with the same strength, it is possible to compare collider and direct detection searches [173].

The various dark matter search channels presented here are thus highly complementary to one another. While the current generation of collider searches can probe very low

WIMP masses, and up to masses of $\sim 1$ TeV, direct and indirect detection experiments can access the WIMP mass region up to 10 TeV and above.

From the above discussions it is evident that various experiments point towards a wide range of different DM mass and no definite conclusion has been reached till date. Naturally, a large number of theoretical models have been proposed to solve the DM mystery. We now proceed to propose one such model for dark matter inspired by the type III seesaw mechanism in the next chapter.

# Chapter 7

# A dark matter candidate in an extended type III seesaw scenario

## 7.1 Introduction

We have seen that the Standard Model (SM) of particle physics has been extremely successful in explaining almost all experimental results. However, extension of the SM is widely expected, to address some yet unexplained observations, which include tiny masses and the mixing pattern of neutrinos and the existence of dark matter (DM) in the Universe as discussed in the previous chapters.

We have already discussed in Chapter 3 that, one possible explanation of small neutrino masses can be obtained by adding $Y = 0$, $SU(2)_L$ lepton triplets to the SM. The active neutrino mixes with the neutral member of such a fermion triplet, allowing $\Delta L = 2$ Majorana mass terms for the neutrinos. The heavy Majorana mass of the neutral member of the fermion triplet ensures smallness of the neutrino mass *via* type-III seesaw mechanism. As neutrino oscillation experiments provide information only on neutrino mass-squared differences, the observed data can be explained if at least two neutrinos are massive. Hence neutrino masses in the type-III seesaw mechanism can be explained if we have at least two fermion triplets.

On the other hand, we have seen in the previous chapter that there is strong empirical evidence for the existence of dark matter in the Universe. A simple and attractive candidate for DM should be a new elementary particle that is electrically neutral and stable on cosmological scales. In this work, we would like to explore a possibility where the neutral member of a fermion triplet can turn out as our missing link.

Our proposal is inspired by the type-III seesaw model for neutrino masses. As two fermion triplets are required to generate neutrino masses, we need to introduce a third

triplet to take care of the DM candidate. In contrast with the two that generate neutrino masses, this triplet needs to be protected by a $Z_2$ symmetry to ensure stability of the DM particle. The $SU(2)$ symmetry will in general demand the charged and neutral components of the fermion triplet to be degenerate. However, we need a mass splitting between the charged and neutral component to obtain a DM particle of mass of the order of the electroweak scale. In some models this mass splitting between the charged and neutral components of the fermion triplet have been obtained through radiative correction. Refs. [269] and [270] discussed TeV scale DM in the context of fermion triplets using radiative correction. The mass of the charged member of the triplet in such a case has to be well above $\sim$ TeV, in order to avoid fast $t$-channel annihilation and a consequent depletion in relic density. As a result, such models end up with somewhat inflexible prediction of DM mass in the region $2.5 - 2.7$ TeV. Alternative models predicting DM mass in the GeV region open up a new way to look into the DM mystery [271].

We propose, as an alternative, two $Z_2$-odd fermion fields, a $Y = 0$ triplet and a neutral singlet that appears as a heavy sterile neutrino. All SM fields and the first two fermion triplets are even under this $Z_2$ symmetry. Mixing between neutral component of the triplet and the sterile neutrino can yield a $Z_2$ odd neutral fermion state that is lighter than all other states in the $Z_2$ odd sector. This fermionic state emerges as the DM candidate in this work [272]. Furthermore, the requisite rate of annihilation is ensured by postulating some $Z_2$ preserving dimension-five operators. These operators, together with the fact that the neutral component of the DM candidate has $W$ couplings, allow a larger region of the parameter space than what we would have had with a sterile neutrino alone. This interplay brings an enriched DM phenomenology compared to models with only singlet or triplets. This, we feel, is a desirable feature of our model given the contradictory claims on the mass of a DM candidate from direct as well as indirect searches. Although choice of a light sterile neutrino can lead to light DM candidates, in our model, we will work with DM masses of more than 62.5 GeV to avoid an unacceptably large invisible Higgs decay width.

We begin by presenting the theoretical framework of our model and introduce the mixing term between $Z_2$ odd triplet $\Sigma$ and sterile neutrino $\nu_s$ in the next section.

## 7.2 Theoretical Framework

In this section we give a description of our model. We have added three fermion triplets to the SM Lagrangian. The fermion triplets $\Sigma = (\Sigma^+, \Sigma^0, \Sigma^-)$ are represented by the $2 \times 2$

matrix [272]

$$\Sigma \;=\; \begin{pmatrix} \Sigma^0/\sqrt{2} & \Sigma^+ \\ \Sigma^- & -\Sigma^0/\sqrt{2} \end{pmatrix}, \tag{7.1}$$

Two of these triplets, which are even under the imposed $Z_2$ symmetry are free to mix with the usual SM particles and therefore responsible for generation of neutrino masses through type III seesaw, explaining the observed mass-squared differences in the neutrino oscillation experiments. On the other hand, the remaining third triplet does not contribute to neutrino mass generation through seesaw, because, it is odd under imposed $Z_2$ symmetry. The neutral component of third triplet mix with the $Z_2$ odd sterile neutrino $\nu_s$ to produce a 'low mass' dark matter candidate. If $\nu_s$ is light enough and its mixing with $\Sigma^0$ is small, the $\nu_s$-like mass eigenstate can be a viable dark matter candidate.

The added part of Lagrangian with the triplet and the sterile neutrino is given by [121, 272–274]: [1]

$$\mathcal{L} = Tr[\overline{\Sigma_a} i\not{D}\Sigma_a] - \frac{1}{2}Tr[\overline{\Sigma_a} M_\Sigma \Sigma_a^c + \overline{\Sigma_a^c} M_\Sigma^* \Sigma_a] - \tilde{\Phi}^\dagger \overline{\Sigma_b}\sqrt{2} Y_\Sigma L - \overline{L}\sqrt{2} Y_\Sigma{}^\dagger \Sigma_b \tilde{\Phi} + \frac{i}{2}\overline{\nu_s}\not{\partial}\nu_s - \frac{1}{2} M_{\nu_s}\overline{\nu_s}\nu_s \,, \tag{7.2}$$

with $L \equiv (\nu, l)^T$, $\Phi \equiv (\phi^+, \phi^0)^T \equiv (\phi^+, (v + H + i\eta)/\sqrt{2})^T$, $\tilde{\Phi} = i\tau_2 \Phi^*$, $\Sigma^c \equiv C\overline{\Sigma}^T$ and summation over $a$ and $b$ are implied, with $a = 1, 2, 3$, $b = 1, 2$, denote generation indices for the triplets. Note that $b$ does not assume the third index as the third generation triplet is odd under $Z_2$.

It should be noted that, in eqn. (7.2), the Yukawa coupling terms for the $Z_2$ odd third triplet and sterile neutrino are prohibited by the exactly conserved $Z_2$ symmetry. Also, in the covariant derivative of eqn. (7.2), no $B_\mu$ terms are present, which in turn restricts the interaction between fermion triplets and $Z_\mu$ boson, this is the speciality of the presence of real triplets in the theory.

The smallness of the $\nu_s$ – $\Sigma^0$ mixing can be generated by dimension-five terms. In general, we add phenomenologically the following terms to the Lagrangian [272]:

$$\mathcal{L}_5 = \left(\alpha_{\Sigma\nu_s} \Phi^\dagger \overline{\Sigma} \Phi \nu_s + \text{h.c.}\right) + \alpha_{\nu_s} \Phi^\dagger \Phi \overline{\nu_s} \nu_s + \alpha_\Sigma \Phi^\dagger \overline{\Sigma} \Sigma \Phi \tag{7.3}$$

where $\alpha_{\Sigma\nu_s}$, $\alpha_{\nu_s}$ and $\alpha_\Sigma$ are three coupling constants of mass dimension $-1$.

[1] We point out that even if the sterile neutrino had a small Majorana mass term, it would not alter our broad conclusions in a significant way because of the wide range of mass values we already have considered for the sterile neutrino in our study.

$\nu_s$ and $\Sigma^0$ mix to produce two mass eigenstates, $\chi$ and $\Psi$, given by [272]

$$\chi = \cos\beta\,\Sigma^0 - \sin\beta\,\nu_s \tag{7.4}$$

$$\Psi = \sin\beta\,\Sigma^0 + \cos\beta\,\nu_s \tag{7.5}$$

We denote $\chi$ as the lighter mass eigenstate and hence as our candidate for dark matter. The mixing angle $\beta$ is determined in terms of the five independent parameters present in the theory, given by [272]

$$M_\Sigma, \qquad M_{\nu_s}, \qquad \alpha_{\Sigma\nu_s}, \qquad \alpha_\Sigma \qquad \text{and} \qquad \alpha_{\nu_s}. \tag{7.6}$$

The $H\chi\chi$ vertex driving the DM annihilation in the $s$-channel, is proportional to [272]

$$\left(\sqrt{2}\alpha_{\Sigma\nu_S}\cos\beta\sin\beta + \alpha_{\nu_S}\sin^2\beta + \frac{\alpha_\Sigma}{2}\cos^2\beta\right). \tag{7.7}$$

In absence of the dimension-five couplings, $\chi$ does not couple to the Higgs. Hence Higgs portal DM annihilation can not take place. As mentioned earlier, $Z$-portal DM annihilation is also not possible. In such a scenario, DM can annihilate *via* $\Sigma^+$ exchange in the $t$-channel to a pair of $W$ bosons. However, in this case, correct relic density can be obtained if the DM mass is larger than 2 TeV as the process is driven by unsuppressed gauge interactions. Introduction of the term $\alpha_\Sigma\Phi^\dagger\overline{\Sigma}\Sigma\Phi$ induces a mixing between $\Sigma^0$ and $\nu_s$ which helps us to get a $\nu_s$-like DM $\chi$. This DM then can self-annihilate *via* suppressed couplings with $H$ and $W$. As we are allowing this dimension-five term, for completeness we have added the other two dimension-5 terms as well, which in turn give more room in the parameter space to manoeuvre.

Clearly if all the $\alpha$s are of the same order, the term $\alpha_\Sigma\Phi^\dagger\overline{\Sigma}\Sigma\Phi$ will be less effective during annihilation, because for a $\nu_s$-like dark matter $\chi$, the value of mixing coefficient $\cos\beta$ will be rather small and that will in turn suppress the effect of parameter $\alpha_\Sigma$ on the observable parameters of the model. However, it cannot be said a priori that the $H\chi\chi$ coupling as a whole gets suppressed because of the choice of a $\nu_s$-like DM.

## 7.3 Results

DM mass depends mainly on the choice of $M_\Sigma$ and $M_{\nu_s}$. But it is also dependent on the higher dimensional parameters. The mass matrix for $\nu_s$ and $\Sigma^0$ is given by [272]

$$\mathcal{M} = \begin{pmatrix} M_{\nu_s} - \alpha_{\nu_s}v^2 & \alpha_{\Sigma\nu_s}v^2 \\ \alpha_{\Sigma\nu_s}v^2 & M_\Sigma - \alpha_\Sigma v^2 \end{pmatrix} \tag{7.8}$$

The DM particle can be identified with the lighter mass eigenstate of $\mathcal{M}$. In the limit when $M_\Sigma \simeq M_{\nu_s}$ the DM mass is a complicated function of all the five free parameters of our model. In the limit where the mixing between $\Sigma^0$ and $\nu_s$ is rather small and $M_\Sigma \gg M_{\nu_s}$, the DM mass is approximately expressed as [272],

$$M_\chi \sim M_{\nu_s} - \alpha_{\nu_s} v^2 + \frac{(\alpha_{\Sigma\nu_s} v^2)^2}{M_\Sigma} \,. \tag{7.9}$$

The flexibility of our model is that, it allows 'low' DM mass for a suitable choice of the relevant parameters, as demonstrated in the following. We use `FeynRules 2.0` [275] in conjunction with `micrOmegas 3.3.13` [276,277] to compute relic density in our model.

In general, two different situation may arise, both of which contribute to the relic density, they are, (i) $M_\Sigma \gg M_{\nu_s}$ and (ii) $M_\Sigma \simeq M_{\nu_s}$. We have also noted that, in the second case, coannihilation between the charged components of the triplet $\Sigma^\pm$, the neutral eigenstate of higher mass $\Psi$ and the dark matter candidate $\chi$ becomes important in calculation of relic density.

If the mass difference between the DM and other $Z_2$-odd particles are within 5–10%, it is expected that coannihilation will dominate over DM self-annihilation [219]. Some idea about the various channels of annihilation can be found from the following benchmark values. When the mass difference between the DM candidate ($\chi$) and other $Z_2$-odd particles is $\approx 200$ GeV with the DM mass $\approx 875$ GeV, then the annihilation channels in decreasing order of dominance are $\chi\chi \to HH$, $\chi\chi \to ZZ$ and $\chi\chi \to W^+W^-$. Similarly, when the mass difference is $\approx 70$ GeV and DM mass $\approx 725$ GeV, the main annihilation channels in similar order are $\chi\chi \to W^+W^-$, $\chi\chi \to HH$ and $\chi\chi \to ZZ$. For a mass difference $\approx 30$ GeV and DM mass $\approx 770$ GeV, coannihilation takes place *via* $\Sigma^-\Psi \to tb$, $\Sigma^-\Psi \to ud$, $\Sigma^-\Psi \to cs$, $\Sigma^-\Sigma^- \to W^-W^-$ and $\Psi\Psi \to W^+W^-$. For mass difference $\approx 700$ GeV (1.3 TeV) and DM mass $\approx 230$ GeV (197 GeV), annihilation proceeds along $\chi\chi \to HH$. Finally, for mass difference $\approx 550$ GeV with DM mass $\approx 425$ GeV, annihilation through both the channels $\chi\chi \to HH$ and $\chi\chi \to W^+W^-$ becomes important.

In Fig. 7.1, we fix $M_\Sigma = 1$ TeV and $\alpha_\Sigma = 0.1$ TeV$^{-1}$. We also choose a benchmark value of $M_{\nu_s} = 200$ GeV. We plot DM relic density against the DM mass $M_\chi$. DM mass is varied by changing $\alpha_{\nu_s}$, but keeping $\alpha_{\Sigma\nu_s}$ fixed at different values. The light shade indicates the region that is excluded when $M_\chi < M_h/2$, where $M_h$ is the Higgs mass, due to the constraint on invisible Higgs decay width. The WMAP [278] and Planck [279] allowed DM relic density being too restrictive, we see from the figure, narrow regions of DM mass $\sim 210$ GeV and $\sim 240$ GeV are allowed. However, for this specific choice of parameters in this plot, only DM mass $\sim 210$ GeV is allowed from LUX direct detection constraints.

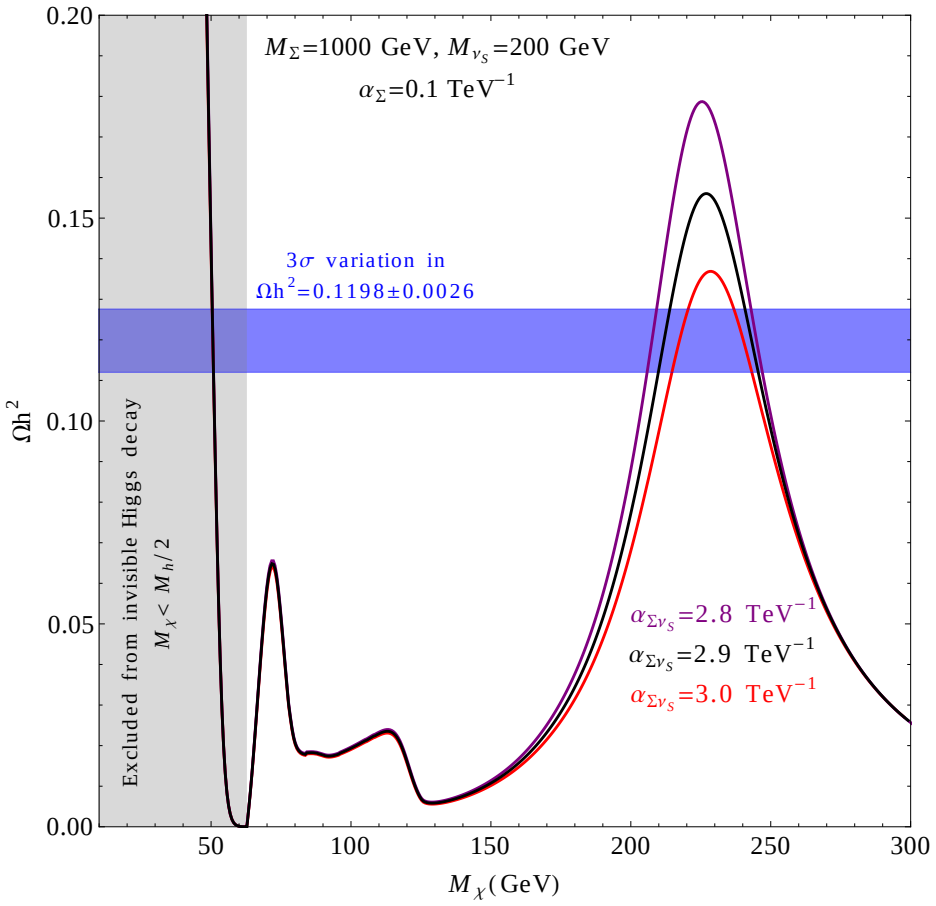


Figure 7.1: *Relic density $\Omega h^2$ vs. dark matter mass $M_\chi$ keeping $\alpha_{\Sigma\nu_s}$ fixed at 2.8 TeV$^{-1}$, 2.9 TeV$^{-1}$ and 3.0 TeV$^{-1}$. $M_\chi$ is varied by changing the remaining parameter $\alpha_{\nu_s}$. We use $M_\Sigma = 1$ TeV, $\alpha_\Sigma = 0.1$ TeV$^{-1}$, $M_{\nu_s} = 200$ GeV. The blue band corresponds to $3\sigma$ variation in relic density according to the WMAP + Planck data.*

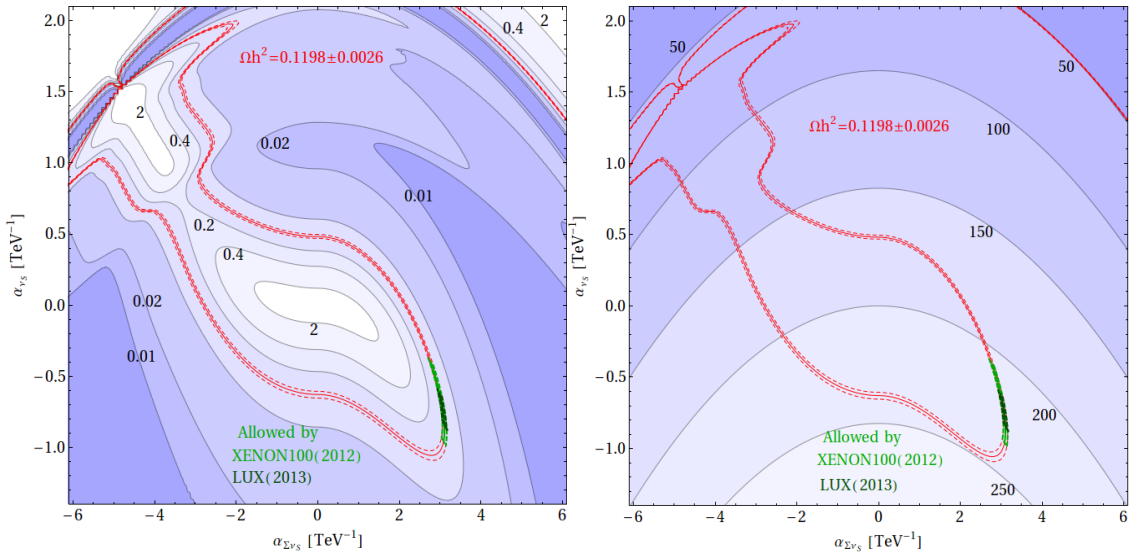


Figure 7.2: *Contour plot in $\alpha_{\Sigma\nu_s} - \alpha_{\nu_s}$ plane for fixed values of $M_\Sigma = 1$ TeV, $M_{\nu_s} = 200$ GeV, $\alpha_\Sigma = 0.1$ TeV$^{-1}$. In* (a) *DM relic density is projected onto the plane, whereas in* (b)*, we project DM mass (in GeV). In both plots the red solid line represents $\Omega h^2 = 0.1198$ and the dashed red lines correspond to the $3\sigma$ variation in $\Omega h^2$. Darker region corresponds to lower values of $\Omega h^2$ or $M_\chi$.*

In order to find the favoured parameter space which satisfies DM relic density constraints, in Fig. 7.2(a) we present contour plots of $\Omega h^2$ in the $\alpha_{\Sigma\nu_s} - \alpha_{\nu_s}$ plane for $M_\Sigma = 1000$ GeV and $M_{\nu_s} = 200$ GeV. The solid red curve denotes $\Omega h^2 = 0.1198$. A $3\sigma$ error band is shown by the dashed red curves. We have varied $\alpha_{\Sigma\nu_s}$ from $-6.0$ to $6.0$ TeV$^{-1}$ and $\alpha_{\nu_s}$ from $-1.5$ to $2.0$ TeV$^{-1}$ to obtain this plot. We have also fixed $\alpha_\Sigma = 0.1$ TeV$^{-1}$ for this plot. In Fig. 7.2(b) we project DM mass $M_\chi$ onto the $\alpha_{\Sigma\nu_s} - \alpha_{\nu_s}$ plane for same values of parameters used in the previous figure. The light green region and the deep green region in both plots corresponding to $M_\chi$ between $205 - 235$ GeV indicate the parameter space which satisfy DM relic density constraints as well as WIMP-nucleon cross section bound as imposed by XENON 100 [239] and LUX [244].

In Fig. 7.3(a) we have plotted the WIMP-nucleon cross section vs. dark matter mass $M_\chi$ keeping $\alpha_\Sigma$ fixed at $0.1$ TeV$^{-1}$. $M_\chi$ is varied by changing the remaining parameters. For illustration, we have varied $M_\Sigma$ between $300$ and $1000$ GeV, $M_{\nu_s}$ between $150$ and $1000$ GeV keeping the mass difference between DM and other $Z_2$ odd fermions greater than $200$ GeV. The remaining parameters $\alpha_{\Sigma\nu_s}$ and $\alpha_{\nu_s}$ were varied between $[-8, +8]$ TeV$^{-1}$ and $[-0.9, +0.9]$ TeV$^{-1}$ respectively. In this case, the DM particle always self-annihilates

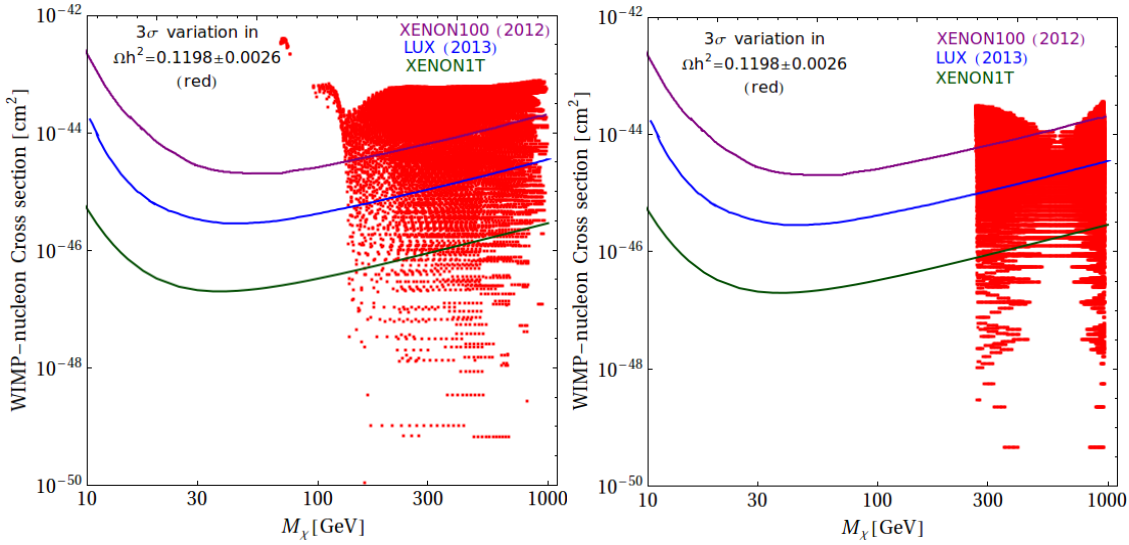


Figure 7.3: (a) *WIMP-nucleon cross section vs. dark matter mass* $M_\chi$ *keeping* $\alpha_\Sigma$ *fixed at* $0.1$ *TeV*$^{-1}$. $M_\chi$ *is varied by changing the remaining parameters. In such a scenario, DM annihilates via self-annihilation only.* $M_{\nu_s}$ *is varied between* $150$ *and* $1000$ *GeV.* (b) *WIMP-nucleon cross section vs. dark matter mass* $M_\chi$ *keeping* $\alpha_\Sigma$ *fixed at* $0.1$ *TeV*$^{-1}$. $M_\chi$ *is varied by changing the remaining parameters. Here coannihilation between the DM candidate with the charged components of the triplet* $\Sigma^\pm$*, the neutral eigenstate of higher mass provides the dominating contribution to relic density. In both the figures different direct detection experimental bounds are indicated and the red points correspond to the* $3\sigma$ *variation in relic density according to the WMAP + Planck data.*

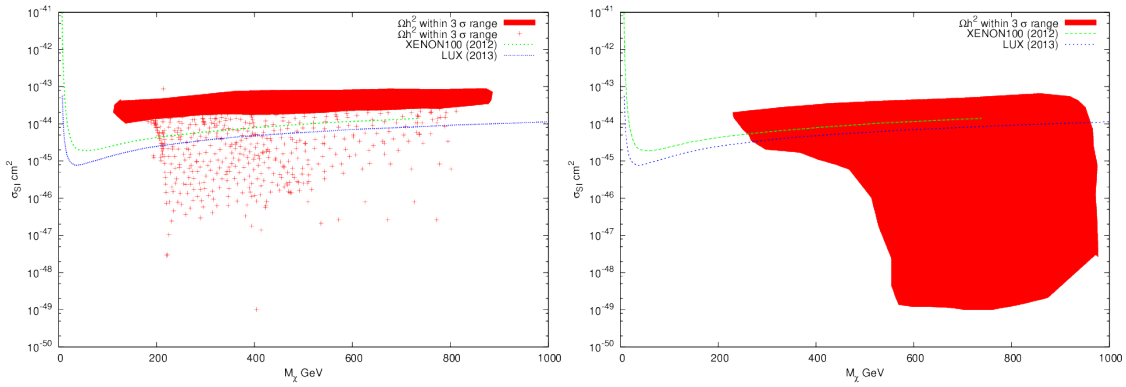


(a) (b)

Figure 7.4: (a) *WIMP-nucleon cross section vs. dark matter mass* $M_\chi$ *keeping* $\alpha_\Sigma$ *fixed at* $0.01$ *TeV*$^{-1}$. $M_\chi$ *is varied by changing the remaining parameters. Here self-annihilation of the DM candidate provides the dominating contribution to relic density* (b) *WIMP-nucleon cross section vs. dark matter mass* $M_\chi$ *keeping* $\alpha_\Sigma$ *fixed at* $0.01$ *TeV*$^{-1}$. $M_\chi$ *is varied by changing the remaining parameters. Here coannihilation between the DM candidate with the charged components of the triplet* $\Sigma^\pm$*, the neutral eigenstate of higher mass provides the dominating contribution to relic density. In both the figures different direct detection experimental bounds are indicated and the red points correspond to the* $3\sigma$ *variation in relic density according to the WMAP + Planck data.*

and DM coannihilation does not take place. It is seen that a large region of parameter space satisfies the bound on WIMP-nucleon cross section as imposed by XENON 100 [239] and LUX [244] experimental data. In Fig. 7.3(b) we have plotted the WIMP-nucleon cross section vs. dark matter mass $M_\chi$ keeping $\alpha_\Sigma$ fixed at $0.1$ TeV$^{-1}$. We varied $M_\Sigma$ between $300$ and $1000$ GeV, $M_{\nu_s}$ between $270$ and $1000$ GeV keeping the mass difference between DM mass and other $Z_2$ odd fermions always smaller than $30$ GeV. The other parameters $\alpha_{\Sigma\nu_s}$ and $\alpha_{\nu_s}$ were varied between $[-8, +8]$ TeV$^{-1}$ and $[-0.9, +0.9]$ TeV$^{-1}$ respectively. In this case, we noted that coannihilation between the charged components of the triplet $\Sigma^\pm$, the neutral eigenstate of higher mass ($\Psi$) and the dark matter candidate ($\chi$) provides the dominant contributions in the calculation of relic density. Again a large region of parameter space satisfies the bound on WIMP-nucleon cross section as imposed by XENON 100 and LUX experimental data [280] in this case too.

In Fig. 7.4(a), we have plotted the WIMP-nucleon cross section vs. dark matter mass $M_\chi$ keeping $\alpha_\Sigma$ fixed at $0.01$ TeV$^{-1}$. Other parameters $\alpha_{\Sigma\nu_s}$ and $\alpha_{\nu_s}$ were varied between $1.2$ TeV$^{-1}$ to $3.0$ TeV$^{-1}$ and $-1.1$ TeV$^{-1}$ to $0.03$ TeV$^{-1}$ respectively. In this case, we varied $M_\Sigma$ between $500$ and $1500$ GeV and $M_{\nu_s}$ between $150$ and $900$ GeV. We obtained wide region of DM mass from $128$ GeV to $872$ GeV that satisfies the correct relic density range and

the constrains imposed on WIMP-nucleon cross section, i.e., $\sigma_{SI}$ by XENON 100 and LUX data. The mass difference between $M_\Sigma$ and $M_{\nu_s}$ was always kept greater than $150$ GeV. In this case also the annihilation of DM particle with itself provides the dominating contribution to the calculation of relic density. In Fig. 7.4(b), we have plotted the WIMP-nucleon cross section vs. dark matter mass $M_\chi$ keeping $\alpha_\Sigma$ fixed at $0.01$ TeV$^{-1}$. Other parameters $\alpha_{\Sigma\nu_s}$ and $\alpha_{\nu_s}$ were varied between $-0.08$ TeV$^{-1}$ to $0.94$ TeV$^{-1}$ and $-0.009$ TeV$^{-1}$ to $0.096$ TeV$^{-1}$ respectively. In this case we varied $M_\Sigma$ between $300$ and $1000$ GeV and $M_{\nu_s}$ in such a way as to make the mass difference between $M_\Sigma$ and $M_{\nu_s}$ smaller than $55$ GeV. In this case also coannihilation process between the charged components of the triplet $\Sigma^\pm$, the neutral eigenstate of higher mass ($\Psi$) and the dark matter candidate ($\chi$) provides the dominant contributions in the calculation of relic density. Here also we got a large region of parameter space that satisfies the correct relic density requirement and the bound imposed by XENON 100 and LUX data on WIMP-nucleon cross section. In both the plots the red points and red regions correspond to those data points that fall within the $3\sigma$ variation in relic density according to the combined WMAP and Planck data.

## 7.4 Conclusion

To explain smallness of neutrino masses, type-III seesaw mechanism employs heavy fermion triplets. In this chapter, we have tried to investigate a scenario inspired by this model to address the dark matter riddle. Previous attempts in this regard employed radiative mass splitting of the members of a lepton triplet, yielding DM masses at the TeV scale. We have in addition introduced a sterile neutrino to bring down the DM mass scale to $\sim 200$ GeV. Both the additional triplet and the sterile neutrino are odd under a postulated $Z_2$ symmetry.

Dark matter direct detection experimental results are rather conflicting. While CDMS [227, 281], DAMA [282], CoGeNT [283], CRESST [284] *etc.* point towards a DM mass of $\sim 10$ GeV, XENON 100 and LUX claim to rule out these observations. Given this scenario, we keep our options open and explore all DM masses allowed by experimental observations.

As we are exploring a Higgs portal dark matter model, to respect the invisible Higgs decay width constraints we have considered DM masses more than $M_h/2 \sim 62.5$ GeV. We have ensured that our results are consistent with XENON 100 and LUX constraints. In addition, we also indicate the constraints on the parameters of our model ensuing from WMAP and Planck data. In our model, the charged triplet fermions, being $Z_2$ odd, do not

couple to SM fermions and as a consequence, can evade detection in the existing colliders including LHC.

We have introduced dimension five terms to satisfy the DM relic density constraints with the help of a sterile neutrino-like DM. The role of these terms is to produce the right amount of $\Sigma^0$–$\nu_s$ mixing to get the appropriate DM mass and DM annihilation.

It is possible to satisfy the relic density constraints in a model with a pure sterile neutrino DM with the dimension five term $\alpha_{\nu_s}\Phi^\dagger\Phi\overline{\nu_s}\nu_s$ alone, without the triplet fermions. However in this model the allowed parameter space is rather restricted compared to our model which offers a lot of flexibility in DM mass.

In short, we have presented a triplet fermion DM model, which can provide us with DM candidates with masses as low as $\approx 200$ GeV. The scenario, however has the flexibility to accommodate a higher mass DM candidate as well, and offers a wide region of parameter space consistent with observations.

# Chapter 8

# Summary and conclusions

In the following we make an attempt to discuss in brief the findings of our research included in this thesis.

The type II seesaw mechanism for neutrino mass generation usually makes use of one complex scalar triplet. The collider signature of the doubly-charged scalar, the most striking feature of this scenario, consists mostly in decays into same-sign dileptons or same-sign $W$ boson pairs. However, certain scenarios of neutrino mass generation, such as those imposing texture zeros by a symmetry mechanism, require at least two triplets in order to be consistent with the type II seesaw mechanism.

In Chapter 1, we have briefly described the Standard Model of particle physics and the need for going beyond it. We presented a partial summary of various neutrino physics experiments and their implications on neutrino masses and mixings, some models for neutrino mass generation and two-zero textures of Majorana neutrino mass matrices in Chapter 2. We also described how the need for explanation of current neutrino data serves as a motivation for searching new physics beyond the SM.

In Chapter 3, we described the seesaw models for Majorana mass generation for neutrinos. In the later part of this chapter we have shown that how the two-zero textures of neutrino mass matrices become inconsistent with type II seesaw mechanism, when only one scalar triplet is present in the scenario.

We developed a model in Chapter 4 with two such complex triplets and showed that, in such a case, mixing between the triplets can cause the heavier doubly-charged scalar mass eigenstate to decay into a singly-charged scalar and a $W$ boson of the same sign. Considering a large number of benchmark points with different orders of magnitude of the $\Delta L = 2$ Yukawa couplings, chosen in agreement with the observed neutrino mass and mixing pattern, we demonstrate that $H_1^{++} \to H_2^+ W^+$ can have more than 99% branching

fraction in the cases where the vacuum expectation values of the triplets are small. It is also shown that the above decay allows one to differentiate a two-triplet case at the LHC, through the ratios of events in various multi-lepton channels.

In Chapter 5, we reconsidered the scenario mentioned in Chapter 4 with one CP-violating phase present in the scalar potential of the model, and all parameters have been chosen consistently with the observed neutrino mass and mixing patterns. We found that a large phase ($\gtrsim 60^\circ$) splits the two doubly-charged scalar mass eigenstates wider apart, so that the decay $H_1^{++} \to H_2^{++}h$ is dominant (with $h$ being the $125$ GeV scalar). We identified a set of benchmark points where this decay dominates. This is complementary to the situation, reported in Chapter 4, where the heavier doubly-charged scalar decays as $H_1^{++} \to H_2^{+}W^{+}$. We pointed out the rather spectacular signal, ensuing from $H_1^{++} \to H_2^{++}h$, in the form of Higgs plus same-sign dilepton peak, which can be observed at the Large Hadron Collider.

We have presented an outline of the Dark Matter problem in Chapter 6. In Chapter 7, we have considered a model to address the DM riddle inspired by the type III seesaw mechanism for neutrino mass generation. The type III seesaw mechanism for neutrino mass generation usually makes use of at least two $Y = 0$, $SU(2)_L$ lepton triplets. We augmented such a model with a third triplet and a sterile neutrino, both of which are odd under a conserved $Z_2$ symmetry. With all new physics confined to the $Z_2$-odd sector, whose low energy manifestation is in some higher-dimensional operators, a fermionic dark matter candidate is found to emerge. We identified the region of the parameter space of the scenario, which is consistent with all constraints from relic density and direct searches, and allows a wide range of masses for the dark matter candidate.

# Bibliography


[1] Y. Nambu and G. Jona-Lasinio, *"Dynamical Model of Elementary Particles Based on an Analogy with Superconductivity. 1."*, *Phys.Rev.* **122**, 345, (1961) .

[2] Y. Nambu and G. Jona-Lasinio, *"Dynamical Model of Elementary Particles Based on an Analogy with Superconductivity. II"*, *Phys.Rev.* **124**, 246, (1961).

[3] J. Goldstone, *"Field Theories with Superconductor Solutions"*, *Nuovo Cim.* **19**, 154, (1961) .

[4] J. Goldstone, A. Salam, and S. Weinberg, *"Broken Symmetries"*, *Phys.Rev.* **127**, 965, (1962).

[5] F. Englert and R. Brout, *"Broken Symmetry and the Mass of Gauge Vector Mesons"*, *Phys.Rev.Lett.* **13**, 321, (1964) .

[6] P. W. Higgs, *"Broken Symmetries and the Masses of Gauge Bosons"*, *Phys.Rev.Lett.* **13**, 508, (1964).

[7] G. Guralnik, C. Hagen, and T. Kibble, *"Global Conservation Laws and Massless Particles"*, *Phys.Rev.Lett.* **13**, 585, (1964).

[8] P. W. Higgs, *"Spontaneous Symmetry Breakdown without Massless Bosons"*, *Phys.Rev.* **145**, 1156, (1966) .

[9] T. Kibble, *"Symmetry breaking in nonAbelian gauge theories"*, *Phys.Rev.* **155**, 1554, (1967).

[10] **ATLAS** Collaboration, G. Aad *et al.*, *"Observation of a new particle in the search for the Standard Model Higgs boson with the ATLAS detector at the LHC"*, Phys.Lett. **B716**, 1, (2012), arXiv:1207.7214.

[11] **CMS** Collaboration, S. Chatrchyan *et al.*, *"Observation of a new boson at a mass of 125 GeV with the CMS experiment at the LHC"*, Phys.Lett. **B716**, 30, (2012) , arXiv:1207.7235.

[12] C. L. Cowan, F. Reines, F. Harrison, H. Kruse and a. McGuire, *"Detection of the Free Neutrino: a Confirmation"*, *Science*, **124**, 103, (1956).

[13] G. Danby, J. M. Gaillard, K. A. Goulianos, L. M. Lederman, N. B. Mistry, M. Schwartz and J. Steinberger, *"Observation of High-Energy Neutrino Reactions and the Existence of Two Kinds of Neutrinos,"* Phys. Rev. Lett. **9**, 36, (1962) .

[14] K. Kodama *et al.* (DONUT Collaboration). *"Observation of tau neutrino interactions."* Phys.Lett. **B504**, 218, (2001) . hep-ex/0012035.

[15] B T. Cleveland, T. Daily, R. Jr. Davis, J. R. Distel, K. Lande *et al. "Measurement of the solar electron neutrino flux with the Homestake chlorine detector."* Astrophys.J. **496**, 505, (1998).

[16] W. Hampel *et al.* (GALLEX Collaboration). *"GALLEX solar neutrino observations: Results for GALLEX IV."* Phys.Lett. **B447**, 127, (1999) .

[17] Q.R. Ahmad *et al.* (SNO Collaboration). *"Direct evidence for neutrino flavor transformation from neutral current interactions in the Sudbury Neutrino Observatory."* Phys.Rev.Lett. **89**, 011301, (2002),. nucl-ex/0204008.

[18] J.N. Abdurashitov *et al.* (SAGE Collaboration). *"Solar neutrino flux measurements by the SovietAmerican Gallium Experiment (SAGE) for half the 22 year solar cycle."* J.Exp.Theor.Phys. **95**, 181,(2002) . astro-ph/0204245.

[19] S. Fukuda *et al.* (Super-Kamiokande Collaboration). *"Solar B-8 and hep neutrino measurements from 1258 days of Super-Kamiokande data."* Phys.Rev.Lett. **86**, 5651 (2001). hep-ex/0103032.

[20] S. N. Ahmed *et al.* (SNO Collaboration). *"Measurement of the total active B-8 solar neutrino flux at the Sudbury Neutrino Observatory with enhanced neutral current sensitivity."* Phys.Rev.Lett. **92**, 181301, (2004). nucl-ex/0309004.

[21] Y. Fukuda *et al.* (Super-Kamiokande Collaboration). *"Evidence for oscillation of atmospheric neutrinos."* Phys.Rev.Lett. **81**, 1562 (1998). hep-ex/9807003.

[22] Y. Ashie *et al.* (Super-Kamiokande Collaboration). *"Evidence for an oscillatory signature in atmospheric neutrino oscillation."* Phys.Rev.Lett. **93**, 101801, (2004). hep-ex/0404034.

[23] M. H. Ahn *et al.* (K2K Collaboration). *"Indications of neutrino oscillation in a 250 km long baseline experiment."* Phys.Rev.Lett. **90**, 041801 (2003). hep-ex/0212007.

[24] D. G. Michael *et al.* (MINOS Collaboration). *"Observation of muon neutrino disappearance with the MINOS detectors and the NuMI neutrino beam."* Phys.Rev.Lett. **97**, 191801 (2006). hep-ex/0607088.

[25] K. Abe *et al.* (T2K Collaboration). *"Evidence of Electron Neutrino Appearance in a Muon Neutrino Beam." Phys.Rev.* **D88**, 032002 (2013). arXiv: 1304.0841.

[26] K. Eguchi *et al.* (KamLAND Collaboration). *"First results from KamLAND: Evidence for reactor anti- neutrino disappearance."* Phys.Rev.Lett. **90**, 021802 (2003). hep-ex/0212021.

[27] T. Araki *et al.* (KamLAND Collaboration). *"Measurement of neutrino oscillation with KamLAND: Evidence of spectral distortion."* Phys.Rev.Lett. **94**, 081801 (2005). hep-ex/0406035.

[28] Y. Abe *et al.* (Double Chooz Collaboration). *"Reactor electron antineutrino disappearance in the Double Chooz experiment." Phys.Rev.* **D86**, 052008 (2012), arXiv: 1207.6632.

[29] J. K. Ahn et al. (RENO collaboration). *"Observation of Reactor Electron Antineutrino Disappearance in the RENO Experiment."* Phys.Rev.Lett. **108**, 191802 (2012), arXiv: 1204.0626.

[30] Daya Bay Collaboration, F. P. An *et al. "Observation of electron-antineutrino disappearance at Daya Bay,"* Phys. Rev. Lett. **108**, 171803 (2012) [arXiv:1203.1669 [hep-ex]].

[31] F. P. An *et al.* (Daya Bay Collaboration). *"Improved Measurement of Electron Antineutrino Disappearance at Daya Bay."* Chin.Phys. **C37**, 011001 (2013), arXiv: 1210.6327.

[32] G. L. Fogli *et al.*, *"Global analysis of neutrino masses, mixings and phases: entering the era of leptonic CP violation seraches"*; *Phys.Rev.* **D86** (2012), arXiv:013012.

[33] A. de Gouvea *et al.*, *"Working Group Report: Neutrinos"*; arXiv:1310.4340 [hep-ex].

[34] R.N. Mohapatra and P. Pal, *Massive neutrinos in physics and astrophysics* (World Scientific, Singapore, 1991).

[35] M. Aglietta *et al.* (The NUSEX), *"Experimental study of atmospheric neutrino flux in the NUSEX experiment"*, Europhys. Lett. **8** (1989) 611.

[36] M. Aglietta *et al.*, *"Experimental study of upward stopping muons in NUSEX"*, Europhys. Lett. **15** (1991) 559.

[37] A. de Bellefon, J. Bouchez, J. Busto, Jean-Eric Campagne, C. Cavata, et al. *"MEMPHYS: A Large scale water Cerenkov detector at Frejus."* (2006). hep-ex/0607026.

[38] C. Berger et al., *"Study of atmospheric neutrino interactions with the Frejus detector"*, Phys. Lett. **B227** (1989) 489.

[39] C. Berger et al., *"A Study of atmospheric neutrino oscillations in the Frejus experiment"*, Phys. Lett. **B245** (1990) 305.

[40] K. Daum, *"Determination of the atmospheric neutrino spectra with the Frejus detector"*, Z. Phys. **C66** (1995) 417.

[41] W. W. M. Allison *et al.*, *"Measurement of the atmospheric neutrino flavour composition in Soudan-2"* , Phys. Lett. **B391** (1997) 491, hep-ex/9611007.

[42] W. W. M. Allison *et al.* (Soudan-2), *"The atmospheric neutrino flavor ratio from a 3.9 fiducial kiloton-year exposure of Soudan 2"*, Phys. Lett. **B449** (1999) 137, hep-ex/9901024.

[43] M. Sanchez *et al.* (Soudan 2), *"Observation of Atmospheric Neutrino Oscillations in Soudan 2"*, *Phys.Rev.* **D68** (2003) 113004, hep-ex/0307069.

[44] W. W. M. Allison *et al.* (Soudan-2), *"Neutrino Oscillation Effects in Soudan-2 Upward-stopping muons"*, *Phys.Rev.* **D72** (2005) 052005, hep-ex/0507068.

[45] M. Ambrosio *et al.* (MACRO), *"Measurement of the atmospheric neutrino-induced upgoing muon flux using MACRO"*, Phys. Lett. **B434** (1998) 451, hep-ex/9807005.

[46] M. Ambrosio *et al.* (MACRO), *"Low energy atmospheric muon neutrinos in MACRO"*, Phys. Lett. **B478** (2000) 5.

[47] M. Ambrosio *et al.* (MACRO), *"Atmospheric neutrino oscillations from upward throughgoing muon multiple scattering in MACRO"*, Phys. Lett. **B566** (2003) 35, hep-ex/0304037.

[48] Masayuki Nakahata *et al.* (Kamiokande), *"Atmospheric neutrino background and pion nuclear effect for Kamioka nucleon decay experiment"*, J. Phys. Soc. Jap. **55** (1986) 3786.

[49] M. Takita *et al.* (Kamiokande II), *"Experimental study of the atmospheric neutrino flux"*, 1988, In 'Tsukuba 1988, Proceedings, Physics at TeV energy scale' 235-246. Tsukuba KEK - KEK-88-010 (88/12,rec.Feb.89) 235- 246, and In 'Les Arcs 1988, Proceedings, Electroweak interactions and unified theories' 447.

[50] Y. Oyama *et al.* (Kamiokande), *"Experimental study of upward going muons in Kamiokande"*, *Phys.Rev.* **D39** (1989) 1481.

[51] K. S. Hirata *et al.* (Kamiokande), *"Observation of a small atmospheric $\nu_\mu/\nu_e$ ratio in Kamiokande"*, Phys. Lett. **B280** (1992) 146.

[52] Y. Fukuda *et al.* (Kamiokande), *"Atmospheric muon-neutrino / electron-neutrino ratio in the multiGeV energy range"*, Phys. Lett. **B335** (1994) 237.

[53] Y. Fukuda *et al.* (Kamiokande), *"Study of neutron background in the atmospheric neutrino sample in Kamiokande"*, Phys. Lett. **B388** (1996) 397.

[54] S. Hatakeyama *et al.* (Kamiokande), *"Measurement of the flux and zenith angle distribution of upward through-going muons in Kamiokande II + III"*, Phys. Rev. Lett. **81** (1998) 2016, hep-ex/9806038.

[55] J. Hosaka *et al.* (Super-Kamiokande), *"Three flavor neutrino oscillation analysis of atmospheric neutrinos in Super-Kamiokande"*, *Phys.Rev.* **D74** (2006) 032002, hep-ex/0604011.

[56] R. Wendell *et al.* (Super-Kamiokande), *"Atmospheric neutrino oscillation analysis with sub-leading effects in Super-Kamiokande I, II, and III"*, *Phys.Rev.* **D81** (2010) 092004, arXiv:1002.3471 [hep-ex].

[57] G. Mitsuka *et al.* (Kamiokande), *"Study of Non-Standard Neutrino Interactions with Atmospheric Neutrino Data in Super-Kamiokande I and II"*, *Phys.Rev.* **D84** (2011) 113008, arXiv:1109.1889 [hep-ex].

[58] K. Abe *et al.* (Super-Kamiokande), *"A Measurement of the Appearance of Atmospheric Tau Neutrinos by Super-Kamiokande"*, Phys.Rev.Lett. **110** (2013) 181802, arXiv:1206.0328 [hep-ex].

[59] K. Abe *et al.* (Super-Kamiokande), *"Limits on Sterile Neutrino Mixing using Atmospheric Neutrinos in Super-Kamiokande"*, *Phys.Rev.* **D91** (2015) 052019, arXiv:1410.2008 [hep-ex].

[60] E. Richard *et al.* (Super-Kamiokande), *"Measurements of the atmospheric neutrino flux by Super-Kamiokande: energy spectra, geomagnetic effects, and solar modulation"*, arXiv:1510.08127 [hep-ex].

[61] R. M. Bionta *et al.* (IMB), *"Contained neutrino interactions in an underground water detector"*, *Phys.Rev.* **D38** (1988) 768.

[62] D. Casper *et al.* (IMB), *"Measurement of atmospheric neutrino composition with IMB-3"*, Phys. Rev. Lett. **66** (1991) 2561.

[63] R. Becker-Szendy *et al.* (IMB), *"A Search for muon-neutrino oscillations with the IMB detector"*, Phys. Rev. Lett. **69** (1992) 1010.

[64] M. Shiozawa [Super-Kamiokande Collaboration]: *"Talk given at the "Neutrino 2002" conference"*, http://neutrino2002.ph.tum.de

[65] R. Davis, Jr., *"Solar neutrinos : Experimental"*, Phys. Rev. Lett., **302** (1964).

[66] K. S. Hirata *et al.* (Kamiokande), *"Search for correlation of neutrino events with solar flares in Kamiokande"*, Phys. Rev. Lett. **61** (1988) 2653.

[67] K. S. Hirata *et al.* (Kamiokande), *"Observation of B-8 solar neutrinos in the Kamiokande-II detector"*, Phys. Rev. Lett. **63** (1989) 16.

[68] K. S. Hirata *et al.* (Kamiokande), *"Constraints on neutrino oscillation parameters from the Kamiokande-II solar neutrino data"*, Phys. Rev. Lett. **65** (1990) 1301.

[69] K. S. Hirata *et al.* (Kamiokande), *"Real time, directional measurement of B-8 solar neutrinos in the Kamiokande-II detector"*, *Phys.Rev.* **D44** (1991) 2241.

[70] Y. Fukuda *et al.* (Kamiokande), *"Solar neutrino data covering solar cycle 22"*, Phys. Rev. Lett. **77** (1996) 1683.

[71] B. Aharmim *et al.* [SNO Collaboration], *"Low Energy Threshold Analysis of the Phase I and Phase II Data Sets of the Sudbury Neutrino Observatory,"* Phys. Rev. **C 81** (2010) 055504, [arXiv:0910.2984 [nucl-ex]].

[72] A. Aguilar-Arevalo *et al.* (LSND Collaboration). *"Evidence for neutrino oscillations from the observation of anti-neutrino(electron) appearance in a anti-neutrino(muon) beam." Phys.Rev.* **D64**, 112007 (2001). hep-ex/0104049.

[73] K. Eitel [KARMEN Collaboration], *"KARMEN: Present neutrino oscillation limits and perspectives after the upgrade,"* hep-ex/9706023.

[74] A.A. Aguilar-Arevalo *et al.* (MiniBooNE Collaboration). *"First Measurement of the Muon Neutrino Charged Current Quasielastic Double Differential Cross Section." Phys.Rev.* **D81**, 092005 (2010), arXiv: 1002.2680.

[75] A.A. Aguilar-Arevalo *et al.* (MiniBooNE Collaboration). *"The Neutrino Flux prediction at MiniBooNE." Phys.Rev.* **D79**, 072002 (2009), arXiv: 0806.1449.

[76] M.H. Ahn *et al.* (K2K Collaboration). *"Measurement of Neutrino Oscillation by the K2K Experiment." Phys.Rev.* **D74**, 072003 (2006). hep-ex/0606032.

[77] A. Gando *et al.* (KamLAND Collaboration). *"Reactor On-Off Antineutrino Measurement with KamLAND."* (2013), arXiv: 1303.4667.

[78] T. Mitsui (KamLAND Collaboration). *"KamLAND results and future."* Nucl.Phys.Proc.Suppl. **221**, 193 (2011).

[79] [Daya Bay Collaboration], *"Prospects For Precision Measurements with Reactor Antineutrinos at Daya Bay,"* arXiv:1309.7961 [hep-ex].

[80] D. A. Dwyer *et al.*, *"Search for Sterile Neutrinos with a Radioactive Source at Daya Bay."* http: //if-neutrino.fnal.gov/whitepapers/littlejohn-db.pdf (2013).

[81] C. Kraus and S. J. M. Peeters (SNO+ Collaboration). *"The rich neutrino programme of the SNO+ experiment."* Prog.Part.Nucl.Phys. **64**, 273 (2010).

[82] P. Adamson *et al.* (MINOS), *"An improved measurement of muon antineutrino disappearance in MINOS*, Phys. Rev. Lett. **108** (2012) 191801, arXiv:1202.2772 [hep-ex].

[83] P. Adamson *et al.* (MINOS), *"Combined analysis of $\nu_\mu$ disappearance and $\nu_\mu \to \nu_e$ appearance in MINOS using accelerator and atmospheric neutrinos"*, Phys.Rev.Lett. **112** (2014) 191801, arXiv:1403.0867 [hep-ex].

[84] Francis Halzen, Spencer R. Klein, *"IceCube: An Instrument for Neutrino Astronomy", Rev. Sci. Instrum. **81** (2010) 081101, arXiv:1007.1247 [astro-ph].*

*[85] M. D. Messier [NOvA Collaboration], " Extending the NOvA Physics Program," arXiv:1308.0106 [hep-ex].*

*[86] A. Ghosh, T. Thakore and S. Choubey, "Determining the Neutrino Mass Hierarchy with INO, T2K, NOvA and Reactor Experiments," JHEP* **1304** *(2013) 009, [arXiv:1212.1305 [hep-ph]].*

*[87] A. B. Balantekin et al., "Neutrino mass hierarchy determination and other physics potential of medium-baseline reactor neutrino oscillation experiments", arXiv:1307.7419 [hep-ex].*

*[88] M. Antonello et al., "Search for 'anomalies' from neutrino and anti-neutrino oscillations at $\Delta m^2 \sim 1eV^2$ with muon spectrometers and large LAr-TPC imaging detectors," arXiv:1203.3432*

*[89] N. Agafonova et al. [OPERA Collaboration], "New results on $\nu_\mu \to \nu_\tau$ appearance with the OPERA experiment in the CNGS beam," JHEP* **1311** *(2013) 036*

*[90] C. Adams et al. [LBNE Collaboration], "The Long-Baseline Neutrino Experiment: Exploring Fundamental Symmetries of the Universe," arXiv:1307.7335 [hep-ex].*

*[91] K. Abe et al. [T2K Collaboration], "T2K neutrino flux prediction,"* Phys.Rev. **D87** *(2013), [arXiv:1211.0469 [hep-ex]].*

*[92] P. Adamson et al., "CHerenkov detectors In mine PitS (CHIPS) Letter of Intent to FNAL," arXiv:1307.5918*

*[93] RENO-50 Collaboration (2013). URL http://home.kias.re.kr/MKG/h/reno50/.*

[94] *B. Pontecorvo, "Superweak interactions and double beta decay, Phys. Lett.* ***B26*** *(1968) 630.*

[95] *Lincoln Wolfenstein, "CP properties of Majorana neutrinos and double beta decay", Phys. Lett.* ***B107*** *(1981) 77.*

[96] *J. Schechter, J. W. F. Valle, "Neutrinoless double-beta decay in SU(2) x U(1) theories",* Phys.Rev. ***D25*** *(1982) 2951.*

[97] *Eiichi Takasugi, "Can the neutrinoless double beta decay take place in the case of Dirac neutrinos?", Phys. Lett.* ***B149*** *(1984) 372.*

[98] *Jose F. Nieves, "Dirac and pseudodirac neutrinos and neutrinoless double beta decay", Phys. Lett.* ***B147*** *(1984) 375.*

[99] *J. D. Vergados, "The Neutrinoless double beta decay from a modern perspective", Phys. Rep.* ***361*** *(2002) 1, hep-ph/0209347.*

[100] *S. M. Bilenky, C. Giunti, J. A. Grifols, E. Masso, "Absolute values of neutrino masses: Status and prospects", Phys. Rep.* ***379*** *(2003) 69, hep-ph/0211462.*

[101] *Craig Aalseth et al., "Neutrinoless double beta decay and direct searches for neutrino mass", hep-ph/0412300.*

[102] *R.N. Mohapatra et al., "Theory of Neutrinos: A White Paper", Rept. Prog. Phys.* ***70*** *(2007) 1757, hep-ph/0510213.*

[103] *W. Rodejohann, "Neutrinoless double beta decay and neutrino physics," J. Phys.* **G39** *(2012) 124008 [arXiv:1206.2560 [hep-ph]].*

[104] *Frank F. Deppisch, Martin Hirsch, Heinrich Pas, "Neutrinoless Double Beta Decay and Physics Beyond the Standard Model", J. Phys.* ***G39*** *(2012) 124007, arXiv:1208.0727 [hep-ph].*

[105] *H. Ejiri. "Comments on Neutrinoless Double Beta Decays." http://if-neutrino.fnal.gov/whitepapers/ejiri-dbd.pdf (2013).*

[106] *M. Auger et al. [EXO-200 Collaboration], "Search for Neutrinoless Double-Beta Decay in* $^{136}$*Xe with EXO-200," Phys. Rev. Lett.* **109** *(2012) 032505 [arXiv:1205.5608 [hep-ex]].*

[107] *M. Danilov et al., "Detection of very small neutrino masses in double beta decay using laser tagging," Phys. Lett.* **B480** *(2000) 12 [hep-ex/0002003].*

[108] *S. Dell'Oro, S. Marcocci, M. Viel, F. Vissani, "Neutrinoless double beta decay: 2015 review", arXiv:1601.07512 [hep-ph].*

[109] *Yu. Zdesenko, "The future of double beta decay research", Rev.Mod.Phys.* **74**, *663 (2002).*

[110] *O. Cremonesi, M. Pavan, "Challenges in Double Beta Decay", Adv. High Energy Phys.* ***2014*** *(2014) 951432, arXiv:1310.4692.*

[111] *Igor Ostrovskiy, Kevin O'Sullivan, "Search for neutrinoless double beta decay", arXiv:1605.00631 [hep-ex].*

[112] *A. de Gouvea, "TASI lectures on neutrino physics," hep-ph/0411274.*

[113] *H. V. Klapdor-Kleingrothaus, A. Dietz, H. L. Harney and I. V. Krivosheina, "Evidence for neutrinoless double beta decay," Mod. Phys. Lett.* **A16** *(2001) 2409 [hep-ph/0201231].*

[114] *B. Monreal and J. A. Formaggio, "Relativistic Cyclotron Radiation Detection of Tritium Decay Electrons as a New Technique for Measuring the Neutrino Mass,"* Phys.Rev. **D80** *(2009) 051301 [arXiv:0904.2860 [nucl-ex]].*

[115] *R. G. H. Robertson [KATRIN Collaboration], "KATRIN: an experiment to determine the neutrino mass from the beta decay of tritium," arXiv:1307.5486*

[116] *R. N. Mohapatra, "ICTP lectures on theoretical aspects of neutrino masses and mixings," hep-ph/0211252.*

[117] *S. Weinberg, "Baryon and Lepton Nonconserving Processes, Phys. Rev. Lett.* **43** *(1979) 1566.*

[118] *P. Minkowski, "$\mu$ to $e\gamma$ at a Rate of One out of One Billion Muon Decays?", Phys. Lett.* **B 67** *(1977) 421;*
*T. Yanagida, in: O. Sawada, et al. (Eds.), "Proceedings of the Workshop on the Unified Theory and the Baryon Number in the Universe, KEK Report, 79-18, Tsukuba, 1979, p. 95";*
*M. Gell-Mann, P. Ramond, R. Slansky, in: P. van Nieuwenhuizen, et al. (Eds.), "Supergravity, North-Holland," 1979, p. 315;*

*S. L. Glashow, in: M. Levy, et al. (Eds.), "Quarks and Leptons, Cargese," 1979, Plenum, 1980, p. 707;*
*R. N. Mohapatra, G. Senjanovic, "Neutrino Mass and Spontaneous Parity Nonconservation", Phys. Rev. Lett.* **44** *(1980) 912;*
*M. Fukugita, T. Yanagida, "Physics of Neutrinos and Applications to Astrophysics," Springer, Berlin, Germany, 2003, 593 .*

[119] *W. Konetschny, W. Kummer, "Nonconservation of total lepton number with scalar bosons", Phys. Lett.* **B 70** *(1977) 433;*
*T. P. Cheng, L. F. Li, "Neutrino masses, mixings, and oscillations in $SU(2) \times U(1)$ models of electroweak interactions",* Phys.Rev. **D22** *(1980) 2860;*
*M. Magg, C. Wetterich, "Neutrino mass problem and gauge hierarchy", Phys. Lett.* **B 94** *(1980) 61;*
*J. Schechter, J. W. F. Valle, "Neutrino masses in $SU(2) \times U(1)$ theories",* Phys.Rev. **D22** *(1980) 2227;*
*G. Lazarides, Q. Shafi, C. Wetterich, "Proton lifetime and fermion masses in an $SO(10)$ model" ,Nucl. Phys.* **B181** *(1981) 287;*
*R. N. Mohapatra, G. Senjanovic, "Neutrino masses and mixings in gauge models with spontaneous parity violation",* Phys.Rev. **D23** *(1981) 165.*

[120] *R. Foot, H. Lew, X. G. He, G. C. Joshi, "See-saw neutrino masses induced by a triplet of leptons" ,Z. Phys.* **C 44** *(1989) 441;*
*J. Chakrabortty, A. Dighe, S. Goswami, S. Ray, "Renormalization group evolution of neutrino masses and mixing in the Type III seesaw mechanism", Nucl. Phys.* **B820** *(2009) 116, arXiv:0812.2776 [hep-ph].*

[121] *A. Abada, C. Biggio, F. Bonnet, M. B. Gavela and T. Hambye, "Low energy effects of neutrino masses," JHEP* **0712** *(2007) 061 [arXiv:0707.4058 [hep-ph]].*

[122] *R. N. Mohapatra, "Mechanism for understanding small neutrino mass in superstring theories", Phys. Rev. Lett.* **56** *(1986), 561;*
*R. N. Mohapatra, J. W. F. Valle, "Neutrino mass and baryon-number nonconservation in superstring models",* Phys.Rev. **D34**, *1642 (1986).*

[123] *A. G. Dias, C. A. de S.Pires, P. S. Rodrigues da Silva and A. Sampieri, "A Simple Realization of the Inverse Seesaw Mechanism,"* Phys.Rev. **D86** *(2012) 035007 [arXiv:1206.2590].*

[124] *A. Zee, "A Theory of Lepton Number Violation, Neutrino Majorana Mass, and Oscillation", Phys. Lett.* **B93**, *389 (1980).*

[125] *X. G. He, "Is the Zee model neutrino mass matrix ruled out?", Eur. Phys. J.* **C34**, *371 (2004), hep-ph/0307172.*

[126] *K. S. Babu, "Model of 'calculable' Majorana neutrino masses", Phys. Lett.* **B203**, *132 (1988).*

[127] *A. Zee, "Quantum numbers of Majorana masses", Nucl. Phys.* **B264**, *99 (1986).*

[128] *K. S. Babu and E. Ma, "Natural Hierarchy of Radiatively Induced Majorana Neutrino Masses", Phys. Rev. Lett.* **61**, *674 (1988).*

[129] *E. Ma, "Verifiable radiative seesaw mechanism of neutrino mass and dark matter",* Phys.Rev. **D73**, *077301 (2006), hep-ph/0601225.*

[130] *P. O. Ludl and W. Grimus, "A complete survey of texture zeros in the lepton mass matrices," JHEP* **1407** *(2014) 090, [arXiv:1406.3546 [hep-ph]].*

[131] *P. O. Ludl and W. Grimus, "A complete survey of texture zeros in general and symmetric quark mass matrices," Phys. Lett.* **B744** *(2015) 38, [arXiv:1501.04942 [hep-ph]].*

[132] *A. Merle, W. Rodejohann, "The Elements of the Neutrino Mass Matrix: Allowed Ranges and Implications of Texture Zeros",* Phys.Rev. ***D73*** *073012 (2006), arXiv:hep-ph/0603111;*
*G. C. Branco, D. E. Costa, M. N. Rebelo and P. Roy, "Four Zero Neutrino Yukawa Textures in the Minimal Seesaw Framework",* Phys.Rev. ***D77*** *053011 (2008), arXiv:0712.0774 [hep-ph];*
*S. Choubey, W. Rodejohann and P. Roy, "Phenomenological consequences of four zero neutrino Yukawa textures" , Nucl.Phys.* ***B808*** *(2009), arXiv:0807.4289 [hep-ph];*
*B. Adhikary, A. Ghosal and P. Roy "$\mu\tau$ symmetry, tribimaximal mixing and four zero neutrino Yukawa textures" , JHEP 0910 (2009)* **040**, *arXiv:0908.2686 [hep-ph];*
*H. Fritzsch, Z. Z. Xing, S. Zhou, "Two-zero Textures of the Majorana Neutrino Mass Matrix and Current Experimental Tests", JHEP 083 (2011)* **09**, *arXiv:1108.4534 [hep-ph];*
*G. Blankenburg and D. Meloni, "Fine-tuning and naturalness issues in the two-zero neutrino mass textures", Nucl.Phys.* ***B867*** *(2013), arXiv:1204.2706 [hep-ph];*

*L. Wang and X. F. Han, "130 GeV gamma-ray line and enhancement of $h \to \gamma\gamma$ in the Higgs triplet model plus a scalar dark matter",* Phys.Rev. ***D87*** *015015 (2013), arXiv:1209.0376 [hep-ph];*
*J. Liao, D. Marfatia and K. Whisnant, "Neutrino seesaw mechanism with texture zeros" , Nucl.Phys.* ***B900*** *(2015), arXiv:1508.07364 [hep-ph];*
*H. Fritzsch , "Texture zero mass matrices and flavor mixing of quarks and leptons" , Mod.Phys.Lett.* ***A30*** *(2015) 28, 1550138,*
*L. M. Cebola, D. E. -Costa and R. G. Felipe, "Confronting predictive texture zeros in lepton mass matrices with current data" ,* Phys.Rev. ***D92*** *(2015) 2, 025005, arXiv:1504.06594 [hep-ph];*
*L. Lavoura , "New texture-zero patterns for lepton mixing" , J.Phys.* ***G42*** *(2015) 105004, arXiv:1502.03008 [hep-ph];*
*A. Ghosal and R. Samanta, "Probing texture zeros with scaling ansatz in inverse seesaw" , JHEP 1505 (2015)* **077** *, arXiv:1501.00916 [hep-ph].*

*[133] P. H. Frampton, S. L. Glashow and D. Marfatia, "Zeroes of the neutrino mass matrix," Phys. Lett.* **B536** *(2002) 79, [hep-ph/0201008].*

*[134] P. O. Ludl, S. Morisi and E. Peinado, "The Reactor mixing angle and CP violation with two texture zeros in the light of T2K," Nucl. Phys.* **B857** *(2012) 411, [arXiv:1109.3393 [hep-ph]].*

*[135] H. Fritzsch, Z. z. Xing and S. Zhou, "Two-zero Textures of the Majorana Neutrino Mass Matrix and Current Experimental Tests," JHEP* **1109** *(2011) 083 [arXiv:1108.4534 [hep-ph]].*

*[136] D. Meloni, A. Meroni and E. Peinado, "Two-zero Majorana textures in the light of the Planck results,"* Phys.Rev. **D89** *(2014) no.5, 053009 [arXiv:1401.3207 [hep-ph]].*

*[137] J. M. Lamprea and E. Peinado, "See-Saw scale discrete dark matter and two-zero texture Majorana neutrino mass matrices," arXiv:1603.02190 [hep-ph].*

*[138] S. Zhou, "Update on two-zero textures of the Majorana neutrino mass matrix in light of recent T2K, Super-Kamiokande and NO$\nu$A results," Chin. Phys.* **C40** *(2016) no.3, 033102 [arXiv:1509.05300 [hep-ph]].*

*[139] J. Liao, D. Marfatia and K. Whisnant, "Neutrino seesaw mechanism with texture zeros," Nucl. Phys.* **B900** *(2015) 449 [arXiv:1508.07364 [hep-ph]].*

[140] *R. Sinha, R. Samanta and A. Ghosal, "Revisiting Allowed Two Zero Textures of Neutrino Mass Matrices through Linear and Inverse Seesaw," arXiv:1508.05227 [hep-ph].*

[141] *L. M. Cebola, D. Emmanuel-Costa and R. G. Felipe, "Confronting predictive texture zeros in lepton mass matrices with current data,"* Phys.Rev. **D92** *(2015) no.2, 025005 [arXiv:1504.06594 [hep-ph]].*

[142] *Z. z. Xing and Z. h. Zhao, "On the four-zero texture of quark mass matrices and its stability," Nucl. Phys.* **B897** *(2015) 302 [arXiv:1501.06346 [hep-ph]].*

[143] *K. Whisnant, J. Liao and D. Marfatia, "Constraints on texture zero and cofactor zero models for neutrino mass," AIP Conf. Proc.* **1604** *(2014) 273.*

[144] *G. B. Gelmini and M. Roncadelli, "Left-handed neutrino mass scale and spontaneously broken lepton number", Phys. Lett.* **99B**, *411 (1981).*

[145] *J. Beringer et al. [Particle Data Group Collaboration],* Phys.Rev. **D86**, *010001 (2012).*

[146] *P. H. Frampton, S. L. Glashow, D. Marfatia, Phys. Lett.* ***B536*** *(2002) 79, [hep-ph/0201008];*
*W. Grimus and L. Lavoura, "On a model with two zeros in the neutrino mass matrix", J. Phys.* ***G31****, 693 (2005) [hep-ph/0412283];*

[147] *A. Chaudhuri and B. Mukhopadhyaya, "CP -violating phase in a two Higgs triplet scenario: Some phenomenological implications,"* Phys.Rev. **D93** *(2016) no.9, 093003 [arXiv:1602.07846 [hep-ph]].*

[148] *E. Ma and U. Sarkar, "Neutrino masses and leptogenesis with heavy Higgs triplets", Phys. Rev. Lett.* ***80****, 5716 (1998) [hep-ph/9802445].*

[149] *S.M. Bilenky, J. Hošek and S.T. Petcov, "On oscillations of neutrinos with Dirac and Majorana masses", Phys. Lett.* ***94B****, 495 (1980);*
*I.Yu. Kobzarev, B.V. Martemyanov, L.B. Okun and M.G. Shchepkin, "The phenomenology of neutrino oscillations", Yad. Fiz.* ***32****, 1590 (1980) [Sov. J. Nucl. Phys.* ***32****, 823 (1981)].*

[150] *J. F. Gunion, R. Vega and J. Wudka, "Higgs triplets in the standard model",* Phys.Rev. **D42**, *1673 (1990);*
*J. F. Gunion, R. Vega and J. Wudka, "Naturalness problems for* $\rho = 1$ *and other large one-loop effects for a standard-model Higgs sector containing triplet fields",* Phys.Rev. **D43**, *2322 (1991);*

*S. Chakrabarti,, D. Choudhury, R. M. Godbole and B. Mukhopadhyaya, "Observing Doubly Charged Higgs Bosons in Photon-Photon Collisions", Phys. Lett.* **B434**, *347 (1998) [hep-ph/9804297];*
*E. J. Chun, K. Y. Lee and S. C. Park, "Testing Higgs Triplet Model and Neutrino Mass Patterns", Phys. Lett.* **B566**, *142 (2003) [hep-ph/0304069];*
*T. Han, H. E. Logan, B. Mukhopadhyaya and R. Srikanth, "Neutrino masses and lepton-number violation in the Littlest Higgs scenario",* Phys.Rev. **D72**, *053007 (2005) [hep-ph/0505260];*
*T. Han, B. Mukhopadhyaya, Z. Si and K. Wang, "Pair Production of Doubly-Charged Scalars: Neutrino Mass Constraints and Signals at the LHC",* Phys.Rev. **D76**, *075013 (2007) [arXiv:0706.0441 [hep-ph]];*
*P. Dey, A. Kundu and B. Mukhopadhyaya, "Some consequences of a Higgs triplet", J. Phys.* **G36**, *025002 (2009) [arXiv:0802.2510 [hep-ph]];*
*M. Aoki, S. Kanemura, T. Shindou and K. Yagyu, "An R-parity conserving radiative neutrino mass model without right-handed neutrinos", JHEP* **1007**, *084 (2010) [Erratum-ibid.* **1011**, *049 (2010)] [arXiv:1005.5159 [hep-ph]];*
*A. G. Akeroyd, H. Sugiyama,* Phys.Rev. **D84**, *035010 (2011) [arXiv:1105.2209 [hep-ph]];*
*M. Aoki, S. Kanemura and K. Yagyu, "Production of doubly charged scalars from the decay of singly charged scalars in the Higgs Triplet Model",* Phys.Rev. **D85**, *055007 (2012) [arXiv:1110.4625 [hep-ph]].*

*[151] Z.-Z. Xing, "Texture zeros and Majorana phases of the neutrino mass matrix", Phys. Lett.* ***B530*** *(2002) 159 [hep-ph/0201151];*
*Z.-Z. Xing, "A full determination of the neutrino mass spectrum from two-zero textures of the neutrino mass matrix", Phys. Lett.* ***B539****, 85 (2002) [hep-ph/0205032];*
*M. Honda, S. Kaneko and M. Tanimoto, "Prediction and its stability in neutrino mass matrix with two zeros," JHEP* **0309**, *028 (2003) [hep-ph/0303227];*
*W.-L. Guo and Z.-Z. Xing, "Calculable CP-violating Phases in the Minimal Seesaw Model of Leptogenesis and Neutrino Mixing", Phys. Lett.* **B583**, *163 (2004) [hep-ph/0310326];*
*M. Honda, S. Kaneko and M. Tanimoto, "Seesaw enhancement of bilarge mixing in two zero textures," Phys. Lett.* **B593**, *165 (2004) [hep-ph/0401059].*

*[152] W. Grimus, A. S. Joshipura, L. Lavoura and M. Tanimoto, "Symmetry realization of texture zeros", Eur. Phys. J.* **C36**, *227 (2004) [hep-ph/0405016].*

[153] *W. Grimus and L. Lavoura, "On a model with two zeros in the neutrino mass matrix", J. Phys.* ***G31****, 693 (2005) [hep-ph/0412283].*

[154] *K. Huitu, J. Maalampi, A. Pietila and M. Raidal, "Doubly charged Higgs at LHC," Nucl. Phys.* **B487***, 27 (1997) [hep-ph/9606311];*
*J. F. Gunion, C. Loomis and K. T. Pitts, "Searching for doubly charged Higgs bosons at future colliders," eConf C* **960625***, LTH096 (1996) [hep-ph/9610237];*
*J. C. Montero, C. A. de S.Pires and V. Pleitez, "Neutrino masses through a type II seesaw mechanism at TeV scale," Phys. Lett.* **B502***, 167 (2001) [hep-ph/0011296];*
*E. Ma, M. Raidal and U. Sarkar, "Phenomenology of the neutrino mass giving Higgs triplet and the low-energy seesaw violation of lepton number," Nucl. Phys.* **B615***, 313 (2001) [hep-ph/0012101];*
*M. Mühlleitner and M. Spira, "A Note on doubly charged Higgs pair production at hadron colliders,"* Phys.Rev. **D68***, 117701 (2003) [hep-ph/0305288].*
*A. G. Akeroyd and M. Aoki, "Single and pair production of doubly charged Higgs bosons at hadron colliders,"* Phys.Rev. **D72***, 035011 (2005) [hep-ph/0506176];*
*B. Bajc, M. Nemevšek and G. Senjanović, "Probing seesaw at LHC,"* Phys.Rev. **D76***, 055011 (2007) [hep-ph/0703080];*
*A. Hektor, M. Kadastik, M. Müntel, M. Raidal and L. Rebane, "Testing neutrino masses in little Higgs models via discovery of doubly charged Higgs at LHC," Nucl. Phys.* **B787***, 198 (2007) [arXiv:0705.1495 [hep-ph]];*
*J. Garayoa and T. Schwetz, "Neutrino mass hierarchy and Majorana CP phases within the Higgs triplet model at the LHC," JHEP* **0803***, 009 (2008) [arXiv:0712.1453 [hep-ph]].*

[155] *W. Grimus, R. Pfeiffer and T. Schwetz, "A 4-neutrino model with a Higgs triplet", Eur. Phys. J.* **C13***, 125 (2000) [hep-ph/9905320].*

[156] *A. Chaudhuri, W. Grimus and B. Mukhopadhyaya, "Doubly charged scalar decays in a type II seesaw scenario with two Higgs triplets," JHEP* **1402** *(2014) 060 [arXiv:1305.5761 [hep-ph]].*

[157] *J. Beringer et al. (Particle Data Group),* Phys.Rev. **D86***, 010001 (2012).*

[158] *https://twiki.cern.ch/twiki/bin/view/AtlasPublic/HiggsPublicResults.*

[159] *N. D. Christensen and C. Duhr, "FeynRules - Feynman rules made easy," Comput. Phys. Commun.* **180***, 1614 (2009) [arXiv:0806.4194 [hep-ph]].*

[160] *C. Degrande, C. Duhr, B. Fuks, D. Grellscheid, O. Mattelaer and T. Reiter, "UFO - The Universal FeynRules Output," Comput. Phys. Commun.* **183**, *1201 (2012) [arXiv:1108.2040 [hep-ph]].*

[161] *A. Pukhov et al., "CompHEP: A package for evaluation of Feynman diagrams and integration over multi-particle phase space", hep-ph/9908288.*

[162] *J. Alwall, M. Herquet, F. Maltoni, O. Mattelaer and T. Stelzer, "MadGraph 5: Going Beyond", JHEP* **1106**, *128 (2011) [arXiv:1106.0522 [hep-ph]].*

[163] *T. Han, B. Mukhopadhyaya, Z. Si and K. Wang, "Pair Production of Doubly-Charged Scalars: Neutrino Mass Constraints and Signals at the LHC",* Phys.Rev. **D76**, *075013 (2007) [arXiv:0706.0441 [hep-ph]].*

[164] *J. C. Pati and A. Salam, "Lepton Number As The Fourth Color,"* Phys.Rev. ***D10*** *(1974) 275;*
*R. N. Mohapatra and J. C. Pati, "A Natural Left-Right Symmetry,"* Phys.Rev. ***D11*** *(1975) 2558;*
*G. Senjanović and R. N. Mohapatra, "Exact left-right symmetry and spontaneous violation of parity,"* Phys.Rev. ***D12*** *(1975) 1502;*
*G. Senjanović, "Spontaneous Breakdown of Parity in a Class of Gauge Theories," Nucl. Phys.* ***B153*** *(1979) 334;*
*M. Fukugita, T. Yanagida, "Physics of Neutrinos and Applications to Astrophysics," Springer, Berlin, Germany, 2003;*
*P. Fileviez Perez, "Type III Seesaw and Left- Right Symmetry," JHEP* **03** *(2009) 142;*
*J. Chakrabortty "Type I and new seesaw in left - right symmetric theories", Phys. Lett.* ***4B****, 690 (2010);*
*G. Senjanović, "SEESAW AT LHC THROUGH LEFTâĂŞRIGHT SYMMETRY", Int. J. Mod. Phys.* ***A26****, 1469 (2011);*
*M. Duerr, P. F. Perez and M. Lindner, "Left-Right Symmetric Theory with Light Sterile Neutrinos",* Phys.Rev. ***D88****, 051701 (2013).*

[165] *N. G. Deshpande and E. Ma, "Pattern of symmetry breaking with two Higgs doublets",* Phys.Rev. ***D18*** *2574 (1078).*

[166] *N. Chakrabarty, U. K. Dey, B. Mukhopadhyaya, "High-scale validity of a two-Higgs doublet scenario: a study including LHC data", JHEP 1412 (2014)* **166**, *arXiv:1407.2145 [hep-ph];*

*N. Chakrabarty, "High-scale validity of a model with Three-Higgs-doublets", arXiv:1511.08137 [hep-ph].*

*[167] M. A. Schmidt, "Renormalization group evolution in the type I + II seesaw model",* Phys.Rev. **D76** *(2007) 073010, arXiv:0705.3841 [hep-ph];*
*J. Elias-Miro, J. R. Espinosa, G. Giudice, G. Isidori, A. Riotto, A. Strumia , "Higgs mass implications on the stability of the electroweak vacuum", Phys.Lett. **B709** (2012), arXiv:1112.3022 [hep-ph];*
*E. Jin. Chun, H. Min. Lee, P. Sharma, "Vacuum Stability, Perturbativity, EWPD and Higgs-to-diphoton rate in Type II Seesaw Models", JHEP 1211 (2012)* **106**, *arXiv:1209.1303 [hep-ph].*

*[168] J. Alwall, R. Frederix, S. Frixione, V. Hirschi, F. Maltoni, O. Mattelaer, H. S. Shao, T. Stelzer, P. Torrielli and M. Zaro, "The automated computation of tree-level and next-to-leading order differential cross sections, and their matching to parton shower simulations," JHEP 1407 (2014)* **079**, *arXiv:1405.0301 [hep-ph].*

*[169] N. Jarosik et al. (WMAP), "Seven-Year Wilkinson Microwave Aniosotropy Probe (WMAP*)$Observations$ :
$SkyMaps, SystematicErrors, AndBasicResults$", $Astrophys.J.Suppl.192(2011)$**14**;
*For an overview see: K. Nakamura et al. (PDG), "Review of Particle Physics", J. Phys. G* **37** *(2010) 075021.*

*[170] WMAP Collaboration, G. Hinshaw et al., "Nine-Year Wilkinson Microwave Anisotropy Probe (WMAP) Observations: Cosmological Parameter Results," Astrophys. J. Suppl. 208 (2013)* **19**, *arXiv:1212.5226.*

*[171] Planck Collaboration, P. Ade et al., "Planck 2013 results. I. Overview of products and scientific results," arXiv:1303.5062.*

*[172] F. Zwicky, "Die Rotverschiebung von extragalaktischen Nebeln", Helv.Phys.Acta* **6**, *110-127 (1933).*

*[173] L. Baudis, "Dark matter searches," Annalen Phys.* **528** *(2016) 74 [arXiv:1509.00869 [astro-ph.CO]].*

*[174] V. C. Rubin, N. Thonnard, and J. Ford, W. K., "Extended rotation curves of high-luminosity spiral galaxies.," Astrophys. J 225 (1978)* **L107**.

*[175] J. A. Tyson, G. P. Kochanski, and I. P. Dell'Antonio, "Detailed mass map of CL0024+1654 from strong lensing",* Astrophys.J. **498** *(1998) L107, [astro-ph/9801193].*

*[176] R. Massey, J. Rhodes, R. Ellis, N. Scoville, A. Leauthaud, et al., "Dark matter maps reveal cosmic scaffolding",* Nature **445** *(2007) 286, [astro-ph/0701594].*

*[177] D. Clowe, M. Bradac, A. H. Gonzalez, M. Markevitch, S. W. Randall, et al., "A direct empirical proof of the existence of dark matter",* Astrophys.J. **648** *(2006) L 109, [astro-ph/0608407].*

*[178] D. N. Spergel et al. [WMAP Collaboration], "Wilkinson Microwave Anisotropy Probe (WMAP) three year results: implications for cosmology," Astrophys. J. Suppl.* **170** *(2007) 377 [astro-ph/0603449].*

*[179] R. H. Cyburt, "Primordial nucleosynthesis for the new cosmology: Determining uncertainties and examining concordance,"* Phys.Rev. **D70** *(2004) 023505 [astro-ph/0401091].*

*[180] D. J. Eisenstein et al. [SDSS Collaboration], "Detection of the baryon acoustic peak in the large-scale correlation function of SDSS luminous red galaxies," Astrophys. J.* **633** *(2005) 560 [astro-ph/0501171].*

*[181] O. Y. Gnedin , J. P. Ostriker, "Limits on Collisional Dark Matter from Elliptical Galaxies in Clusters", Astrophys. J.* **561**, *61 (2001);*
*J. F. Hennawi, J. P. Ostriker, "Observational Constraints on the Self-interacting Dark Matter Scenario and the Growth of Supermassive Black Holes", Astrophys. J.* **572**, *41 (2002);*
*J. Miralda-Escude, "A Test of the Collisional Dark Matter Hypothesis from Cluster Lensing", Astrophys. J.* **564**, *60 (2002);*
*S. W. Randall et al., "Constraints of the Self-Interaction Cross Section of Dark Matter from Numerical Simulations of the Merging Galaxy Cluster 1E 0657-56", Astrophys. J.* **679**, *1173 (2008).*

*[182] E. Otten and C. Weinheimer, "Neutrino mass limit from tritium beta decay",* Rept.Prog.Phys. **71** *(2008) 086201, [arXiv:0909.2104].*

*[183] S. Tremaine and J. Gunn, "Dynamical Role of Light Neutral Leptons in Cosmology",* Phys.Rev.Lett. **42** *(1979) 407.*

[184] *K. Griest, "Galactic Microlensing as a Method of Detecting Massive Compact Halo Objects"*, Astrophys.J. **366** *(1991) 412.*

[185] *B. J. Carr, "Baryonic dark matter"*, Ann.Rev.Astron.Astrophys. **32** *(1994) 531.*

[186] *R. Peccei and H. R. Quinn, "CP Conservation in the Presence of Instantons"*, Phys.Rev.Lett. **38** *(1977) 1440.*

[187] *M. S. Turner, "Windows on the Axion"*, Phys.Rept. **197** *(1990) 67.*

[188] *G. G. Raffelt, "Astrophysical methods to constrain axions and other novel particle phenomena"*, Phys.Rept. **198** *(1990) 1.*

[189] *L. Visinelli and P. Gondolo, "Dark Matter Axions Revisited"*, Phys.Rev. **D80** *(2009) 035024, [arXiv:0903.4377].*

[190] *P. Sikivie, "Dark matter axions"*, Int.J.Mod.Phys. **A25** *(2010) 554, [arXiv:0909.0949].*

[191] *M. Archidiacono, S. Hannestad, A. Mirizzi, G. Raffelt, and Y. Y. Wong, "Axion hot dark matter bounds after Planck"*, JCAP **1310** *(2013) 020, [arXiv:1307.0615].*

[192] *K. S. Jeong, M. Kawasaki, and F. Takahashi, "Axions as Hot and Cold Dark Matter"*, JCAP **1402** *(2014) 046, [arXiv:1310.1774].*

[193] *E. Di Valentino, E. Giusarma, M. Lattanzi, A. Melchiorri, and O. Mena, "Axion cold dark matter: status after Planck and BICEP2", [arXiv:1405.1860].*

[194] *S. Profumo,* "Neutralino dark matter: where particle physics meets cosmology ". *PhD thesis, UC, Santa Cruz & UC, Santa Cruz, Inst. Part. Phys., 2005.*

[195] *L. Calibbi, J. M. Lindert, T. Ota, and Y. Takanishi, "Cornering light Neutralino Dark Matter at the LHC"*, JHEP **1310** *(2013) 132, [arXiv:1307.4119].*

[196] *G. Bélanger, G. Drieu La Rochelle, B. Dumont, R. M. Godbole, S. Kraml, et al., "LHC constraints on light neutralino dark matter in the MSSM", Phys.Lett.* **B726** *(2013) 773, [arXiv:1308.3735].*

[197] *T. Han, Z. Liu, and S. Su, "Light Neutralino Dark Matter: Direct/Indirect Detection and Collider Searches", [arXiv:1406.1181].*

[198] *L. Lopez Honorez, E. Nezri, J. F. Oliver, and M. H. Tytgat, "The Inert Doublet Model: An Archetype for Dark Matter"*, JCAP **0702** *(2007) 028, [hep-ph/0612275].*

[199] *A. Arhrib, Y.-L. S. Tsai, Q. Yuan, and T.-C. Yuan, "An Updated Analysis of Inert Higgs Doublet Model in light of the Recent Results from LUX, PLANCK, AMS-02 and LHC", [arXiv:1310.0358].*

[200] *G. Servant and T. M. Tait, "Is the lightest Kaluza-Klein particle a viable dark matter candidate?"*, Nucl.Phys. **B650** *(2003) 391–419, [hep-ph/0206071].*

[201] *G. Servant and T. M. Tait, "Elastic scattering and direct detection of Kaluza-Klein dark matter"*, New J.Phys. **4** *(2002) 99, [hep-ph/0209262].*

[202] *K. Kong and K. T. Matchev, "Precise calculation of the relic density of Kaluza-Klein dark matter in universal extra dimensions"*, JHEP **0601** *(2006) 038, [hep-ph/0509119].*

[203] *M. Kakizaki, S. Matsumoto, Y. Sato, and M. Senami, "Relic abundance of LKP dark matter in UED model including effects of second KK resonances"*, Nucl.Phys. **B735** *(2006) 84, [hep-ph/0508283].*

[204] *M. Kakizaki, S. Matsumoto, Y. Sato, and M. Senami, "Significant effects of second KK particles on LKP dark matter physics"*, Phys.Rev. **D71** *(2005) 123522, [hep-ph/0502059].*

[205] *T. Flacke, D. Hooper, and J. March-Russell, "Improved bounds on universal extra dimensions and consequences for LKP dark matter"*, Phys.Rev. **D73** *(2006) 095002, [hep-ph/0509352].*

[206] *F. Burnell and G. D. Kribs, "The Abundance of Kaluza-Klein dark matter with coannihilation"*, Phys.Rev. **D73** *(2006) 015001, [hep-ph/0509118].*

[207] *T. Flacke and D. W. Maybury, "Constraints on UED KK-neutrino dark matter from magnetic dipole moments"*, Int.J.Mod.Phys. **D16** *(2007) 1593, [hep-ph/0601161].*

[208] *M. Kakizaki, S. Matsumoto, and M. Senami, "Relic abundance of dark matter in the minimal universal extra dimension model"*, Phys.Rev. **D74** *(2006) 023504, [hep-ph/0605280].*

[209] *S. Arrenberg, L. Baudis, K. Kong, K. T. Matchev, and J. Yoo, "Kaluza-Klein Dark Matter: Direct Detection vis-a-vis LHC"*, Phys.Rev. **D78** *(2008) 056002, [arXiv:0805.4210].*

[210] *G. Belanger, M. Kakizaki, and A. Pukhov, "Dark matter in UED: The Role of the second KK level"*, JCAP **1102** *(2011) 009, [arXiv:1012.2577].*

*[211] S. Arrenberg, L. Baudis, K. Kong, K. T. Matchev, and J. Yoo, "Kaluza-Klein Dark Matter: Direct Detection vis-a-vis LHC (2013 update)", [arXiv:1307.6581].*

*[212] S. D. M. White, C. S. Frenk and M. Davis, "Clustering in a Neutrino Dominated Universe," Astrophys. J.* **274** *(1983) L1.*

*[213] K. N. Abazajian et al., "Light Sterile Neutrinos: A White Paper," arXiv:1204.5379 [hep-ph].*

*[214] A. Kusenko, "Sterile neutrinos: The Dark side of the light fermions," Phys. Rept.* **481** *(2009) 1 [arXiv:0906.2968 [hep-ph]].*

*[215] A. Boyarsky, O. Ruchayskiy and M. Shaposhnikov, "The Role of sterile neutrinos in cosmology and astrophysics," Ann. Rev. Nucl. Part. Sci.* **59** *(2009) 191 [arXiv:0901.0011 [hep-ph]].*

*[216] E. W. Kolb and M. S. Turner, "The Early Universe",* Front.Phys. **69** *(1990).*

*[217] J. D. Wells, "Annihilation cross-sections for relic densities in the low velocity limit", [hep-ph/9404219].*

*[218] M. Srednicki, R. Watkins, and K. A. Olive, "Calculations of Relic Densities in the Early Universe",* Nucl.Phys. **B310** *(1988) 693.*

*[219] K. Griest and D. Seckel, "Three exceptions in the calculation of relic abundances",* Phys.Rev. **D43** *(1991) 3191.*

*[220] G. Jungman, M. Kamionkowski, and K. Griest, "Supersymmetric dark matter",* Phys.Rept. **267** *(1996) 195, [hep-ph/9506380].*

*[221] J. Lewin and P. Smith, "Review of mathematics, numerical factors, and corrections for dark matter experiments based on elastic nuclear recoil," Astropart. Phys.* **6** *(1996) 87.*

*[222] T. Marrodan Undagoitia and L. Rauch, "Dark matter direct-detection experiments," J. Phys.* **G43** *(2016) no.1, 013001 [arXiv:1509.08767].*

*[223] C. E. Aalseth et al. [CoGeNT Collaboration], "Search for An Annual Modulation in Three Years of CoGeNT Dark Matter Detector Data," arXiv:1401.3295 [astro-ph.CO].*

[224] *C. E. Aalseth et al. [CoGeNT Collaboration], "CoGeNT: A Search for Low-Mass Dark Matter using p-type Point Contact Germanium Detectors,"* Phys.Rev. **D88** *(2013) 012002 [arXiv:1208.5737 [astro-ph.CO]].*

[225] *J. H. Davis, C. McCabe and C. Boehm, "Quantifying the evidence for Dark Matter in CoGeNT data," JCAP* **1408** *(2014) 014 doi:10.1088/1475-7516/2014/08/014 [arXiv:1405.0495 [hep-ph]].*

[226] *Z. Ahmed et al. [CDMS Collaboration], "Search for Weakly Interacting Massive Particles with the First Five-Tower Data from the Cryogenic Dark Matter Search at the Soudan Underground Laboratory," Phys. Rev. Lett.* **102** *(2009) 011301 [arXiv:0802.3530 [astro-ph]].*

[227] *Z. Ahmed et al. [CDMS-II Collaboration], "Dark Matter Search Results from the CDMS II Experiment," Science* **327** *(2010) 1619 [arXiv:0912.3592 [astro-ph.CO]].*

[228] *Z. Ahmed et al. [CDMS-II Collaboration], "Search for annual modulation in low-energy CDMS-II data," arXiv:1203.1309 [astro-ph.CO].*

[229] *R. Agnese et al. [SuperCDMS Collaboration], "Search for Low-Mass Weakly Interacting Massive Particles with SuperCDMS," Phys. Rev. Lett.* **112** *(2014) no.24, 241302 [arXiv:1402.7137 [hep-ex]].*

[230] *R. Agnese et al. [SuperCDMS Collaboration], "New Results from the Search for Low-Mass Weakly Interacting Massive Particles with the CDMS Low Ionization Threshold Experiment," Phys. Rev. Lett.* **116** *(2016) no.7, 071301 [arXiv:1509.02448 [astro-ph.CO]].*

[231] *S. T. Lin et al. [TEXONO Collaboration], "New limits on spin-independent and spin-dependent couplings of low-mass WIMP dark matter with a germanium detector at a threshold of 220 eV,"* Phys.Rev. **D79** *(2009) 061101 [arXiv:0712.1645 [hep-ex]].*

[232] *E. Armengaud et al. [EDELWEISS Collaboration], "Final results of the EDELWEISS-II WIMP search using a 4-kg array of cryogenic germanium detectors with interleaved electrodes," Phys. Lett.* **B702** *(2011) 329 [arXiv:1103.4070 [astro-ph.CO]].*

[233] *G. Angloher et al. [CRESST Collaboration], "Probing low WIMP masses with the next generation of CRESST detector," arXiv:1503.08065 [astro-ph.IM]*

*[234] G. Angloher et al. [CRESST Collaboration], "Results on light dark matter particles with a low-threshold CRESST-II detector," Eur. Phys. J.* **C76** *(2016) no.1, 25 [arXiv:1509.01515 [astro-ph.CO]].*

*[235] EURECA Collaboration, G. Angloher et al., "EURECA Conceptual Design Report," Phys. Dark Univ.* **3** *(2014) 41.*

*[236] S. Cebrian et al., "First results of the ROSEBUD dark matter experiment," Astropart. Phys.* **15** *(2001) 79 [astro-ph/0004292].*

*[237] P. Agnes et al. [DarkSide Collaboration], "First Results from the DarkSide-50 Dark Matter Experiment at Laboratori Nazionali del Gran Sasso," Phys. Lett.* **B743** *(2015) 456 [arXiv:1410.0653 [astro-ph.CO]].*

*[238] J. Angle et al. [XENON10 Collaboration], "A search for light dark matter in XENON10 data," Phys. Rev. Lett.* **107** *(2011) 051301 [arXiv:1104.3088 [astro-ph.CO]].*

*[239] E. Aprile et al. [XENON100 Collaboration], "Dark Matter Results from 225 Live Days of XENON100 Data," Phys. Rev. Lett.* **109** *(2012) 181301 [arXiv:1207.5988 [astro-ph.CO]].*

*[240] E. Aprile et al. [XENON100 Collaboration], "Search for Event Rate Modulation in XENON100 Electronic Recoil Data," Phys. Rev. Lett.* **115** *(2015) no.9, 091302 [arXiv:1507.07748 [astro-ph.CO]].*

*[241] E. Aprile et al. [XENON100 Collaboration], "Exclusion of Leptophilic Dark Matter Models using XENON100 Electronic Recoil Data," Science* **349** *(2015) no.6250, 851 [arXiv:1507.07747 [astro-ph.CO]].*

*[242] E. Aprile [XENON1T Collaboration], "The XENON1T Dark Matter Search Experiment," Springer Proc. Phys.* **148** *(2013) 93 [arXiv:1206.6288 [astro-ph.IM]].*

*[243] D. S. Akerib et al. [LUX Collaboration], "The Large Underground Xenon (LUX) Experiment," Nucl. Instrum. Meth.* **A704** *(2013) 111 [arXiv:1211.3788 [physics.ins-det]].*

*[244] D. S. Akerib et al. [LUX Collaboration], "First results from the LUX dark matter experiment at the Sanford Underground Research Facility," Phys. Rev. Lett.* **112** *(2014) 091303 [arXiv:1310.8214 [astro-ph.CO]].*

*[245] D. Malling et al., "After LUX: The LZ Program," arXiv:1110.0103.*

[246] *X. Cao et al. [PandaX Collaboration], "PandaX: A Liquid Xenon Dark Matter Experiment at CJPL," Sci. China Phys. Mech. Astron.* **57** *(2014) 1476 [arXiv:1405.2882 [physics.ins-det]].*

[247] *X. Xiao et al. [PandaX Collaboration], "Low-mass dark matter search results from full exposure of the PandaX-I experiment,"* Phys.Rev. **D92** *(2015) no.5, 052004 [arXiv:1505.00771 [hep-ex]].*

[248] *M. Felizardo et al., "Final Analysis and Results of the Phase II SIMPLE Dark Matter Search," Phys. Rev. Lett.* **108** *(2012) 201302 [arXiv:1106.3014 [astro-ph.CO]].*

[249] *C. Amole et al. [PICO Collaboration], "Dark Matter Search Results from the PICO-2L $C_3F_8$ Bubble Chamber," Phys. Rev. Lett.* **114** *(2015) no.23, 231302 [arXiv:1503.00008 [astro-ph.CO]].*

[250] *M. Schumann, "Dark Matter 2013," Braz. J. Phys.* **44** *(2014) 483 [arXiv:1310.5217 [astro-ph.CO]].*

[251] *K. Choi, "talk 906 at ICRC 2013".*

[252] *M. G. Aartsen et al. [IceCube Collaboration], "Search for dark matter annihilations in the Sun with the 79-string IceCube detector," Phys. Rev. Lett.* **110** *(2013) no.13, 131302 [arXiv:1212.4097 [astro-ph.HE]].*

[253] *J. J. Hernandez-Rey, "talk 316 at ICRC 2013".*

[254] *M. G. Aartsen et al. [IceCube Collaboration], "The IceCube Neutrino Observatory Part IV: Searches for Dark Matter and Exotic Particles," arXiv:1309.7007 [astro-ph.HE].*

[255] *M. Wolf, "talk 330 at ICRC 2013".*

[256] *C. Weniger, "A Tentative Gamma-Ray Line from Dark Matter Annihilation at the Fermi Large Area Telescope," JCAP* **1208** *(2012) 007 [arXiv:1204.2797 [hep-ph]].*

[257] *D. P. Finkbeiner, M. Su and C. Weniger, "Is the 130 GeV Line Real? A Search for Systematics in the Fermi-LAT Data," JCAP* **1301** *(2013) 029 [arXiv:1209.4562 [astro-ph.HE]].*

[258] *O. Adriani et al. [PAMELA Collaboration], "An anomalous positron abundance in cosmic rays with energies 1.5-100 GeV," Nature* **458** *(2009) 607 [arXiv:0810.4995 [astro-ph]].*

*[259] M. Boezio, "review 1284 at ICRC 2013".*

*[260] M. Aguilar et al. [AMS Collaboration], "First Result from the Alpha Magnetic Spectrometer on the International Space Station: Precision Measurement of the Positron Fraction in Primary Cosmic Rays of 0.5-350 GeV," Phys. Rev. Lett.* **110** *(2013) 141102.*

*[261] S. Ting, "review 1259 at ICRC 2013".*

*[262] G. Aad et al. [ATLAS Collaboration], "Search for dark matter in events with a Z boson and missing transverse momentum in pp collisions at $\sqrt{s}$=8 TeV with the ATLAS detector,"* Phys.Rev. **D90** *(2014) no.1, 012004 [arXiv:1404.0051 [hep-ex]].*

*[263] G. Aad et al. [ATLAS Collaboration], "Search for dark matter candidates and large extra dimensions in events with a jet and missing transverse momentum with the ATLAS detector," JHEP* **1304** *(2013) 075 [arXiv:1210.4491 [hep-ex]].*

*[264] S. Chatrchyan et al. [CMS Collaboration], "Search for dark matter and large extra dimensions in monojet events in $pp$ collisions at $\sqrt{s} = 7$ TeV," JHEP* **1209** *(2012) 094 [arXiv:1206.5663 [hep-ex]].*

*[265] O. Buchmueller, M. J. Dolan and C. McCabe, "Beyond Effective Field Theory for Dark Matter Searches at the LHC," JHEP* **1401** *(2014) 025 [arXiv:1308.6799 [hep-ph]].*

*[266] A. De Simone, G. F. Giudice and A. Strumia, "Benchmarks for Dark Matter Searches at the LHC," JHEP* **1406** *(2014) 081 [arXiv:1402.6287 [hep-ph]].*

*[267] S. A. Malik et al., "Interplay and Characterization of Dark Matter Searches at Colliders and in Direct Detection Experiments," Phys. Dark Univ.* **9** *(2015) 51 [arXiv:1409.4075 [hep-ex]].*

*[268] G. Belanger, B. Dumont, U. Ellwanger, J. F. Gunion and S. Kraml, "Status of invisible Higgs decays," Phys. Lett.* **B723** *(2013) 340 [arXiv:1302.5694 [hep-ph]].*

*[269] E. Ma and D. Suematsu, "Fermion Triplet Dark Matter and Radiative Neutrino Mass," Mod. Phys. Lett.* **A24**, *583 (2009) [arXiv:0809.0942 [hep-ph]].*

*[270] W. Chao, "Dark Matter, LFV and Neutrino Magnetic Moment in the Radiative Seesaw Model with Triplet Fermion," arXiv:1202.6394 [hep-ph].*

*[271] M. Hirsch, R. A. Lineros, S. Morisi, J. Palacio, N. Rojas and J. W. F. Valle, "WIMP dark matter as radiative neutrino mass messenger," JHEP* **1310**, *149 (2013) [arXiv:1307.8134 [hep-ph]].*

*[272] A. Chaudhuri, N. Khan, B. Mukhopadhyaya and S. Rakshit, "Dark matter candidate in an extended type III seesaw scenario,"* Phys.Rev. **D91** *(2015) 055024 [arXiv:1501.05885 [hep-ph]].*

*[273] A. Abada, C. Biggio, F. Bonnet, M. B. Gavela and T. Hambye, "$\mu \to e\gamma$ and $\tau \to l\gamma$ decays in the fermion triplet seesaw model,"* Phys.Rev. **D78**, *033007 (2008) [arXiv:0803.0481 [hep-ph]].*

*[274] C. Biggio and F. Bonnet, "Implementation of the Type III Seesaw Model in FeynRules/MadGraph and Prospects for Discovery with Early LHC Data," Eur. Phys. J.* **C72**, *1899 (2012) [arXiv:1107.3463 [hep-ph]].*

*[275] A. Alloul, N. D. Christensen, C. Degrande, C. Duhr and B. Fuks, "FeynRules 2.0 - A complete toolbox for tree-level phenomenology," Comput. Phys. Commun.* **185** *(2014) 2250 [arXiv:1310.1921 [hep-ph]].*

*[276] G. Belanger, F. Boudjema, P. Brun, A. Pukhov, S. Rosier-Lees, P. Salati and A. Semenov, "Indirect search for dark matter with micrOMEGAs2.4," Comput. Phys. Commun.* **182**, *842 (2011) [arXiv:1004.1092 [hep-ph]].*

*[277] G. Belanger, F. Boudjema, A. Pukhov and A. Semenov, "micrOMEGAs 3: A program for calculating dark matter observables," Comput. Phys. Commun.* **185**, *960 (2014) [arXiv:1305.0237 [hep-ph]].*

*[278] C. L. Bennett et al. [WMAP Collaboration], "First year Wilkinson Microwave Anisotropy Probe (WMAP) observations: Preliminary maps and basic results," Astrophys. J. Suppl.* **148**, *1 (2003) [astro-ph/0302207]. D.N. Spergel et al. [WMAP Collaboration], Astrophys. J. Suppl.* **170**, *377 (2007); G. Hinshaw et al. [WMAP Collaboration], arXiv:1212.5226 [astro-ph.CO]*

*[279] P. A. R. Ade et al. [Planck Collaboration], "Planck 2013 results. XVI. Cosmological parameters," Astron. Astrophys.* **571**, *A16 (2014) [arXiv:1303.5076 [astro-ph.CO]].*

*[280] http://dendera.berkeley.edu/plotter/entryform.html and http://dmtools.brown.edu/*

[281] *R. Agnese et al. [CDMS Collaboration], "Silicon detector results from the first five-tower run of CDMS II,"* Phys.Rev. **D88**, *031104 (2013) [Erratum-ibid. D* **D88**, *no. 5, 059901 (2013)] [arXiv:1304.3706 [astro-ph.CO]].*

[282] *R. Bernabei et al. [DAMA Collaboration], "First results from DAMA/LIBRA and the combined results with DAMA/NaI," Eur. Phys. J.* **C56**, *333 (2008) [arXiv:0804.2741 [astro-ph]];*
*R. Bernabei et al. [DAMA and LIBRA Collaborations], "New results from DAMA/LIBRA," Eur. Phys. J.* **C67**, *39 (2010) [arXiv:1002.1028 [astro-ph.GA]].*

[283] *C.E. Aalseth et al. [CoGeNT collaboration], Phys. Rev. Lett.* **106**, *131301 (2011).*

[284] *G. Angloher, M. Bauer, I. Bavykina, A. Bento, C. Bucci, C. Ciemniak, G. Deuter and F. von Feilitzsch et al., "Results from 730 kg days of the CRESST-II Dark Matter Search," Eur. Phys. J.* **C72**, *1971 (2012) [arXiv:1109.0702 [astro-ph.CO]].*